NASA CR-167952

Turbofan Noise Generation
Volume 1: Analysis

by
C.S. Ventres
M.A. Theobald
W.D. Mark

July 1982

Prepared Under Contract No. NAS3-21252
by
Bolt Beranek and Newman Inc.
Cambridge, Mass. 02138

for

NASA

National Aeronautics and
Space Administration
Lewis Research Center
Cleveland, Ohio 44135

Technical Report Documentation Page

1. Report No.	2. Government Accession No.	3. Recipient's Catalog No.

4. Title and Subtitle

Turbofan Noise Generation: Volume I, Analysis

5. Report Date

6. Performing Organization Code

7. Author(s)

C.S. Ventres, M.A. Theobald, W. Mark

8. Performing Organization Report No.

4770

9. Performing Organization Name and Address

Bolt Beranek and Newman Inc.
10 Moulton Street
Cambridge, MA 02238

10. Work Unit No. (TRAIS)

11. Contract or Grant No.

NAS3-21252

12. Sponsoring Agency Name and Address

National Aeronautics and Space Administration
Lewis Research Center
Cleveland, Ohio 44135

13. Type of Report and Period Covered

14. Sponsoring Agency Code

15. Supplementary Notes

16. Abstract Computer programs have been developed which calculate the in-duct acoustic modes excited by a fan/stator stage operating at subsonic tip speed. The following three noise source mechanisms are included:

a) sound generated by the rotor blades interacting with turbulence ingested into, or generated within, the inlet duct;
b) sound generated by the stator vanes interacting with the turbulent wakes of the rotor blades; and
c) sound generated by the stator vanes interacting with the mean velocity deficit wakes of the rotor blades.

The fan/stator stage is modeled as an ensemble of blades and vanes of zero camber and thickness enclosed within an infinite hard-walled annular duct. The amplitude of each propagating mode is computed and summed to obtain the sound power flux within the duct, for both upstream and downstream propagating modes.

Turbulence drawn into or generated within the inlet duct is modeled as nonhomogeneous and anisotropic random fluid motion, superimposed upon a uniform axial mean flow, and convected with that flow. The flow downstream of the rotor is also modeled as anisotropic and nonhomogeneous random fluid motion, superimposed upon a steady, but in this case spatially nonuniform mean flow.

Equations for the duct mode amplitudes, or expected values of the amplitudes, are derived in this volume, documentation for the computer programs is supplied in a second volume.

17. Key Words	18. Distribution Statement

19. Security Classif. (of this report)	20. Security Classif. (of this page)	21. No. of Pages	22. Price
Unclassified	Unclassified	112	

Report No. 4770

TURBOFAN NOISE GENERATION:
VOLUME 1: ANALYSIS

C.S. Ventres
M.A. Theobald
W.D. Mark

July 1982

Prepared for:

National Aeronautics and Space Administration
Lewis Research Center
Cleveland, Ohio 44135

TABLE OF CONTENTS

TABLE OF CONTENTS (Cont.)

LIST OF FIGURES

SUMMARY

A package of computer programs has been developed which calculates the in-duct acoustic modes excited by a fan/stator stage operating at subsonic tip speed. The following three noise source mechanisms are included:

a) sound generated by the rotor blades interacting with turbulence ingested into, or generated within, the inlet duct;
b) sound generated by the stator vanes interacting with the turbulent wakes of the rotor blades; and
c) sound generated by the stator vanes interacting with the velocity deficits in the mean wakes of the rotor blades.

The first two interaction mechanisms generate random noise (although most of the resulting energy may, in some circumstances, be clustered around multiples of the blade passage frequency), while the third mechanism generates tonal noise at the blade passage frequency and its harmonics.

The fan/stator stage is modeled as an ensemble of blades and vanes of zero camber and thickness enclosed within an infinite hard-walled annular duct. The acoustic pressure within the duct is calculated by distributing pressure dipoles on the surface of the rotor blades or stator vanes and calculating the pressure at an arbitrary point within the duct via the normal mode expansion of the Green's function for an annular duct. By this procedure one obtains an infinite series for the sound pressure within the duct. Each term contains a normal mode of the duct multiplied by the amplitude of that mode. The amplitude (or the expected value of the amplitude spectral density) of each *propagating* mode is computed and summed to obtain the sound power flux (or the expected value of the sound power spectral density) within the duct. These calculations are carried through for both upstream and downstream propagating modes.

The equations relating the duct acoustic mode amplitudes to the pressure dipole distribution on the rotor or stator blades make no assumptions about the ratio of the wavelength of the sound generated to the blade chord. However, to simplify the computation of the dipole distribution generated by a given periodic or random inflow variation, the so-called strip theory approximation is used. Specifically, the dipole distribution is calculated by deleting, from the convected wave equation, all terms containing derivatives with respect to radius, but retaining the radius as a parameter in the boundary conditions (which derive from the blade geometry and the incident fluid flow). At each radius, therefore, the equations to be solved are those for a linear cascade in subsonic flow. Although radial derivatives are deleted from the wave equation in calculating the chordwise pressure distribution on the blades, radial variations in the amplitude and phase of the pressure distribution are taken into account in integrating over the blade/vane surface to obtain the amplitudes of the propagating duct modes.

Turbulence drawn into or generated within the inlet duct is modeled as nonhomogeneous and anisotropic random fluid motion, superimposed upon a uniform axial mean flow, and convected with that flow. In the computer programs, the inlet turbulence velocity auto-correlation function is computed by a set of subprograms. It is intended that the form of the correlation function be chosen to fit turbulence data collected from a transducer fixed in the inlet duct (as opposed to rotating with the fan). To allow some flexibility in selecting the functional form of the velocity auto-correlation function without requiring an excessive amount of data for its definition, the auto-correlation function has been expressed as the product of three functions. Each function depends upon only a single variable, one of the three cylindrical polar coordinates of a point within the duct: r, ϕ, x. Rational methods for selecting these three functions are suggested in a companion report (Ref. 1).

The flow downstream of the rotor is also modeled as anisotropic and nonhomogeneous random fluid motion, superimposed upon a steady, but in this case spacially

nonuniform, mean flow. The mean (time-averaged) component of the flow is assumed to have no radial component, so that the mean flow streamlines form cylindrical surfaces. It is further assumed that if one of these cylinders is unwrapped to form a plane, the mean flow streamlines will be parallel. This is equivalent to ignoring the effects of viscous and turbulent diffusion in the rotor wakes, a justifiable approximation as regards the calculation of the forces on the stator vane, provided that the wake thickness chosen is that which is obtained at the axial station of the stator vanes themselves. The magnitude of the mean flow velocity is constant on lines parallel to the mean flow streamlines, but varies periodically in the direction normal to the mean flow streamlines.

Rotor wake turbulence is modeled as anisotropic and inhomogeneous turbulence carried along with the mean flow downstream of the rotor. The intensity of the turbulence is constant on lines parallel to the mean flow streamlines, but periodically varies in the direction normal to them. The turbulence velocity auto-correlation function is expressed, in rotor-fixed coordinates, as the product of three functions, each of which is a function of only one of the three spatial variables r, ϕ, x, just as for inlet turbulence.

Equations for the duct mode amplitudes, or expected values of the amplitudes, are derived in Volume 1, while documentation for the computer programs is supplied in Volume 2.

CHAPTER 1

INTRODUCTION

This is the final report of a project designed to develop a computer program which calculates the modal content of the acoustic fields set up in the inlet and exhaust ducts of a turbofan by the actions of nonsteady vortical velocity fluctuations convected past the rotor and stator blades. Such a program, supplemented by mathematical models of the impedance of the inlet and exhaust terminations, can be used to calculate the far field noise. The program can also be used to provide the initial conditions required for the investigation of duct liners, particularly liners tailored to suppress a specific mode or set of modes.

The fluctuating flows come from three distinct sources: 1) turbulence drawn into the inlet duct, 2) the turbulent component of the rotor blade wakes, and 3) the mean component of the rotor blade wakes. The first two motions are random, while the third is periodic (as seen by an observer fixed in the duct). It is characteristic of all three flows that the pressure fluctuations associated with them are an order of magnitude smaller than the velocity fluctuations, and that all three are embedded in, or convected with, the mean flow. When the velocity fluctuations are carried past a rigid surface, such as a fan or stator blade, the requirement that the flow conform to the shape of the blade sets up additional (acoustic) disturbances, which propagate both upstream and downstream in the duct.

The acoustic pressure in the duct can be calculated in a straightforward manner, using the Green's function for the duct, provided that the pressure distributions on the surfaces of the rotor or stator blades are known. If the Green's function is expressed as an infinite series of the normal modes of the duct, the modal amplitudes of the acoustic pressure are obtained directly. The problem remaining, therefore, is to determine the pressure distributions on the surfaces of the rotor or stator blades generated by the convected vortical velocity disturbances.

This is accomplished by modeling the blades as surfaces of zero thickness and camber, which support an unknown but continuous distribution of pressure dipoles. The particle velocity normal to the blades on the blades themselves is calculated from the unknown dipole distribution; this velocity is then *required* to nullify the normal component of the vortical disturbance velocity (so that the total fluid velocity conforms to the shape of the blades). The result is an integral equation for the dipole distribution, which, depending upon the approximations introduced, may admit an analytic solution, or may require numerical treatment.

The approximations required to arrive at an analytic solution are considerable: essentially they ignore the annular or circular geometry of the fan (or stator), the three dimensionality of the disturbance, the interaction between blades, and the compressibility of the fluid. What remains is incompressible flow around an isolated airfoil in two dimensions, the solution of which, for a sinusoidal vortical gust, is known as Sear's function. This was the approach used by Kemp and Sears (Refs. 2 and 3) in their original investigations of the interactions between blade rows in axial flow turbo-machinery. The incompressible approximation has since been shown to be unacceptable. For example, Fleeter (Ref. 4) found that compressibility can change the pressure on the rotor or stator values by as much as a factor of two, while Kaji (Ref. 5) calculated even greater changes (20 dB; a factor of 10) in the sound pressure level upstream of the blade row due to source non-compactness.

At the opposite extreme, as regards complexity, are calculations carried out by Kobayashi (Ref. 6) and Kobayashi and Groeneweg (Ref. 7), using equations derived by Namba (Refs. 8, 9) for an annular blade row in compressible flow. Because of the annular geometry the kernel function, which relates the dipole distribution to the velocity normal to the blades, is elaborate in form and time-consuming to compute. The associated integral equation is two-dimensional (i.e., both the spanwise and chordwise distributions of pressure dipoles must be determined). In his numerical work, Kobayashi made comparisons between his "exact" aerodynamic theory and various approximate methods of calculating the normal

component of the induced velocity. One of these, which he called the "quasi-three-dimensional" approximation, coincides with what most would call a "strip theory" approximation. In calculating the induced velocity, derivatives with respect to radius are deleted from the convected wave equation, so that one is left with the kernel function of a linear cascade in nonsteady compressible flow. The particular geometry of the cascade, as well as the vortical inflow velocity, depends on the radius, and this parametric dependence is retained in calculating the induced velocity (and hence ultimately the dipole distribution). The effects of radial or spanwise variations in the amplitude and phase of the vortical disturbance velocity, as well as radial variations in blade chord, inter-blade gap, and stagger angle, are thereby taken into account, even if in an approximate manner. Kobayashi found that this procedure introduced errors no greater than 2 dB in the computed magnitudes of the acoustic modes set up in the duct upstream and downstream of the rotor.

The strip theory approximation, as described above, has practical advantages. It is considerably easier than the "exact" method to implement numerically, and it accommodates more conveniently a variety of vortical inflow disturbances (e.g. random as well as deterministic motions). For these reasons, it has been selected for use in the computer codes developed in this project.

The role of atmospheric turbulence in generating either broadband or tone-like noise, depending upon the extent to which the turbulence is distorted as it is drawn into the turbofan inlet, is by now widely known and well understood. Measurements made by Hanson (Ref. 10) and others have shown that when initially isotropic (or nearly isotropic) turbulence is drawn into a duct moving at zero or very low forward speed, the streamwise component of the turbulence velocity is reduced as compared to the transverse components. Elongated turbulence eddies are intercepted by many rotor blades as they pass through the fan; because each blade experiences essentially the same velocity fluctuation, the noise generated is tone-like in nature, containing prominent peaks at multiples of the blade passage frequency. On the other hand, when the

forward speed of the turbofan is comparable to the velocity within the duct, the turbulence remains roughly isotropic, and the spectrum of the sound generated is less peaked.

Modeling inlet turbulence requires that the velocity correlation function of the turbulence be anisotropic. We have chosen to write the turbulence velocity correlation function as the product of three functions, each of which depends only upon the quotient of one space coordinate and the corresponding length scale. This model is not based upon or suggested by any physical model of fluid turbulence, but has the advantage of being easily adjusted to fit measured turbulence spectra, without requiring an excessive number of measurements for the purpose. Other models of inlet turbulence, such as the axisymmetric turbulence model used by Kerschen (Ref. 11), could easily be incorporated if desired.

Laksminarayana et al. have collected an extensive set of measurements of the mean and fluctuating components of the flow downstream of a multibladed fan operating at subsonic tip speed, using a transducer rotating at the same rate as the fan (Refs. 12, 13, 14). Their measurements of the mean (or time-averaged) component of the flow at locations remote from the blade hub or tip indicate that the radial velocity immediately downstream of the fan blade trailing edges is substantial, but that this velocity decays rapidly, so that at distances greater than about one-half blade chord downstream the circumferential and axial components of the mean velocity predominate. Measurements of the velocity defect profiles show marked asymmetry about the streamlines on which the minimum velocity occurs, but this asymmetry also disappears within a half-chord length downstream of the fan blade trailing edges. At greater distances, the normalized velocity defect profiles all show a Gaussian distribution, there being one such velocity defect profile for each fan blade. Due to the diffusion of momentum in the flow, the widths of the velocity defect profiles increase with distance downstream, while the maximum velocity defect decreases. But for the purpose of calculating the noise radiated by the stator, it is sufficient to model the wake flow in the vicinity of the stator. This can be done by ignoring momentum diffusion,

provided that the wake thickness and velocity defect are assigned the values they attain in the vicinity of the stator, say at the leading edges of the stator vanes.

With these approximations, the mean flow streamlines down-stream of the fan become a series of parallel lines, as viewed by a cylindrical surface opened out to form a flat plane. The velocity defect profiles are Gaussian, with the wake width and maximum velocity defect left as parameters to be specified. The flow velocity, being periodic in the azimuthal direction, is conveniently expressed as a Fourier series for the purpose of calculating the inflow velocity fluctuations normal to the stator vanes.

One additional aspect of the mean wake geometry is noteworthy. At each radius the mean flow streamlines all bear the same angle to the centerline of the duct, but this angle is a function of the radius, the precise nature of which depends upon the radial variation of design lift coefficient and chord length of the rotor blades. The locus of centerlines of any given wake form a surface whose shape depends upon the radial variation of the wake angle; this surface will in general intersect any selected stator vane at only one point, and this point will move along the leading edge of the stator vane as the fan rotates. Particularly if the gap between the fan and stator is large, each stator vane will at any given instant intersect many rotor blade wakes, and for each wake intersected, there will be two changes in the sign of the disturbance velocity seen by the stator vane. The pressure induced on the stator vane will have as many sign reversals as the inflow velocity, and will tend to excite duct acoustic modes with that same number of circular nodes. If, at the frequency of interest (which of course must be the blade passage frequency or one of its harmonics), few or none of the duct modes with that number of radial nodes propagate in the duct, the stator will not, at that frequency, be an effective generator of sound. The significance of this wake roll-up phenomenon in the generation of sound by the stator was pointed out previously by Bliss, et al. (Ref. 15). In their discussion, they chose to emphasize the radial trace velocity of the vane/wake intercept instead of the number of nodes in the normal

component of the inflow velocity. Their criteria for efficient sound generation, namely that the trace velocity of the points of intersection of the wake centerlines with the stator vanes be supersonic, is perhaps more appropriate to an unshrouded rotor/stator combination, but the two criteria are roughly equivalent when the ratio of hub and tip radii is close to one, and are exactly equivalent for a set of two linear cascades in relative motion between two infinite parallel planes.

In the equations derived in this report, and in the computer programs developed from them, the radial variation of the the angle between the mean wake streamlines and the duct centerlines may be specified arbitrarily, so that the effects of wake roll-up are properly accounted for.

Wake turbulence measurements made by Laksminarayana, et al. (Refs. 13, 14) using a transducer rotating at the same speed as the rotor indicated that the turbulence on the centerline of the mean velocity defect wakes is both more intense and contains more energy at high frequencies than does the turbulence in the region between wakes. The maximum turbulence intensity coincides roughly with the maximum mean velocity defect, and the fall-off in intensity with distance normal to the wake centerline follows roughly the same Gaussian distribution as the mean wake velocity defect. The width of the turbulent wake is also roughly the same as the width of the mean wake.

Based upon these observations, we have chosen to model rotor wake turbulence as homogeneous turbulence modulated by a function which is constant on the wake centerlines, but which varies periodically along lines drawn normal to the wake centerline. This model is at variance with the observations quoted above in that the turbulence midway between wake centerlines has the same frequency content (but at diminished intensity) as the turbulence on the centerlines. But because of the diminished intensity of the "between wake" turbulence, it cannot figure significantly in the noise generated by the stator.

Only one other model of rotor wake turbulence (as applied to acoustic calculations) has been published to

date. In his model, Hanson (Ref. 16) took a very different tack by modeling both the mean and turbulent components of the wake flow as a series of velocity defects of randomly varying amplitude and position. The mean value of the amplitude of the wake defect coincides, of course, with that of the mean wake velocity defect, and the functional form (or shape) of the velocity defect must likewise conform to that of the mean wakes. In this regard, Hanson's model is less flexible than the one used in this report. Also, in calculating the noise radiated by the stator, Hanson modeled the stator vanes as point dipoles. He was therefore unable to account for the (quite reasonable) possibility that the radial integral scale of the turbulence might be considerably shorter than the span of the stator vanes. The point dipole model also requires that the wavelength of the radiated sound be considerably greater than the chord of the stator vanes, which at high frequencies is not the case.

No attempt has been made to model the flow field downstream of the rotor hub or tip; such work is beyond the scope of this investigation.

The remainder of the report is arranged as follows: pertinent aspects of the geometry of the duct, rotor and stator are discussed in Chapter 2. In Chapter 3, a brief discussion of the acoustics of annular ducts is presented, along with a derivation of the amplitudes (or expected values of the amplitudes) of the duct modes excited by a given pressure distribution on the fan or stator blades. The computation of the blade or vane pressure distribution caused by a given vortical inflow velocity is outlined in Chapter 4, and mathematical models of the fan blade mean velocity defect wakes, rotor inlet turbulence, and rotor wake turbulence are provided in Chapters 5, 6, and 7, respectively. Finally in Chapter 8, selected aspects of the numerical procedures used in the computer programs are discussed. Program listings and documentation are supplied in Volume 2.

CHAPTER 2

GEOMETRY OF DUCT, ROTOR, AND STATOR

For our purposes, a turbofan is a rotor and stator combination mounted in an annular duct of infinite length (i.e., reflection of acoustic waves from the ends of the duct are to be ignored). A sketch of the rotor/stator combination is shown in Fig. 1. As shown in the figure, a cylindrical polar coordinate system is established in the duct, with the polar axis lying along the duct centerline. The axial coordinate x increases in the direction of air flow, and the rotor rotates in the sense of increasing ϕ. The outer radius of the duct is r_D and the inner radius is r_H. The rotor has B identical evenly spaced blades, and the stator has V identical evenly spaced vanes.

The rotor blades and stator vanes are modelled as twisted sheets of zero thickness and camber, whose pitch angle and chord vary with the radius, r. The axial and azimuthal sweep, if any, of the rotor blades are defined by extending a radial line from the axis of rotation through the mid-chord point of the blade at the hub (radius = r_H). The location of the mid-chord point at any other radius r is defined by the two component vector $\underline{\delta} \equiv (\delta_1, \delta_2)$ which gives the displacement of this point from the radial line. (δ_1 = axial displacement and δ_2 = azimuthal displacement.) In general, both δ_1 and δ_2 are functions of the radius r, and by definition $\delta_1 = \delta_2 = 0$ at the hub ($r = r_H$). See Figure 2.

The intersections of the rotor blades and stator vanes with a cylindrical surface of radius r is shown in Fig. 3. The stagger angle of the blades is χ, and that of the vanes is θ (both are functions of r). The spacing between the blades is $2\pi r/B$, and between the vanes, $2\pi r/V$. The local semichord of the blades is b (a function of r). The same symbol is used for the semichord of the vanes. The distance between the rotor and stator is d.

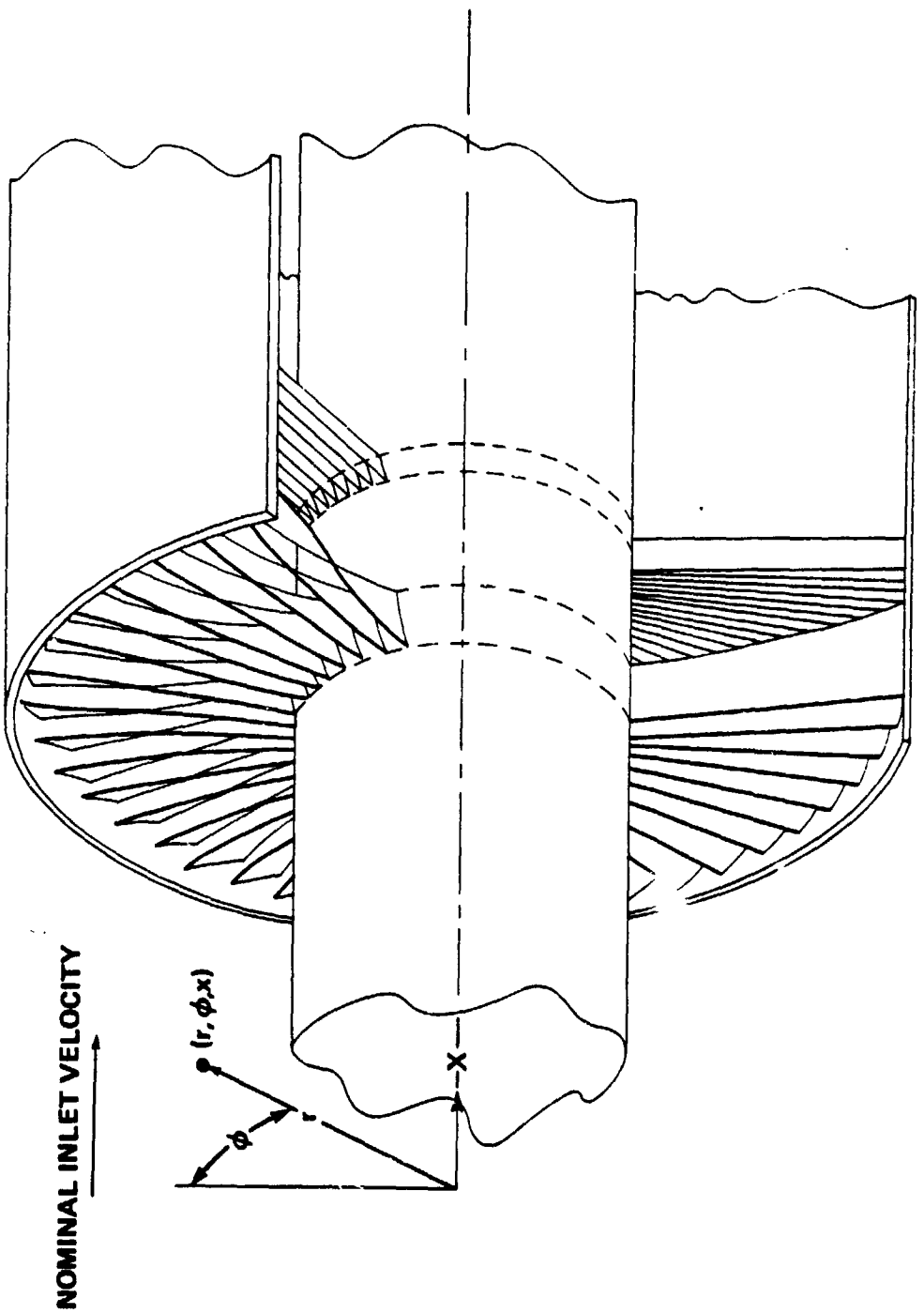

FIGURE 1. Sketch of Rotor/Stator Combination

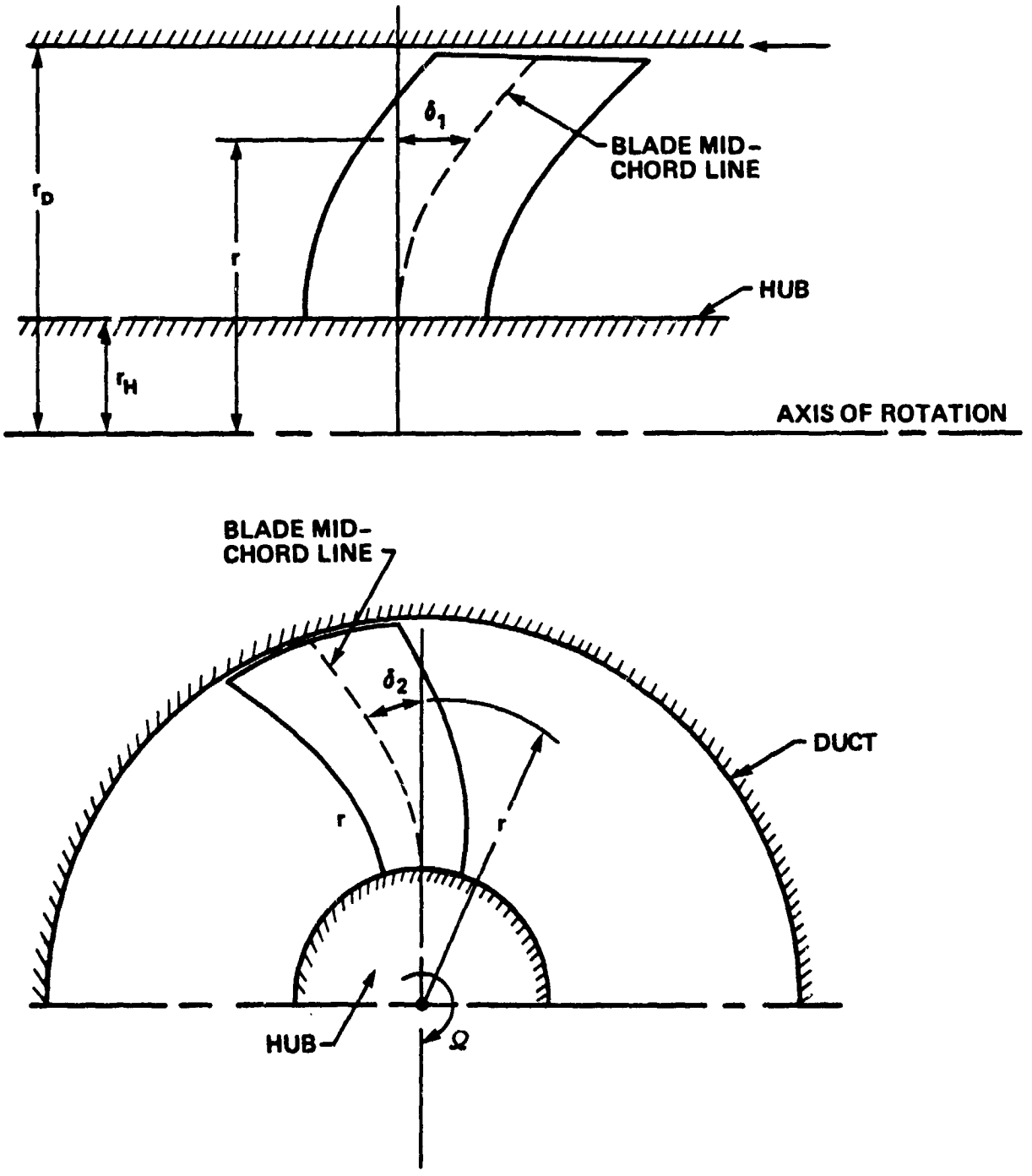

Figure 2. Blade Geometry

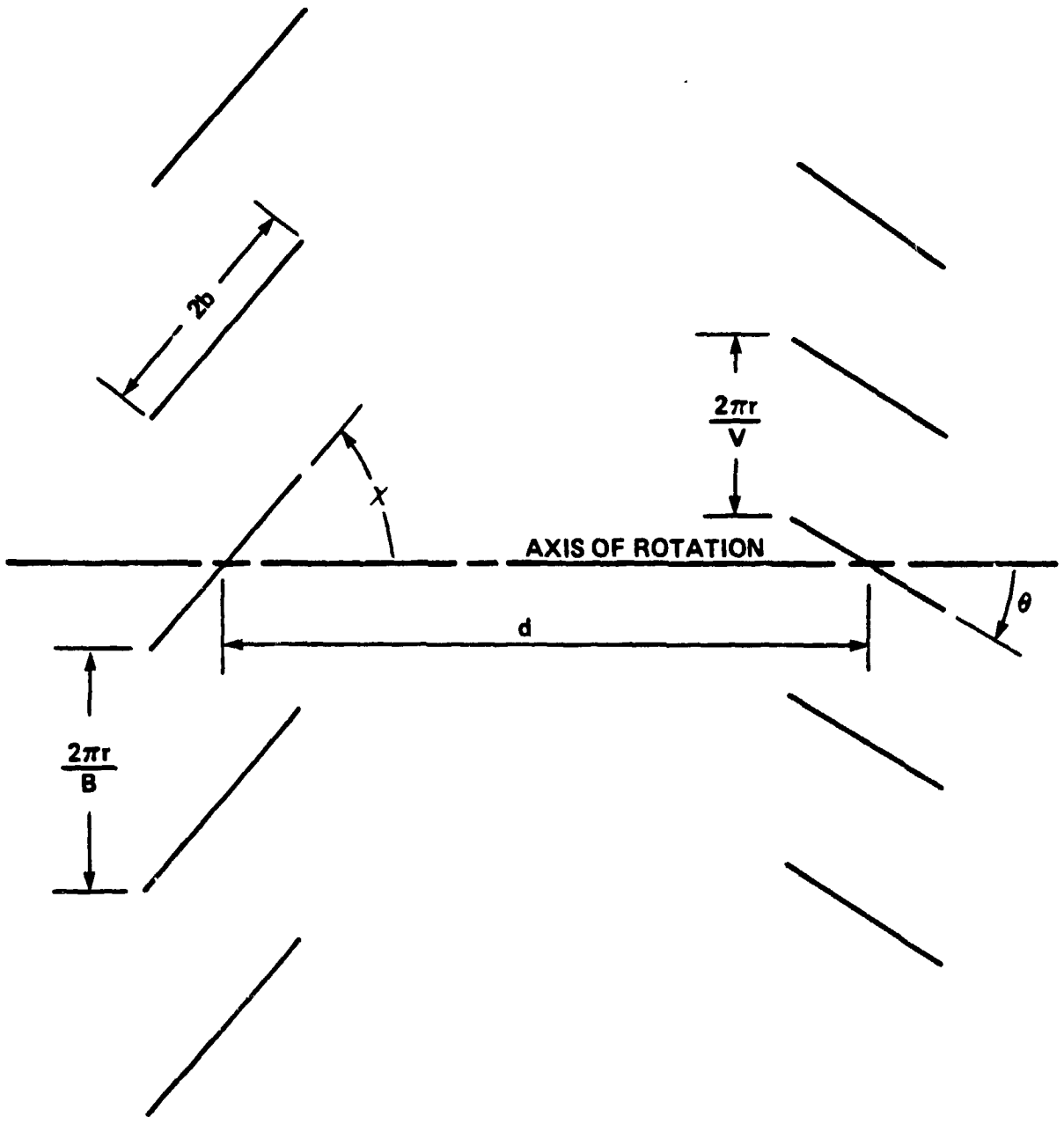

Figure 3. Rotor/Stator Geometry

CHAPTER 3
DUCT ACOUSTICS

3.1 Normal Modes in an Annular Duct

The normal modes of an annular duct with hard walls are the set of solutions to the two-dimensional Helmholtz equation having the special form.

$$\Psi(r,\phi) = f(r)\exp(im\phi) \tag{1}$$

where m is any integer, positive, negative, or zero. The Helmholtz equation is, in polar coordinates,

$$\left(\frac{\partial^2}{\partial r^2} + \frac{1}{r}\frac{\partial}{\partial r} + \frac{1}{r^2}\frac{\partial^2}{\partial \phi^2}\right)\Psi + \kappa^2\Psi = 0 \quad . \tag{2}$$

In this equation κ is an undefined constant. As is shown below, the equation has non-trivial solutions which fit the appropriate boundary conditions on the walls of the annular duct only for certain specific values of κ. If Eq. (1) is substituted into Eq. (2), we obtain

$$\frac{d^2f}{dr^2} + \frac{1}{r}\frac{df}{dr} + \left(\kappa^2 - \frac{m^2}{r^2}\right) f = 0 \quad . \tag{3}$$

Substituting $u \equiv \kappa r$ for r reduces Eq. (3) to Bessel's equation of order m:

$$\frac{d^2f}{du^2} + \frac{1}{u}\frac{df}{du} + \left(1 - \frac{m^2}{u^2}\right) f = 0 \quad .$$

The solutions are mth order Bessel functions of the first and second kind, i.e., $f(u) = \psi_m(\kappa r)$, where

$$\psi_m(\kappa r) = AJ_m(\kappa r) + BY_m(\kappa r) \quad . \tag{4}$$

If we specify that $\Psi(r,\phi) = \psi_m(\kappa r)\exp(im\phi)$ is either the pressure or the velocity potential, then the radial derivatives of ψ_m must vanish at the inner and outer walls of the duct, so if A and B are to be not both zero,

$$\begin{vmatrix} J'_m(\kappa r_H) & Y'_m(\kappa r_H) \\ J'_m(\kappa r_D) & Y'_m(\kappa r_D) \end{vmatrix} = 0 \quad . \tag{5}$$

This transcendental equation has a countably infinite number of roots κ for every integer m; if we denote these roots by $\kappa_{m,n}$, n = 1,2,3,..., and arrange them in order of increasing magnitude, then the functions $\psi_m(\kappa_{m,n}r)$ have (n-1) zeros in the interval $r_H \leq r \leq r_D$. These functions are also orthogonal with respect to the weight function r over the same interval; that is,

$$\int_{r_H}^{r_D} r\, \psi_m(\kappa_{m,n}r)\, \psi_m(\kappa_{m,\ell}r)\, dr = 0$$

unless $\ell = n$. Using this fact, plus the fact that the functions $\exp(im\phi)$, m = any integer, are orthogonal on the interval $0 \leq \phi \leq 2\pi$, it is easy to show that the normal modes $\psi_m(\kappa_{m,n}r)\exp(im\phi)$ are orthogonal over the cross-section of the duct. Specifically,

$$\int_{r_H}^{r_D}\int_{0}^{2\pi} \{\psi_m(\kappa_{m,n}r)\exp(im\phi)\} \cdot \{\psi_k(\kappa_{k,\ell}r)\exp(-ik\phi)\} r\, d\phi\, dr$$

$$= 0 \text{ if } k \neq m \textit{ or } \ell \neq n$$

$$= 2\pi \int_{r_H}^{r_D} \psi_m^2(\kappa_{m,n}r) r\, dr \quad , \tag{6}$$

if $k = m$ *and* $\ell = n$. It is convenient to adjust the constants A and B in Eq. (4) [which are determined by Eq. (5) only to within an arbitrary multiplicative factor] so that

$$\int_{r_H}^{r_D} \psi_m^2(\kappa_{m,n}r) r\, dr = \frac{r_d^2 - r_n^2}{2} \quad .$$

The orthogonality relation [Eq. (6)] then becomes

$$\int_{r_n}^{r_d} \int_{0}^{2\pi} \{\psi_m(\kappa_{m,n}r)\exp(im\phi)\} \cdot \{\psi_k(\kappa_{k,\ell}r)\exp(-ik\phi)\}rd\phi dr$$

$$= \pi(r_D^2-r_H^2)\ \delta_{mk}\delta_{n\ell} \quad . \tag{8}$$

A special FORTRAN program has been written which calculates $\kappa_{m,n}$ and the constants A and B in Eq. (4) subject to the normalization given in Eq. (8); for details see Appendix C.

The significance of the normal modes is that they can be used to represent pressure patterns which propagate within the duct without change in form, and that any acoustic field within the duct, however generated, can be represented as a suitable combination of these patterns.

The wave equation in a duct containing a fluid moving at a uniform *axial* velocity U is*

$$\nabla^2 p + \frac{\partial^2 p}{\partial x^2} - \frac{1}{c_0^2}\left(\frac{\partial}{\partial t} + U\frac{\partial}{\partial x}\right)^2 p = 0 \quad , \tag{9}$$

where p is the acoustic pressure, and ∇^2 is the two-dimensional Laplace operator,

$$\nabla^2 \equiv \frac{\partial^2}{\partial r^2} + \frac{1}{r}\frac{\partial}{\partial r} + \frac{1}{r^2}\frac{\partial^2}{\partial \phi^2} \quad .$$

Now assume that p is the real or imaginary part of

$$\psi_m(\kappa_{m,n}r)\ \exp[i(m\phi-\gamma x-\omega t)] \quad . \tag{10}$$

This pressure pattern has m diametral nodes (like the spokes of a wheel), and (n-1) concentric circular nodes. If we substitute expression (10) into Eq. (9), and recall that

$$\nabla^2\{\psi_m(\kappa_{m,n}r)\exp(im\phi)\} = -\kappa_{m,n}^2\psi_m(\kappa_{m,n}r)\exp(im\phi),$$

the following relation is obtained:

*Between the rotor and stator an appreciable circumferential velocity exists as well. This velocity is not accounted for in Fig. (9).

$$-\kappa_{m,n}^2 - \gamma^2 + \left(\frac{\omega}{c_0} + \frac{U\gamma}{c_0}\right)^2 = 0 \ .$$

Solving for γ in terms of $\kappa_{m,n}$ and ω, we find that $\gamma \equiv \gamma_{n,m}(\omega)$, where

$$\gamma_{n,m}(\omega) \equiv \frac{1}{\beta^2}\left(\frac{M\omega}{c_0} \pm \sqrt{\left(\frac{\omega}{c_0}\right)^2 - \beta^2\kappa_{m,n}^2}\right). \tag{11}$$

Equation (11) shows that γ is real whenever ω is real and $\omega/c_0 > \beta\kappa_{m,n}$. Under these conditions, the pressure pattern propagates unchanged along spiral paths normal to the lines

$$m\phi - \gamma x - \omega t = \text{const.}$$

If ω is real but $\omega/c_0 < \beta\kappa_{m,n}$, then γ is complex and the pattern grows or decays exponentially along the duct depending on which sign is selected in Eq. (11).

Modal pressure patterns such as

$$\psi_m(\kappa_{m,n}r)\exp\{i[m\phi - \gamma_{n,m}(\omega)x - \omega t]\} \tag{12}$$

can be superimposed to form a general description of the acoustic pressure field in a turbomachine. Thus, if we multiply the pattern above by an arbitrary function of ω, say $\bar{p}_{m,n}(\omega)$, integrate over frequency $(\omega/2\pi)$, and sum over m,n, we obtain*

$$p(\underset{\sim}{x},t) = \sum_m \sum_n \psi_m(\kappa_{m,n}r)\int \bar{p}_{mn}(\omega)\exp\{i[m\phi + \gamma_{n,m}(\omega)x - \omega t]\}\,\frac{d\omega}{2\pi} \tag{13}$$

where now $\underset{\sim}{x}$ is the point (r,x,ϕ) in the duct. Note that in general $p(\underset{\sim}{x},t)$ is composed of both propagating and non-propagating modal pressure patterns. The Fourier transform of this equation, namely,

$$\bar{p}(\underset{\sim}{x},\omega) = \sum_m \sum_n \bar{p}_{mn}(\omega)\psi_m(\kappa_{m,n}r)\exp[im\phi + i\gamma_{n,m}(\omega)x] \tag{14}$$

---

*Where no integration limits are specified, $-\infty$ to $+\infty$ is implied.

exhibits more explicitly the role of the functions $\bar{p}_{mn}(\omega)$ as complex modal amplitudes.

3.2 Acoustic Energy Flux

In a duct containing a fluid flowing at a uniform axial velocity U, the instantaneous acoustic intensity is (Ref. 17).

$$I = \left(\frac{p}{\rho_0} + Uu\right)(\rho_0 u + U\rho) \tag{15}$$

where ρ_0 is the nominal fluid density and p, ρ, and u are the instantaneous acoustic perturbation pressure, density, and axial velocity, respectively. The acoustic pressure and density perturbations are proportional to one another ($p = c_0^2\rho$), so Eq. (15) can be written in terms of the pressure and axial velocity only:

$$I = (1+M^2)\, pu + \frac{M}{\rho_0 c_0} p^2 + \rho_0 c_0 M u^2 \tag{16}$$

where $M = U/c_0$ is the nominal axial flow Mach number.

Now introduce the Fourier transforms of p and u, defined as follows:

$$\bar{p}(\underset{\sim}{x},\omega) \equiv \int p(\underset{\sim}{x},t)\exp(i\omega t)dt \tag{17}$$

$$p(\underset{\sim}{x},t) = \int \bar{p}(\underset{\sim}{x},\omega)\exp(-i\omega t)\,\frac{d\omega}{2\pi} \tag{18}$$

with the corresponding definition for $\bar{u}(\underset{\sim}{x},\omega)$. (In both integrals above the limits of integration are understood to be $\pm\infty$. This convention will be adhered to throughout this report.) The axial intensity can now be written as a double inverse Fourier transform:

$$I = \iint\{(1+M^2)\bar{p}(\underset{\sim}{x},\omega)\bar{u}^*(\underset{\sim}{x},\nu) + \frac{M}{\rho_0 c_0}\bar{p}(\underset{\sim}{x},\omega)\bar{p}^*(x,\nu)$$

$$+ \rho_0 c_0 M\,\bar{u}(\underset{\sim}{x},\omega)\bar{u}^*(\underset{\sim}{x},\nu)\}\cdot\exp[-i(\omega-\nu)t]\,\frac{d\omega}{2\pi}\,\frac{d\nu}{2\pi}\,. \tag{19}$$

where the superscript * denotes the complex conjugate. Both $\bar{p}(\underset{\sim}{x},\omega)$ and $\bar{u}(\underset{\sim}{x},\omega)$ can be written as sums of modal pressure patterns, as in Eq. (14). Thus,

$$\bar{p}(\underset{\sim}{x},\omega) = \sum_m \sum_n \bar{p}_{mn}(\omega)\psi_m(\kappa_{m,n}r)\exp[im\phi - i\gamma_{n,m}(\omega)x] \tag{20}$$

$$\bar{u}(\underset{\sim}{x},\nu) = \sum_k \sum_\ell \bar{u}_{k\ell}(\nu)\psi_n(\kappa_{k,\ell}r)\exp[ik\phi - i\gamma_{\ell,k}(\nu)x] \ . \tag{21}$$

The modal coefficients $\bar{p}_{mn}(\omega)$ and $\bar{u}_{mn}(\omega)$ are not independent, but are related through the axial momentum equation,

$$\frac{\partial u}{\partial t} + U\frac{\partial u}{\partial x} + \frac{1}{\rho_0}\frac{\partial p}{\partial x} = 0 \ .$$

If Eqs. (20) and (21) are substituted into the Fourier transform of this equation, the following relationship is obtained:

$$\bar{u}_{mn}(\omega) = -\frac{A_{mn}(\omega)}{\rho_0 U}\bar{p}_{mn}(\omega) \tag{22}$$

where

$$A_{mn}(\omega) \equiv \frac{\gamma_{n,m}(\omega)}{\frac{\omega}{U} + \gamma_{n,m}(\omega)} \ . \tag{23}$$

The axial intensity can now be written entirely in terms of p_{mn}:

$$I = \sum_m \sum_n \sum_k \sum_\ell \psi_m(\kappa_{m,n}r)\psi_k(\kappa_{k,\ell}r)\exp[i(m-k)\phi]\cdot$$

$$\frac{1}{\rho_0 U}\iint [M^2-(1+M^2)A^*_{k\ell}(\nu) + A_{mn}(\omega)A^*_{k\ell}(\nu)]\cdot \tag{24}$$

$$\cdot \exp\{-i[\gamma_{n,m}(\omega)-\gamma_{\ell,k}(\nu)]x - i(\omega-\nu)t]\}\cdot\hat{p}_{mn}(\omega)\hat{p}^*_{k\ell}(\nu)\frac{d\omega}{2\pi}\frac{d\nu}{2\pi} \ .$$

The instantaneous sound power is found by integrating the intensity over the cross-section of the duct. That is:

$$\text{Power} = \int_{r_H}^{r_D}\int_{0}^{2\pi} I\, r d\phi dr = \frac{\pi(r_d^2-r_n^2)}{\rho_0 U} \sum_m \sum_n \iint [M^2-(1+M^2)A^*_{mn}(\nu)$$

$$+ A_{mn}(\omega)A^*_{mn}(\nu)]\exp\{i[\gamma_{n,m}(\omega)-\gamma^*_{n,m}(\nu)]x$$

$$-i(\omega-\nu)t\}\ \bar{p}_{mn}(\omega)\bar{p}^*_{mn}(\nu)\ \frac{d\omega}{2\pi}\ \frac{d\nu}{2\pi} \quad . \tag{25}$$

The noise generated by the stator blades interacting with the mean wake momentum deficits of the rotor is periodic, the period being the blade passage interval. Thus

$$\bar{p}_{mn}(\omega) = 2\pi \sum_s p_{mns}\delta(\omega-\Omega Bs)$$

$$\bar{p}^*_{mn}(\nu) = 2\pi \sum_r p^*_{mnr}\delta(\nu-\Omega Br) \tag{26}$$

and the sound power flux in the duct is

$$\text{Power} = \frac{\pi(r_D^2-r_H^2)}{\rho_0 U} \sum_m \sum_n \sum_r \sum_s \{M^2-(1+M^2)A^*_{mn}(rB\Omega)$$

$$+ A_{mn}(sB\Omega)A^*_{mn}(rB\Omega)]\exp\{i[\gamma_{n,m}(sB\Omega)-\gamma^*_{n,m}(rB\Omega)]x$$

$$-i(s-r)B\Omega t]\}p_{mns}p^*_{mnr} \quad . \tag{27}$$

Those terms in this equation with $r \neq s$ represent fluctuations in the power. The time average sound power is

$$\overline{\text{Power}} = \frac{\pi(r_D^2-r_H^2)}{\rho_0 U} \sum_m \sum_n \sum_s \{M^2-(1+M^2)A^*_{mn}(sB\Omega)+|A_{mn}(sB\Omega)|^2\}|p_{mns}|^2. \tag{28}$$

The term in braces {···} can be simplified:

$$\{\cdots\} = \frac{\mp M^2\beta^4(sB\Omega/U)k_{n,m}(sB\Omega)}{[sB\Omega/c_0 \pm Mk_{n,m}(sB\Omega)]^2} \quad . \tag{29}$$

The upper set of signs apply upstream of the rotor (where the energy flows upstream or in the negative x-direction) and the lower set apply downstream.

When the sound in the duct is random, Eq. (24) can be used to calculate the ensemble-averaged or expected value of the power, say <Power>, in terms of the expected value of the mode spectrum in the duct, $\langle \bar{p}_{mn}(\omega)\, \bar{p}^*_{mn}(\nu)\rangle$. If the mode spectrum is correlated at differing frequencies (i.e., if $\langle p_{mn}(\omega)\, p^*_{mn}(\nu)\rangle \neq 0$ when $\omega \neq \nu$), then the sound power within the duct fluctuates. For example, as will be shown later on, when turbulence is convected past either the rotor or the stator, a modal spectral density of the form

$$\langle \bar{p}_{mn}(\omega)\bar{p}^*_{mn}(\nu)\rangle = 2\pi \sum_s \bar{p}_{mns}(\omega)\delta(\omega-\nu-sB\Omega) \quad . \tag{30}$$

is produced. If this expression is substituted into Eq. (24), the following result is obtained for the expected value of the acoustic power:

$$\langle \text{Power}\rangle = \frac{\pi(r_D^2-r_H^2)}{\rho_0 U} \sum_m \sum_n \sum_s \exp(isB\Omega t)\cdot \int [M^2-(1-M^2)A^*_{mn}(\omega+sB\Omega)$$

$$+A_{mn}(\omega)A^*_{mn}(\omega+sB\Omega)]\exp\{i[\gamma_{n,m}(\omega)-\gamma_{n,m}(\omega+sB\Omega)]x\}\bar{p}_{mns}(\omega)\,\frac{d\omega}{2\pi} \quad . \tag{31}$$

All terms with $s \neq 0$ correspond to fluctuations in the power in the duct. If we average over one period, only the $s = 0$ term remains:

$$\langle \overline{\text{Power}}\rangle = \frac{\pi(r_D^2-r_H^2)}{\rho_0 U} \sum_m \sum_n \int [M^2-(1-M^2)A^*_{mn}(\omega)+|A_{mn}(\omega)|^2]\bar{p}_{mno}(\omega)\,\frac{d\omega}{2\pi} \quad . \tag{32}$$

The integrand is the power spectral density. That is,

$$\overline{\langle \text{Power} \rangle} = \int S(\omega) \frac{d\omega}{2\pi} \quad ,$$

where

$$S(\omega) \equiv \frac{\pi(r_D^2 - r_H^2)}{\rho_0 U} \sum_m \sum_n [M^2 - (1-M^2)A_{mn}^*(\omega) + |A_{mn}(\omega)|^2] p_{mno}(\omega) \quad . \tag{33}$$

But $p_{mno}(\omega)$ is just the time average of the amplitude spectral density of the (m,n)th duct mode, which later on we will denote by $P_{mn}(\omega)$. Thus, we can write

$$S(\omega) = \frac{\pi(r_D^2 - r_H^2)}{\rho_0 U} \sum_m \sum_n \{M^2 - (1-M^2)A_{mn}^*(\omega) + |A_{mn}(\omega)|^2\} P_{mn}(\omega) \quad . \tag{34}$$

Again, the quantity in braces in this equation can be simplified:

$$\{\ \} = \frac{\overline{+}M^2 \beta^4 (\omega/U) k_{n,m}(\omega)}{[\omega/c_0 \pm M k_{n,m}(\omega)]^2} \quad . \tag{35}$$

3.3 Duct Acoustic Modes Excited by Fluctuating Loads on the Rotor or Stator

In this section, we shall derive equations which relate the acoustic modes in the inlet or exhaust ducts to fluctuating loads on the rotor or stator blades. The starting point is Eq. (4.13) in Goldstein's book *Aeroacoustics** (Ref. 17).

*Goldstein's equation has the density fluctuation $\rho(\underline{x},t)$ on the left-hand side; the version shown on the following page is actually his equation multiplied through by c_0^2.

$$p(\underset{\sim}{x},t) = \int_{-\infty}^{+\infty} \int_{S(\tau)} \nabla G(\underset{\sim}{x},\underset{\sim}{y},t-\tau)\cdot \underset{\sim}{f}(\underset{\sim}{y},\tau) ds(\underset{\sim}{y})\, d\tau \quad , \quad (36)$$

which gives the pressure fluctuation $p(\underset{\sim}{x},t)$ at any point $\underset{\sim}{x}$ within the duct in terms of the force/unit area $\underset{\sim}{f}$ exerted by the blades on the fluid. In this equation, $G(\underset{\sim}{x},\underset{\sim}{y},t-\tau)$ is the time-dependent Green's function for a hard-walled annular duct. If we introduce a cylindrical coordinate system such that the field point $\underset{\sim}{x}$ is (r,x_1,ϕ) while the integration point $\underset{\sim}{y}$ is $(r',y_1,\tilde{\phi})$, then G can be written as follows:

$$G(\underset{\sim}{x},\underset{\sim}{y},t-\tau) = \frac{-1}{4\pi i} \sum_m \sum_n \frac{\psi_m(\kappa_{m,n}r)\psi_m(\kappa_{m,n}r')}{\Gamma} \exp[im(\phi-\tilde{\phi})]$$

$$\cdot \int \frac{1}{k_{n,m}} \exp[-i\omega(t-\tau)+\gamma_{n,m}(y_1-x_1)]d\omega \quad , \quad (37)$$

where

$$\gamma_{n,m} \equiv \frac{M\omega}{\beta^2 c_0} + \frac{k_{n,m}}{\beta^2} \operatorname{sgn}(y_1-x_1) \quad (38)$$

$$k_{n,m} \equiv \sqrt{\left(\frac{\omega}{c_0}\right)^2 - \beta^2\kappa_{m,n}^2} \quad (39)$$

In Eq. (36), $\psi_m(\kappa_{m,n}r)\exp(im\phi)$ is a normal mode of the duct, and $\psi_m(\kappa_{m,n}r')\exp(-im\phi')$ is the complex conjugate of the same normal mode, evaluated at $(r',\tilde{\phi})$ instead of (r,ϕ).

If the fluid is assumed to be inviscid, the force $\underset{\sim}{f}$ will be normal to the surface,

$$\underset{\sim}{f} = p\underset{\sim}{n} \quad ,$$

where p is the local pressure. Thus,

$$p(\underset{\sim}{x},t) = \iint_{S(y)} \underset{\sim}{n}(\underset{\sim}{y})\cdot\nabla G(\underset{\sim}{x},\underset{\sim}{y},t-\tau)\; p(\underset{\sim}{y},\tau)dS(\underset{\sim}{y})\; d\tau \quad . \quad (40)$$

The integration is to be carried out over both faces of each blade. On each blade, we can divide the integral in the equation above into two parts, one over the forward or upstream face of the blade, and the other over the downstream face. Calling the upstream face + and the downstream face -, we have, because the blades are very thin,

$$p_+\underset{\sim}{n}_+ + p_-\underset{\sim}{n}_- \doteq (p_+-p_-)\;\underset{\sim}{n} \quad ,$$

where $\underset{\sim}{n}$ is a unit normal vector erected on the middle surface of the blade. Define Δp as $\Delta p \equiv p_- - p_+$. Then

$$p(\underset{\sim}{x},t) = -\int\int_{S_m} \underset{\sim}{n}(\underset{\sim}{y})\cdot\nabla G(\underset{\sim}{x},\underset{\sim}{y},t-\tau)\cdot\Delta p(\underset{\sim}{y},\tau)dS(\underset{\sim}{y})d\tau \quad , \quad (41)$$

where now the integration is over the blade surfaces (as opposed to the two blade faces).

Because we are interested in frequency spectra rather than pressure time histories, it is convenient to calculate the Fourier transform of Eq. (41), using the Fourier transform pair as defined in Eqs. (17,18). Before this can be done, however, we must first introduce the following change of variable: $\phi' \equiv \tilde{\phi}-\Omega\tau$. The angle ϕ' remains fixed as the rotor rotates, so the order of the time and space integrations in Eq. (41) can be interchanged. With the above substitution, G contains τ in the combination $\exp[i(\omega-m\Omega)\tau]$, so, carrying out the τ integration, we identify

$$\int_{-\infty}^{+\infty} \Delta p(\underset{\sim}{y}',\tau)\exp[i(\omega-m\Omega)\tau]d\tau = \Delta\bar{p}(\underset{\sim}{y}',\omega-m\Omega) \quad . \quad (42)$$

Because t appears in Eq. (37) only as the factor $\exp(-i\omega t)$, the ω integration is effectively an inverse Fourier transform. Thus,

$$\bar{p}(\underset{\sim}{x},\omega) = \sum_m \sum_n \psi_m(\kappa_{m,n}r)\exp(im\phi - i\gamma_{n,m}x_1)\cdot \tag{43}$$

$$\frac{1}{2i\Gamma k_{n,m}} \int_{S_m} \psi_m(\kappa_{m,n}r')\underset{\sim}{n}(\underset{\sim}{y})\cdot\nabla[\exp(-im\phi' + i\gamma_{n,m}y_1)]\Delta\bar{p}(\underset{\sim}{y},\omega-m\Omega)dS(\underset{\sim}{y})$$

Note that

$$\psi_m(\kappa_{m,n}r)\exp(im\phi - i\gamma_{n,m}x_1)$$

is a rotating pressure pattern of the type discussed previously.* Equation (43) is thus a normal mode expansion of the Fourier transform of the acoustic pressure within the duct:

$$\bar{p}_{mn}(\omega) \equiv \frac{1}{2i\Gamma k_{n,m}} \int_{S_m} \psi_m(\kappa_{m,n}r')$$

$$\underset{\sim}{n}(\underset{\sim}{y})\cdot\nabla[\exp(-im\phi' + i\gamma_{n,m}y_1)]\Delta\bar{p}(\underset{\sim}{y},\omega-m\Omega)ds(\underset{\sim}{y}) \quad , \tag{44}$$

and

$$\bar{p}(\underset{\sim}{x},\omega) = \sum_m \sum_n \bar{p}_{mn}(\omega)\psi_m(\kappa_{m,n}r)\exp(im\phi - i\gamma_{n,m}x_1) \quad . \tag{45}$$

*Except for the factor $\exp(-i\omega t)$.

In Eq. (44), the integration is to be carried out over all B rotor blades. To reduce the region of integration to one blade, arbitrarily select one blade as a reference blade. Assign this blade the number 0, and the remaining blades, in the direction of decreasing ϕ', the numbers 1 through (B-1). Let the pressure on the sth blade, s = 1, B-1, be $\Delta\bar{p}_s(\underset{\sim}{y}_0,\omega-m\Omega)$, where $\underset{\sim}{y}_0$ is the point (r',y_1,ϕ'). Then the corresponding point on blade s is $(r',y_1,\phi'-2\pi s/B$. The total contribution of all B blades is thus

$$\bar{p}_{mn}(\omega) = \frac{1}{2i\Gamma k_{n,m}} \int_{S_0} \psi_m(\kappa_{m,n}r')\cdot\underset{\sim}{n}(\underset{\sim}{y}_0)\cdot\nabla[\exp(-im\phi'+i\gamma_{n,m}y_1)]\cdot$$

$$\{\sum_s \Delta\bar{p}_s(\underset{\sim}{y}_0,\omega-m\Omega)\exp(i2\pi ms/B)\}\,dS(\underset{\sim}{y}_0). \qquad (46)$$

The normal vector on the reference rotor blade is $\underset{\sim}{n} = (0,-\sin\chi,-\cos\chi)$, so

$$\underset{\sim}{n}\cdot\nabla[\exp(-im\phi'+i\gamma_{n,m}y_1] = \left(\frac{im}{r'}\cos\chi - i\gamma_{n,m}\sin\chi\right)\exp(-im\phi'+i\gamma_{n,m}y_1)$$

To facilitate the integration over the blade surface, establish an intrinsic chordwise coordinate z', varying from z' = -b at the leading edge to z = +b at the trailing edge. Then, following the discussion of blade geometry in Chapter 1, coordinates y_1 and ϕ' are given by

$$y_1 = \delta_1' + z'\cos\chi'$$

$$\phi' = -(\delta_2'+z'\sin\chi)/r' \quad , \qquad (48)$$

where $\chi'(r')$ is the angle between the local blade chord and the axis of rotation, and (δ_1',δ_2') is the displacement

of the blade mid-chord line from a radial line drawn through the mid-chord of the blade at the hub. Using r' and z' as integration variables, Eq. (46) becomes

$$\bar{p}_{mn}(\omega) = \frac{1}{2\Gamma k_{n,m}} \int_{r_n}^{r_d} \psi_m(\kappa_{m,n} r') \left(\frac{m}{r'} \cos\chi' - \gamma_{n,m} \sin\chi'\right) \exp(i\gamma_{n,m}\delta_1' + \frac{m}{r'}\delta_2') \cdot$$

$$\int_{-b}^{+b} \left\{ \sum_{s=0}^{B-1} \Delta\bar{p}_s(r', z', \omega - m\Omega) \exp\left(\frac{i2\pi ms}{B}\right) \right\}$$

$$\exp[i(\gamma_{n,m}\cos\chi' + \frac{m}{r'}\sin\chi')z']dz'dr \quad . \tag{49}$$

The corresponding equation for the sound generated by the stator is obtained from Eq. (49) by changing B to V, and by setting $\Omega = 0$ and $\chi' = -\theta'$:

$$\bar{p}_{mn}(\omega) = \frac{1}{2\Gamma k_{n,m}} \int_{r_H}^{r_D} \psi_m(\kappa_{m,n} r') \left(\frac{m}{r'} \cos\theta' + \gamma_{n,m} \sin\theta'\right) \exp(i\gamma_{n,m}\delta_1' + \frac{m}{r'}\delta_2') \cdot$$

$$\int_{-b}^{+b} \left\{ \sum_{s=0}^{V-1} \Delta\bar{p}_s(r', z', \omega) \exp\frac{i2\pi ms}{V} \right\}$$

$$\exp[i(\gamma_{n,m}\cos\theta' - \frac{m}{r'}\sin\theta')z']dz'dr' \quad . \tag{50}$$

CHAPTER 4

ROTOR/STATOR CASCADE RESPONSE

The pressure distribution on the rotor or stator blades can be calculated by dividing the rotor or stator into a series of radial "slices," and calculating the pressure on each "slice" as though it were a linear cascade of thin flat plates. In this approximation, the radial variation of the inflow to the blades is ignored — an application of "strip-theory" to rotor aerodynamics.

The fluid velocity relative to the rotor blades (or stator vanes) is supposed to be a random or deterministic fluctuation $u(r,x_1,x_2,t)$ superimposed on a nominal flow $U_r(r)$, which is a function of the radius only. We are interested only in the fluctuating portion of the loading on the blades, which in the linear approximation is dependent only on the component of the velocity fluctuation that is normal to the blades, say $w(r,\underset{\sim}{x},t)$, where $\underset{\sim}{x} \equiv (x_1,x_2)$. This velocity component can be expressed as a sum of traveling waves:

$$w(r,\underset{\sim}{x},t) = \iiint \hat{\hat{w}}(r,\underset{\sim}{k},\omega)\exp[i(\underset{\sim}{k}\cdot\underset{\sim}{x}-\omega t)]\,\frac{d^2k}{(2\pi)^2}\,\frac{d\omega}{2\pi} \qquad (51)$$

where $d^2k \equiv dk_1dk_2$

In the coordinate system shown in Fig. 4, the mid-chord points of the rotor blades are located at the points $(0,sh)$, where s is any integer. The normal velocity that would exist if the blades were not present is found by substituting $\underset{\sim}{x} = z\underset{\sim}{c} + s\underset{\sim}{h}$ into Eq. (51), where $\underset{\sim}{c} = (\cos\chi,\sin\chi)$ is a unit vector directed along the blade chords, and $\underset{\sim}{h} = (0,h)$ is the vector separation between any two neighboring blades. The coordinate z is equal to -b at the blade leading edges and +b at the trailing edges. Thus the velocity that would exist if the blades were not present is

$$w(r,z\underset{\sim}{c}+s\underset{\sim}{h},t) = \exp(is\underset{\sim}{k}\cdot\underset{\sim}{h}) \iiint \hat{\hat{w}}(r,\underset{\sim}{k},\omega)\exp[i(\underset{\sim}{k}\cdot\underset{\sim}{c}z-\omega t)]\,\frac{d^2k}{(2\pi)^2}\,\frac{d\omega}{2\pi}\,. \qquad (52)$$

Because the blades are impermeable, they induce an additional velocity which negates the normal inflow velocity at the blades themselves. This induced velocity field has

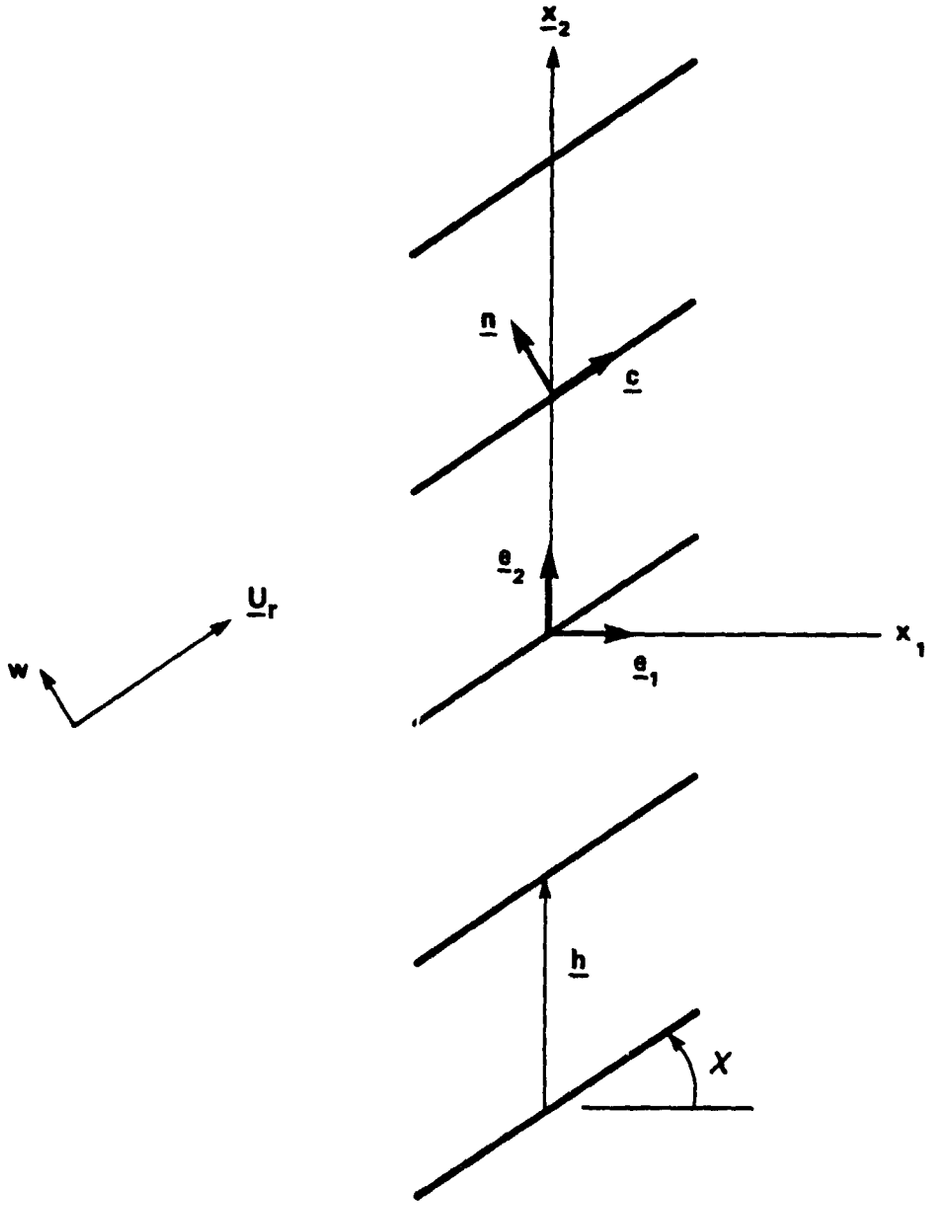

FIGURE 4. Cascade Geometry

associated with it a pressure distribution which is continuous except on the blades where a discontinuity, say $\Delta p_s(r,z,t)$, exists. The problem of calculating the chordwise pressure discontinuity (or pressure loading) on a cascade of blades exposed to the normal inflow velocity

$$\hat{\bar{w}}(r,\underset{\sim}{k},\omega)\ \exp[i\underset{\sim}{k}\cdot(\underset{\sim}{c}z+s\underset{\sim}{h})-i\omega t]$$

can be reduced to the solution of an integral equation of the following form:

$$\rho_0 U_r\ \hat{\bar{w}}(r,\underset{\sim}{k},\omega)\exp[i\underset{\sim}{k}\cdot(\underset{\sim}{c}z+s\underset{\sim}{h})] = \int_{-b}^{+b} K_c(z-y)\ \Delta\bar{p}_s(r,y)\ \frac{dy}{b}\ . \tag{53}$$

The kernel function K_c is derived in Appendix B. For our purpcses, it is convenient to normalize Eq. (53) by dividing both sides by $\rho_0 U_r \hat{\bar{w}}(r,\underset{\sim}{k},\omega)\exp(is\underset{\sim}{k}\cdot\underset{\sim}{h})$:

$$\exp(i\underset{\sim}{k}\cdot\underset{\sim}{c}z) = \int_{-b}^{+b} K_c(z-y)\left\{\frac{\Delta\bar{p}_s(r,y)\ \exp(-is\underset{\sim}{k}\cdot\underset{\sim}{h})}{\rho_0 U_r \hat{\bar{w}}(r,\underset{\sim}{k},\omega)}\right\}\frac{dy}{b}\ . \tag{54}$$

By assumption (see Appendix B) the quantity in braces is independent of s; we denote it by $f(r,z,\underset{\sim}{k},\omega)$. The solution of Eq. (54) for $f(r,z,\underset{\sim}{k},\omega)$ is obtained numerically. The chordwise pressure distribution is then

$$\Delta\bar{p}_s(r,z,\underset{\sim}{k},\omega) = \rho_0 U_r\ \hat{\bar{w}}(r,\underset{\sim}{k},\omega)f(r,z,\underset{\sim}{k},\omega)\exp(is\underset{\sim}{k}\cdot\underset{\sim}{h})\ . \tag{55}$$

Because the problem is assumed to be linear, the pressure loading due to an arbitrary normal inflow velocity [as in Eq. (51)] can be obtained by multiplying Eq. (55) by $\exp(-i\omega t)$ and integrating over ω, k_1, and k_2. Thus,

$$\Delta p_s(r,z,t) = \rho_0 U_r \iiint \hat{\bar{w}}(r,\underset{\sim}{k},\omega)f(r,z,\underset{\sim}{k},\omega)\cdot\exp(-i\omega t+is\underset{\sim}{k}\cdot\underset{\sim}{h})\ \frac{d\omega}{2\pi}\ \frac{d^2k}{(2\pi)^2} \tag{56}$$

Given the complex wavenumber-frequency spectrum $\hat{\hat{w}}(r,k,\omega)$, Eq. (56) allows us to calculate the pressure loading on each blade as a function of position (r,z) and time t. Where the Fourier transform (in time) of Δp_s is required, it is given by

$$\Delta\bar{p}_s(r,z,\omega) = \rho_0 U_r \iint \hat{\hat{w}}(r,\underset{\sim}{k},\omega) f(r,z,\underset{\sim}{k},\omega)\cdot\exp(is\underset{\sim}{k}\cdot\underset{\sim}{h})\,\frac{d^2k}{(2\pi)^2} \quad . \tag{57}$$

For future reference, it is worthwhile to note here that $\hat{\hat{w}}(r,\underset{\sim}{k},\omega)$ is the triple Fourier transform of the inflow to the rotor or stator, calculated in a coordinate system fixed to the rotor or stator, as the case may be. That is,

$$\hat{\hat{w}}(r,\underset{\sim}{k},\omega) \equiv \iiint w(r,\underset{\sim}{x},t)\exp(i\omega t - i\underset{\sim}{k}\cdot\underset{\sim}{x})\,d^2x\,dt \quad . \tag{58}$$

Because the inflow is necessarily periodic in x_2, $w(r,\underset{\sim}{x},t)$ can also be written as a Fourier series:

$$w(r,\underset{\sim}{x},t) = \sum_n w_n(r,x_1,t)\exp\left[i\left(\frac{nx_2}{r}\right)\right] \quad , \tag{59}$$

where

$$w_n(r,x_1,t) \equiv \frac{1}{2\pi r}\int_{-\pi r}^{+\pi r} w(r,\underset{\sim}{x},t)\exp\left[-i\left(\frac{nx_2}{r}\right)\right]dx_2 \quad . \tag{60}$$

If Eq. (59) is substituted into Eq. (58), we obtain

$$\hat{\hat{w}}(r,\underset{\sim}{k},\omega) = 2\pi \sum_n \hat{\hat{w}}_n(r,k_1,\omega)\ \delta\left(k_2 - \frac{n}{r}\right)$$

and, in turn,

$$\Delta\bar{p}_s(r,z,\omega) = \rho_0 U_r \sum_n \exp(isnh/r) \int \hat{\bar{w}}_n(r,k_1,\omega)$$

$$f[r,z,k_1,(n/r),\omega] \frac{dk_1}{2\pi} \quad . \tag{61}$$

This expression for the pressure on blade s is convenient for calculating the duct modes excited by the rotor mean velocity deficit wakes, because it displays clearly the periodic nature of the rotor wake.

CHAPTER 5

MEAN ROTOR WAKE

5.1 Rotor/Wake Model

In this section, we derive an expression for the complex amplitudes of the duct modes excited by the interaction of the rotor blade wakes with the stator vanes. We are concerned here only with the mean value (time average) of the rotor wakes, which, being periodic, generate sound at harmonics of the blade passage rate, ΩB. Broadband noise generated by the turbulence contained within the rotor blade wakes is dealt with in Chapter 6.

Consider an imaginary cylinder of radius r, centered on the duct axis of symmetry. The intersection of this surface with the rotor and stator is depicted in Fig. 5. In this figure, two sets of coordinate axes are shown; axes (X_1,X_2) are fixed in the rotor, while axes (x_1,x_2) are fixed in the stator. The relation between them is

$$\underset{\sim}{X} = \underset{\sim}{x} + \underset{\sim}{D} + \Omega rt\underset{\sim}{e}_2 \quad , \tag{62}$$

where $\underset{\sim}{e}_2$ is a unit vector in the azimuthal direction and $\underset{\sim}{D} = \underset{\sim}{D}(\tilde{r})$ is the vector distance from a rotor blade to a stator vane, both selected arbitrarily. $\underset{\sim}{D}$ is defined only to within an additive vector $r\phi\underset{\sim}{e}_2$, where ϕ represents an arbitrary angle of rotation of the rotor.

So as to arrive at a reasonably simple model of the rotor wake, which will be valid in the vicinity of the stator vanes, it is convenient to introduce two plausible assumptions. They are

1. no radial flow occurs, and
2. pressure gradients and turbulent or viscous diffusion can be neglected over the chord of the stator.

The fluid velocity then has only two components, $(0,W_1,W_2)$ in (r,X_1,X_2) coordinates, and the equations of motion of the fluid reduce to

$$(\underset{\sim}{W}\cdot\nabla)\underset{\sim}{W} = 0 \tag{63}$$

$$\nabla \cdot (\rho_0\underset{\sim}{W}) = 0 \quad . \tag{64}$$

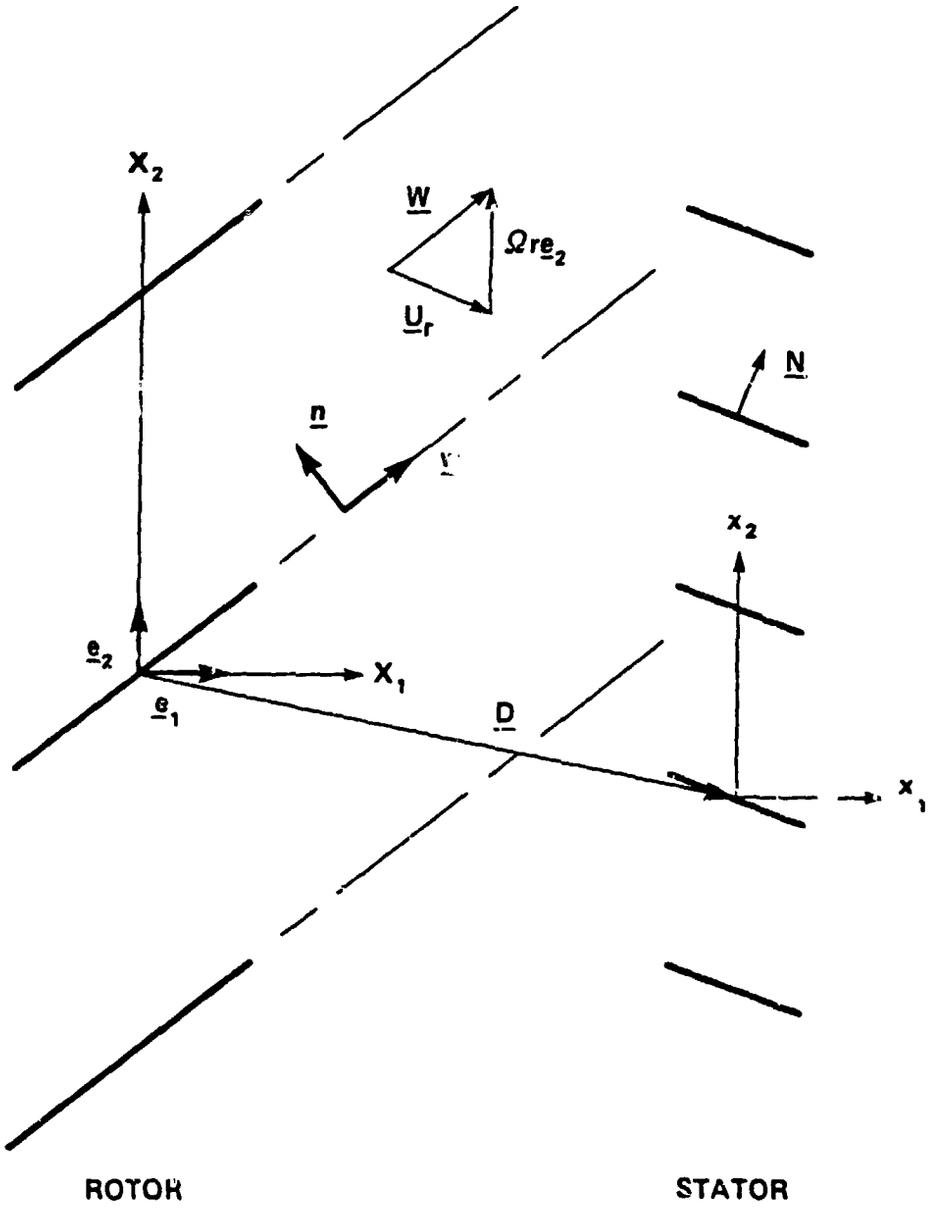

Figure 5. Rotor/Stator Geometry for Mean Wake Analysis

A parallel flow of the form

$$\underset{\sim}{W} = W(\underset{\sim}{X}\cdot\underset{\sim}{n})\underset{\sim}{w} \quad , \tag{65}$$

where $\underset{\sim}{w}$ and $\underset{\sim}{n}$ are constant orthogonal unit vectors (see Fig. 5) is a solution to these equations, and is the form we will assume for the wake. The velocity is everywhere parallel to the unit vector $\underset{\sim}{w} = (\cos\chi,\sin\chi)$, and is constant in magnitude on the lines $\underset{\sim}{X}\cdot\underset{\sim}{n}$ = constant. The variation of the magnitude across the wakes is determined by the as-yet-unspecified function $W(\underset{\sim}{X}\cdot\underset{\sim}{n})$.

$W(\underset{\sim}{X}\cdot\underset{\sim}{n})$ is periodic, because all the wakes are assumed to be identical, the period being the normal distance between wake centerlines, $h\cos\chi$. $W(\underset{\sim}{X}\cdot\underset{\sim}{n})$ can therefore be written as a Fourier series, i.e.,

$$W(\underset{\sim}{X}\cdot\underset{\sim}{n}) = \sum_q W_q \exp\left(\frac{iqB}{r\cos\chi}\,\underset{\sim}{X}\cdot\underset{\sim}{n}\right) , \tag{66}$$

where we have substituted $2\pi r/B$ for h, the gap between rotor blades, measured azimuthally. The unit vector $\underset{\sim}{n}$ has components $(-\sin\chi,\cos\chi)$, so the Fourier series may also be cast in the following form,

$$W = \sum_q W_q \exp\left[\frac{iqB}{r}\,(X_2 - X_1\tan\chi)\right] \quad , \tag{67}$$

which indicates that the rotor wake velocity is periodic in the azimuthal direction also (as opposed to the direction normal to the wakes). The azimuthal period is, of course, $2\pi r/B$.

In principle, the Fourier coefficients W_q of the wake flow could be determined experimentally by processing a sufficient number of flow measurements collected from a transducer mounted behind the rotor, and if only the first few harmonics of the blade passage frequency are of interest (it will transpire that the qth harmonic in the wake flow interacts with the stator to generate sound in the qth harmonic of the blade passage

frequency), this is a feasible proposition. However, by assuming an explicit (and plausible) form for the wake velocity profile, it is possible to characterize the wake velocity profile by only two independent attributes of the flow, as, for example, the mean wake velocity and the root-mean-square deviation from the mean velocity, or the mean velocity and the velocity deficit on the centerlines of the wakes. To do this, we express the wake velocity deficit as a series of "haystack" functions, all of the same form but displaced from one another by the gap between the rotor blades, $h = 2\pi r/B$. That is, momentarily setting $X_1 = 0$, we write

$$w(X_2) = A\left[1 - \varepsilon \sum_m f(X_2 - 2\pi rm/B)\right] , \tag{68}$$

where the constants A and ε are yet to be evaluated, and the function $f(X_2)$ is a function such as

$$f(X_2) = \exp\left[-(X_2/\delta)^2 \ln 2\right] . \tag{69}$$

or any similar function which has the value 1 when $X_2 = 0$, and which decreases monotonically to 0 as $X_2 \to \infty$. In Eq. (69), δ is the half-velocity width of the mean wake, that is

$$f(\delta) = 1/2 . \tag{70}$$

If Eq. (68) above is written as a Fourier series, we find that the Fourier coefficients are proportional to the Fourier transform of $f(X_2)$, i.e.,

$$W_q = -\frac{\varepsilon AB}{2\pi r} \hat{f}\left(\frac{qB}{r}\right) , \quad q \neq 0 . \tag{71}$$

The zeroth-order Fourier coefficient need not be calculated because, as with any Fourier series, it is equal to the mean value of the wake velocity, $\bar{W}$. The constant εA can be evaluated either of two ways; one is to compute the root-mean-square value of the deviation of the wake velocity from its mean value,

$$\left\{\frac{B}{2\pi r}\int_0^{2\pi r/B}[W(X_2)-\bar{W}]^2dx\right\}^{\frac{1}{2}} = \left\{\sum_{q\neq 0}|W_q|^2\right\}^{\frac{1}{2}}$$

$$= \frac{\varepsilon AB}{2\pi r}\left\{\sum_{q\neq 0}|\hat{f}(\frac{qB}{r})|^2\right\}^{1/2}.$$

Denote by S_2 the sum

$$\left\{\sum_{q\neq 0}|\hat{f}(\frac{qB}{r})|^2\right\}^{1/2} \tag{71}$$

and by $(\Delta W)_{rms}$ the square root of the average of the square of the deviation of the wake velocity from its mean value. Then, the Fourier coefficients of the wake velocity have the following values:

$$\begin{aligned} W_0 &= \bar{W} \\ W_q &= -\frac{(\Delta W)_{rms}}{S_2}\hat{f}(\frac{qB}{r}) \quad , q \neq 0 \end{aligned} \tag{72}$$

and the velocity in the wake at any point (X_1,X_2) is

$$W(\underset{\sim}{X}) =$$

$$\bar{W} - \frac{(\Delta W)_{rms}}{S_2}\sum_{q\neq 0}\hat{f}(\frac{qB}{r})\exp\left[\frac{iqB}{r}(X_2-X_1\tan\chi)\right] . \tag{73}$$

An alternative scheme is to define εA in terms of the mean velocity $\bar{W}$ and the velocity at the wake centerlines, say W_c. Then, we find

$$W(\underset{\sim}{X}) =$$

$$\bar{W} + \frac{(W_c-\bar{W})}{S_1}\sum_{q\neq 0}\hat{f}(\frac{qB}{r})\exp\left[\frac{iqB}{r}(X_2-X_1\tan\chi)\right] \tag{74}$$

where

$$S_1 \equiv \sum_{q\neq 0} \hat{f}\left(\frac{qB}{r}\right) \quad . \tag{75}$$

For the Gaussian profile of Eq. (69), whose Fourier transform is

$$\hat{f}(\alpha) = \delta \sqrt{\pi/\ln 2}\, \exp[-(\alpha\delta)^2/4 \ln 2] \tag{76}$$

the sums S_1 and S_2 are defined as follows:

$$S_1 = 2\delta\sqrt{\pi/\ln 2} \sum_{m=1}^{\infty} \exp[-(mB\delta/r)^2/4 \ln 2] \tag{77}$$

$$S_2 = \delta\left\{\frac{2\pi}{\ln 2} \sum_{m=1}^{\infty} \exp[-(mB\delta/r)^2/2 \ln 2]\right\}^{1/2} \quad . \tag{78}$$

5.2 Duct Modes Generated by Mean Wake/Stator Interaction

To calculate the duct modes excited by the interaction of the stator vanes with the mean rotor wake, we have first to calculate the loading on the stator vanes themselves. To do this, calculate the wake velocity relative to the stator vanes,

$$\underset{\sim}{U}_r = \underset{\sim}{W} - \Omega r \underset{\sim}{e}_2 \quad , \tag{79}$$

find the component of this velocity that is normal to the vanes,

$$w = \underset{\sim}{U}_r \cdot \underset{\sim}{N} \quad , \tag{80}$$

and substitute into this expression the coordinate transformation given in Eq. (62). To calculate the normal velocity on any specific vane, say vane s, substitute for $\underset{\sim}{x}$,

$$\underset{\sim}{x} = z\underset{\sim}{c} + s\underset{\sim}{H} \quad , \tag{81}$$

where again z is a chordwise variable, equal to -b at the vane leading edges, and +b at the trailing edges. The result of these several steps is

$$w = \sum_q w_q \exp\left(ik_q z + \frac{2\pi sqB}{V} - iqB\Omega t\right), \tag{82}$$

where

$$w_q = W_q \sin(\theta+\chi) \exp\left[-\frac{iqB}{r}(D_2 - D_1 \tan\chi)\right] \tag{83}$$

and

$$k_q = \frac{qB}{r}(\sin\theta + \cos\theta\tan\chi) \quad . \tag{84}$$

In these equations, $\underset{\sim}{D}$ and $\underset{\sim}{U}_r$ are both functions of the radius r.

The vane pressure loading generated by this normal inflow velocity is obtained numerically by solving an integral equation just as discussed in Chap. 4. Specifically, let $f_q(r,z)$ be the solution of the following equation:

$$\exp(ik_q z) = \int_{-b}^{+b} K_c(z-y)\, f_q(r,z)\frac{dy}{b} \quad , \tag{85}$$

where K_c is the cascade kernel function derived in Appendix B. The parameters needed to calculate K_c for this situation are listed below:

Frequency: $\omega = qB\Omega$

Chordwise wavenumber: $k_q = \frac{qB}{r}(\sin\theta + \tan\chi\cos\theta)$

Inter-blade phase angle: $\sigma = 2\pi qB/V$ (See Appendix B)

Inter-blade gap: $h = 2\pi r/V$

Stagger angle: $-\theta$

Given the elemental stator vane loading function $f_q(r,z)$, the pressure loading on stator vane s is

$$\Delta p_s = \rho_0 U_r\, w_q\, f_q(r,z)\, \exp(i2\pi sqB/V) \quad . \tag{86}$$

This is the qth harmonic of the pressure on vane s. To calculate the (m,n)th duct mode generated by this vane pressure, multiply both sides of Eq. (86) by $\exp(-iqB\Omega t)$, calculate the Fourier transform, substitute this into Eq. (50), and invert back into the time domain. The sum over vane number in Eq. (50) can be evaluated explicitly:

$$\sum_{s=0}^{V-1} \exp\left\{\frac{i2\pi s}{V}\,(m+qB)\right\}$$

$$= V \text{ if } m + qB = pV$$

$$= 0 \text{ otherwise,}$$

where p is any integer. The final result is

$$p_{mnq} = \frac{\rho_0 U_r V}{2\pi k_{m,n,q}} \int_{r_H}^{r_D} \psi_m(\kappa_{m,n} r)\; w_q(r)$$

$$\left(\frac{m}{r}\cos\theta + \gamma_{n,m,q}\sin\theta\right) \exp\left(i\gamma_{n,m,q}\delta_1 + \frac{m}{r}\delta_2\right) \tag{87}$$

$$\cdot \int_{-b}^{+b} f_q(r,z)\, \exp[i(\gamma_{n,m,q}\cos\theta - \frac{m}{r}\sin\theta)z]\, dz dr \quad ,$$

where

$$k_{n,m,q} \equiv \sqrt{\left(\frac{qB\Omega}{c_0}\right)^2 - \beta_r^2 \kappa_{m,n}^2} \tag{88}$$

$$\gamma_{n,m,q} \equiv \frac{1}{\beta_r^2}\left(\frac{MqB\Omega}{c_0} \pm k_{n,m,q}\right) \quad . \tag{89}$$

The quantity $p_{m,n,q}$ is the complex amplitude of the (m,n)th mode at the qth harmonic of the blade passage frequency. As is evident from Eq. (87) above, $p_{m,n,q}$ is proportional to w_q, the qth-order Fourier coefficient of the mean rotor wake. In its present form, the computer code computes these coefficients from Eq. (74), which assumes a Gaussian profile for the individual rotor wakes, and which relates each harmonic in the Fourier series to the mean wake velocity and the velocity at the centerlines of the wakes. As mentioned previously, however, the code can easily be modified to accept the Fourier coefficients of the wake velocity as inputs, and compute the duct modes directly from them.

5.3 Sound Power

The flux of sound power in the duct is found by substituting Eq. (87) into Eq. (28). The result is given below:

$$\overline{\text{Power}} =$$

$$\frac{\pi(r_D^2 - r_H^2)}{\rho_0 U} \sum_p \sum_n \sum_q G_{mn}(qB\Omega)\left|P_{mnq}\right|^2$$

where $G(qB\Omega)$ is the quantity in braces in Eq. (29), but with the integer s replaced by q. In the equation above, the index m is related to the summation indices p and q through the equation $m=pV-qB$. Finally, if the sound power flux at one specific harmonic of the blade passage frequency is desired, the summation over q is deleted, and q is set equal to the desired harmonic number.

CHAPTER 6

INLET TURBULENCE

6.1 Inlet Turbulence Velocity Correlation Function

Figure 6 shows a cylindrical slice of the rotor which has been opened out to form a linear cascade. Axes (x_1,x_2) are fixed in the duct, while axes (X_1,X_2) move with the rotor blades. The equation relating the two sets of axes is

$$\underset{\sim}{X} = \underset{\sim}{x} + \Omega r t \underset{\sim}{e}_2 \quad . \tag{90}$$

The nominal inflow velocity is assumed to be purely axial, so it can be written as $\underset{\sim}{U} = U\underset{\sim}{e}_1$, where $\underset{\sim}{e}_1$ is a unit vector along the x_1 and X_1 axes.

Let w be the component of the inflow turbulence which is normal to the rotor blades. We assume that this turbulence is convected with the mean flow $\underset{\sim}{U}$, i.e., a sample velocity field expressed in duct-fixed coordinates would be

$$w(r,\underset{\sim}{x}-\underset{\sim}{U}t) \quad .$$

Many such samples are recorded and averaged to form the inflow velocity correlation function:

$$\langle w(r_1,\underset{\sim}{x}-\underset{\sim}{U}t)\ w(r_2,\underset{\sim}{y}-\underset{\sim}{U}\tau)\rangle = \varepsilon_D^2 U^2 \Phi_D(r_1,r_2,\underset{\sim}{x}-\underset{\sim}{U}t,\underset{\sim}{y}-\underset{\sim}{U}\tau). \tag{91}$$

If we assume that the inflow turbulence is homogeneous at any radius r, and stationary in time, then Φ_D does not depend on $\underset{\sim}{x}-\underset{\sim}{U}t$ and $\underset{\sim}{y}-\underset{\sim}{U}\tau$ separately, but only on their difference $\underset{\sim}{x}-\underset{\sim}{y}-\underset{\sim}{U}(t-\tau)$; we can write Φ_D as follows:

$$\Phi_D = \Phi_D(\underset{\sim}{x}-\underset{\sim}{y}-\underset{\sim}{U}(t-\tau),r,\Delta r) \quad , \tag{92}$$

where

$$r = \frac{1}{2}(r_1+r_2)$$
$$\Delta r = r_1 - r_2 \quad . \tag{93}$$

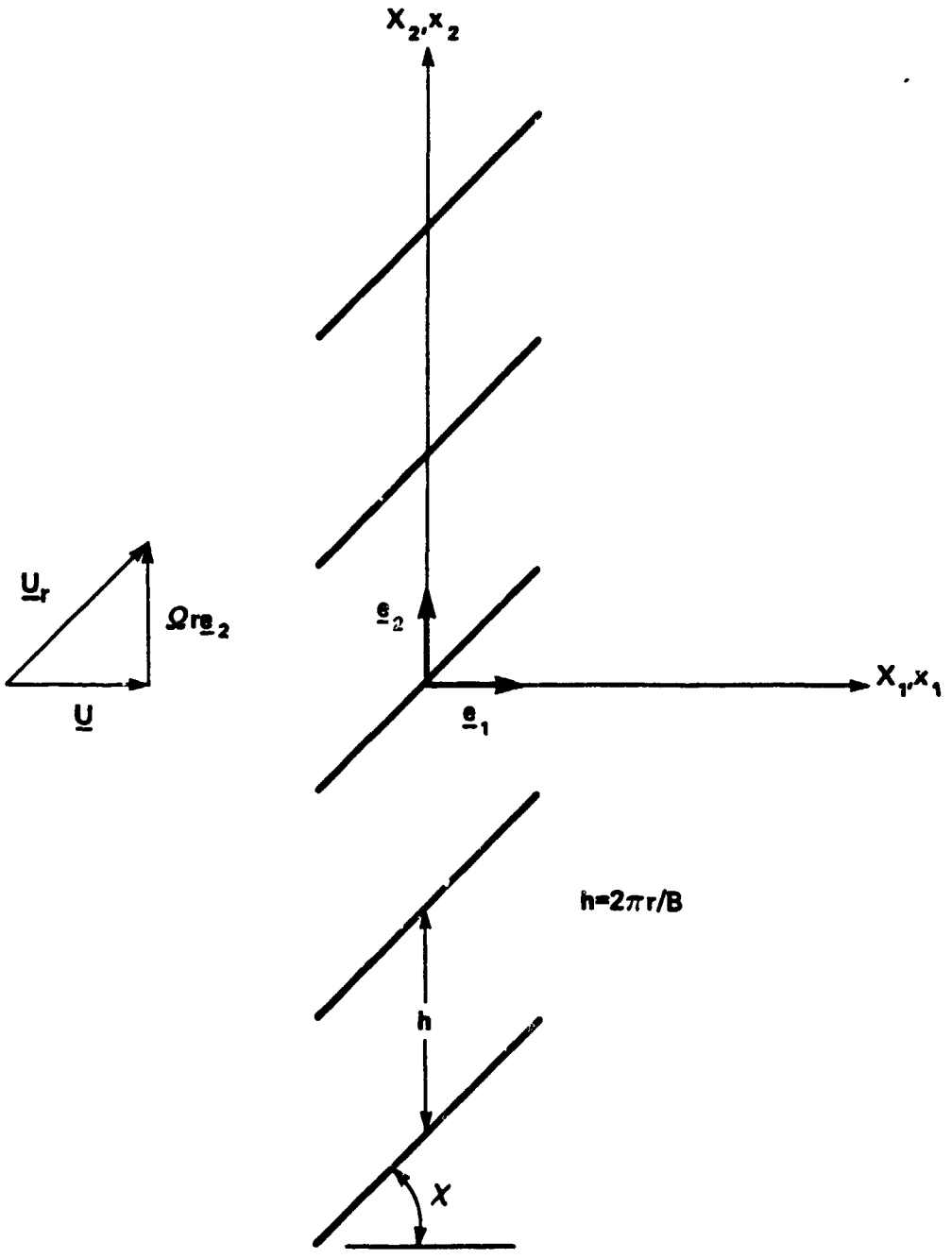

Figure 6. Rotor with Fixed and Moving Coordinate Systems

The mean-square turbulence intensity is obtained by setting $\underset{\sim}{x} = \underset{\sim}{y}$ and $t = \tau$. If Φ_D is normalized so that $\Phi_D(\underset{\sim}{0},r,0) = 1$, then ε_D is the root mean-square turbulence intensity expressed as a fraction of the nominal flow velocity in the duct:

$$\varepsilon_D = \frac{\sqrt{\overline{<w^2>}}}{U} \quad . \tag{94}$$

6.2 Wavenumber-Frequency Spectrum in Rotor-Fixed Coordinates

In order to calculate the power spectral density of the sound generated by the interaction of inlet turbulence with the moving rotor blades, we must calculate the expected value of the inflow wavenumber-frequency spectrum in rotor-fixed coordinates:

$$<\hat{\hat{w}}(r_1,\underset{\sim}{k},\omega)\ \hat{\hat{w}}^*(r_2,\underset{\sim}{K},\nu)> \equiv$$

$$\int\int\int\int\int\int <w(r_1,\underset{\sim}{x}-\underset{\sim}{U}t)\ w(r_2,\underset{\sim}{y}-\underset{\sim}{U}\tau)>$$

$$\exp(i\omega t - i\nu\tau - i\underset{\sim}{k}\cdot\underset{\sim}{X} + i\underset{\sim}{K}\cdot\underset{\sim}{Y})\ d^2X\ d^2Y\ d\tau dt \quad . \tag{95}$$

The expected value of the inlet turbulence is given in Eq. (91). If we substitute this expression into the equation given above and introduce new integration variables $\underset{\sim}{x}$ and $\underset{\sim}{y}$, where

$$\underset{\sim}{X} = \underset{\sim}{x} + \Omega r t \underset{\sim}{e}_2$$

$$\underset{\sim}{Y} = \underset{\sim}{y} + \Omega r \tau \underset{\sim}{e}_2 \quad , \tag{96}$$

then we obtain the following integral:

$$\langle \hat{\hat{w}}(r_1,\underset{\sim}{k},\omega)\ \hat{\hat{w}}(r_2,\underset{\sim}{K},\nu)\rangle =$$

$$\varepsilon_D^2 U^2 \iiiint\!\!\iiint \Phi(\underset{\sim}{x}-\underset{\sim}{y}-\underset{\sim}{U}\tau)$$

$$\exp\{i(\omega-\Omega r k_2)\ t - i(\nu-\Omega r K_2)\tau$$

$$- i\underset{\sim}{k}\cdot\underset{\sim}{x} + i\underset{\sim}{K}\cdot\underset{\sim}{y}\}\ d^2x\ d^2y\ d\tau dt \quad . \tag{97}$$

Now substitute $\xi = \underset{\sim}{x} - \underset{\sim}{y} - \underset{\sim}{U}(t-\tau)$ for x, and integrate with respect to t, τ, and $\underset{\sim}{y}$, recalling the following integral expression for the delta function:

$$\int \exp(i\alpha x)\ dx = 2\pi\ \delta(\alpha) \quad . \tag{98}$$

The result is,

$$\langle \hat{\hat{w}}(r_1,\underset{\sim}{k},\omega)\ \hat{\hat{w}}(r_2,\underset{\sim}{K},\nu)\rangle =$$

$$(2\pi)^4 \varepsilon_D^2 U^2\ \delta(\omega-\Omega r k_2-\underset{\sim}{U}\cdot\underset{\sim}{k})$$

$$\cdot\ \delta(\nu-\Omega r K_2-\underset{\sim}{U}\cdot\underset{\sim}{k})\ \delta(\underset{\sim}{K}-\underset{\sim}{k})\ \hat{\hat{\Phi}}_D(\underset{\sim}{k},r,\Delta r) \ , \tag{99}$$

where $\hat{\hat{\Phi}}_D(\underset{\sim}{k},r,\Delta r)$ is the double Fourier transform of the turbulence velocity correlation function:

$$\hat{\hat{\Phi}}_D(\underset{\sim}{k},r,\Delta r) \equiv \iint \Phi_D(\underset{\sim}{x},r,\Delta r)\ \cdot$$

$$\exp(-i\underset{\sim}{k}\cdot\underset{\sim}{y})\ d^2y \quad . \tag{100}$$

Because the inlet duct is annular, the turbulence velocity correlation function is a periodic function, the period being $2\pi r e_2$. Φ_D can be written as a Fourier Series, i.e.,

$$\Phi_D(\underset{\sim}{x},r,\Delta r) = \sum_m \Phi_m(x_1,r,\Delta r)\ \exp\ (imx_2/r) \tag{101}$$

where

$$\Phi_m(x_1,r,\Delta r) \equiv \frac{1}{2\pi r} \int_{-\pi r}^{+\pi r} \Phi_D(\underset{\sim}{x},r,\Delta r) \tag{102}$$

$$\cdot\ \exp(-imx_2/r)dx_2 \ .$$

Now let the nonperiodic function $\phi(\underset{\sim}{x},r,\Delta r)$ be defined as follows:

$$\phi(\underset{\sim}{x},r,\Delta r) = \Phi_D(\underset{\sim}{x},r,\Delta r) \quad \text{if } |x_2|<\pi r, \tag{103}$$

$$= 0 \quad \text{otherwise}$$

Then the Fourier coefficients of Φ_D [Eq. (102)] can be written as the Fourier transform of ϕ:

$$\phi_m(x_1,r,\Delta r) = \frac{1}{2\pi r}\hat{\phi}(x_1,m/r,r,\Delta r) \tag{104}$$

where

$$\hat{\phi}(\underset{\sim}{x}_1,m/r,r,\Delta r) = \int \phi(\underset{\sim}{x},r,\Delta r)\, \exp(-imx_2/r)\, dx_2. \tag{105}$$

The double Fourier transform of Φ_D is then

$$\hat{\hat{\Phi}}_D(\underset{\sim}{k},r,\, r) = \frac{1}{r}\sum_s \hat{\hat{\phi}}(k_1,s/r,r,\Delta r)\, \delta(k_2-s/r) \tag{106}$$

Equation (99), the expected value of the complex wavenumber-frequency spectrum, contains five delta functions. [Note that $\delta(\underset{\sim}{k}-\underset{\sim}{K})$ is a short-hand notation for the product of two delta functions: $\delta(k_1-K_1)\,\delta(k_2-K_2)$.] The five delta functions in Eq. (99) can be rewritten in the following exactly equivalent form:

$$\delta(\omega-s\Omega-\underset{\sim}{k}\cdot\underset{\sim}{U})\,\delta(\nu-\omega)\cdot$$

$$\cdot\,\delta(\underset{\sim}{k}-\underset{\sim}{K})\,\delta(k_2-s/r)\ .$$

The final expression for the complex wavenumber-frequency spectrum is as follows:

$$\langle\hat{\hat{w}}(r_1,\underset{\sim}{k},\omega)\,\hat{\hat{w}}^*(r_2,\underset{\sim}{K},\nu)\rangle =$$

$$\frac{\epsilon_D^2U^2(2\pi)^4}{r}\,\delta(\nu-\omega)$$

$$\delta(\underset{\sim}{k}-\underset{\sim}{K})\sum_s \delta(k_2-s/r)\,\hat{\phi}(k_1,s/r,r,\Delta r)\,\delta(\omega-s\Omega-\underset{\sim}{U}\cdot\underset{\sim}{k}) \tag{107}$$

6.3 Inflow Velocity Spectral Density in Fixed And Rotating Reference Frames*

Equation (107), which has been cast in the form most convenient for calculating the power spectrum of the sound

*This section is adapted from Ref. 1, pages 37-47.

radiated by the rotating rotor blades, does not itself have an obvious physical interpretation. It is worthwhile, therefore, to calculate the spectral density of the inflow turbulence as "seen" by both fixed and rotating sensors. Comparing the two spectra provides some insight into the effects of rotation.

The mean-square velocity of the inlet turbulence can be calculated by setting $r_1 = r_2 = r$ in Eq. (107), multiplying it by $(2\pi)^{-5} \exp[i(\nu-\omega)t+i(\underset{\sim}{k}-\underset{\sim}{K})\cdot\underset{\sim}{x}]$ and integrating over all values of ν, $\underset{\sim}{k}$, and $\underset{\sim}{K}$:

$$\langle w^2(\underset{\sim}{x},t)\rangle =$$

$$= \iiiiint \langle \hat{\hat{\underset{\sim}{w}}}(r,\underset{\sim}{k},\omega)\ \hat{\hat{\underset{\sim}{w}}}^*(r,\underset{\sim}{K},\nu)\rangle \cdot \tag{108}$$

$$\exp[i(\nu-\omega)t+i(\underset{\sim}{k}-\underset{\sim}{K})\cdot x]\ \frac{d^2K\ d^2k\ d\nu}{(2\pi)^5}$$

The result is,

$$\langle w^2\rangle =$$

$$\frac{\varepsilon_D^2 U}{r} \sum_m \int \hat{\hat{\phi}}\left(\frac{\omega - m\Omega}{U}\ ,\ \frac{m}{r}\ ,\ 0,0\right) \frac{d\omega}{2\pi} \quad . \tag{109}$$

The velocity spectral density (per Hertz) is the integrand:

$$S_D(\omega) = \frac{\varepsilon_D^2 U}{r} \sum_m \hat{\hat{\phi}}\left(\frac{\omega - m\Omega}{U}\ ,\ \frac{m}{r}\ ,\ 0,0\right) \quad . \tag{110}$$

If we set $\Omega = 0$, we obtain the corresponding velocity spectral density in nonrotating coordinates:

$$S_D(\omega) = \frac{\varepsilon_D^2 U}{r} \sum_m \hat{\hat{\phi}}\left(\frac{\omega}{U}\ ,\ \frac{m}{r},\ 0,0\right) \quad . \tag{111}$$

At this point, it is necessary to introduce the integral scales of the turbulence. One such scale exists for each

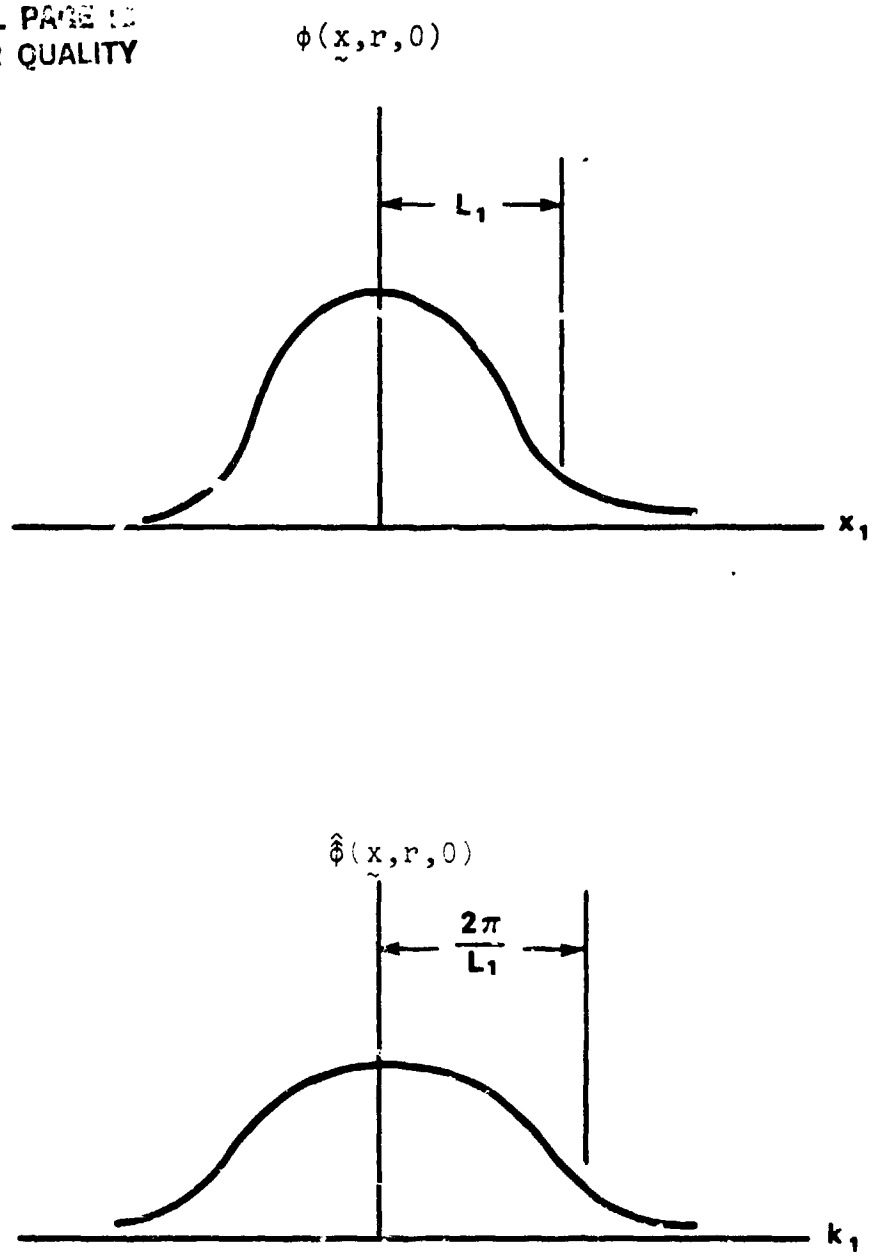

FIGURE 7. Velocity Correlation Function and its Fourier Transform (Adapted from Figs. 9 and 11 of Ref. 1)

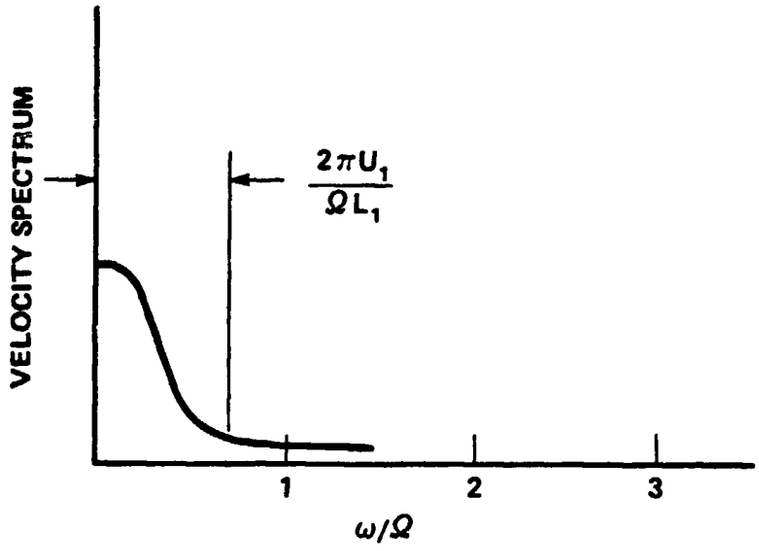

a) Fixed coordinates

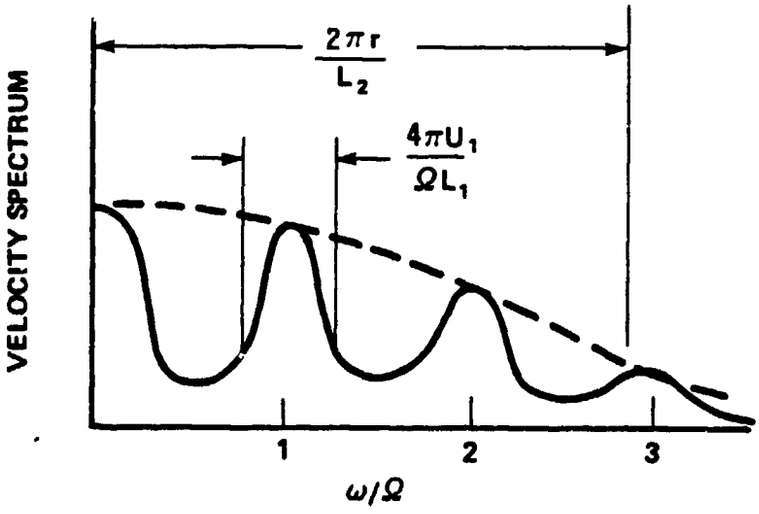

b) Moving Coordinates

FIGURE 8. Velocity Spectrum in Fixed and Rotating Coordinates (Adapted from Figs. 12 and 13 of Ref. 1)

of the three coordinate axes, but we need now consider only the axial and circumferential scales. They are defined as follows:

$$\int \phi(x_1,0,0,0)\, dx_1 \equiv L_1$$

$$\int \phi(0,x_2,0,0)\, dx_2 \equiv L_2 \quad .$$

The velocity correlation function $\phi(\underset{\sim}{x},r,0)$ is plotted as a function of the axial coordinate x_1 in the upper curve of Fig. 7 . A plot of $\phi(\underset{\sim}{x},r,0)$ vs x_2 would be qualitatively similar. Note that ϕ becomes very small when x_1 exceeds the axial integral scale L_1. The Fourier transform of ϕ is plotted in the lower part of Fig. 7 , where we see that the transform of the correlation function is small when k_1 exceeds $2\pi/L_1$. Similar behavior is demonstrated by the correlation function and its transform when plotted vs x_2 and k_2. In Eq. (111), the terms

$$\hat{\phi}\left(\frac{\omega}{U},\ \frac{m}{r},\ r,0\right)$$

are small when either $\omega/U > 2\pi/L_1$ or $m/r > 2\pi/L_2$. Considered as a function of ω, each term in the sum is similar in form, but of course becomes smaller as m/r increases. The result is a spectrum similar to the one shown in Fig. 8 . The spectrum decays monotonically as ω increases. The bandwidth of the spectrum is roughly $\omega_b = 2\pi U/L_1$. When this is expressed as a fraction of the rotation rate, we obtain the following:

$$\frac{\omega_b}{\Omega} = \frac{2\pi/\Omega}{L_1/U} \quad .$$

The numerator is the period of rotation, whereas the denominator is roughly the time required for one coherent eddy to flow past the rotor. Thus, the bandwidth exceeds the rotation rate only if the axial length is small enough that the eddy passage time is less than the period of rotation.

On the other hand, each term in the expression for the velocity spectrum in rotating coordinates [Eq. (110)]

peaks at a different multiple of the rotation rate. Moreover, the mth term, considered as a function of frequency, is small whenever ω is outside an interval of width $4\pi U/L_1$ centered on $m\Omega$. But the frequency interval between peaks is Ω, so the peaks are distinct whenever $4\pi U/L_1 < \Omega$ or

$$\frac{2\pi/\Omega}{L_1/U} < \frac{1}{2} .$$

Thus the spectrum seen in rotor-fixed coordinates consists of distinct peaks at multiples of the rotation frequency whenever the eddy passage time considerably exceeds the period of rotation. Equivalently, the spectrum in rotor-fixed coordinates is peaked whenever the bandwidth of the spectrum in nonrotating coordinates is appreciably less than the rotation rate.

The heights of the successive peaks diminish as the rotation order m increases, and cease to be appreciable when $m/r > 2\pi/L_2$, or $m > 2\pi r/L_2$. Many peaks occur only if the azimuthal integral scale is considerably shorter than the rotor circumference, $2\pi r$. The requirement for many distinct peaks is thus that the axial integral scale be long and the azimuthal integral scale be short. These conditions are met when atmospheric turbulence is drawn into the inlet of a turbofan operating at low or zero forward speed, as has been pointed out by Hanson (Ref. 10) and others. The peaked spectrum which results is shown in Fig. 8 ; when the axial integral scale is short, a broad-band spectrum without sharp peaks is found.

6.4 Spectral Density of Duct Modes Excited by Inlet Turbulence/Rotor Interaction

In this section, we will derive an equation for the power spectrum of the sound generated by the rotor blades as they rotate through turbulence in the inlet duct. The starting point is Eq. (49), which gives the Fourier transform of the complex amplitude of the (m,n)th duct acoustic mode generated by a given pressure distribution on the rotor blades. From this equation, we can write out an equation for the expected value of the (m,n)th mode (in the frequency domain):

$$\langle \bar{p}_{mn}(\omega)\ \bar{p}^{*}_{mn}(\nu)\rangle = \frac{1}{4r^2 k_{n,m}(\nu)\ k_{n,m}(\omega)} \cdot$$

$$\cdot \int_{r_H}^{r_D} R(r',\omega) \int_{r_H}^{r_D} R(r'',\nu) \int_{-b'}^{+b'} \exp[i\mu(r',\omega)z']$$

$$\cdot \int_{-b''}^{+b''} \exp[-i\mu(r'',\omega)z''] \cdot \left\{ \sum_{j=0}^{B-1} \exp(i2\pi mj/B) \cdot \right.$$

$$\sum_{\ell=0}^{B-1} \exp(-i2\pi m\ell/B) \langle \Delta p_j(r'',z'',\omega-m\Omega) \cdot$$

$$\left. \Delta\hat{p}^{*}_{\ell}(r'',z'',\nu-m\Omega)\rangle \right\} dz''\ dz'\ dr''\ dr' \quad , \tag{112}$$

where

$$R(r,\omega) \equiv \psi_m(\kappa_{m,n} r)\ [(m/r)\cos\chi - \gamma_{n,m}(\omega)\sin\chi] \tag{113}$$

$$\mu(r,\omega) \equiv \gamma_{n,m}(\omega)\ \cos\chi + (m/r)\sin\chi \quad . \tag{114}$$

The expected value of the blade loading can be obtained from Eq. (55):

$$\langle \Delta\bar{p}_j(r',z',\omega-m\Omega)\ \Delta\bar{p}^{*}_{\ell}(r'',z'',\nu-m\Omega)\rangle =$$

$$(\rho_0 U_r)^2 \iint f(r',z',\underset{\sim}{k},\omega-m\Omega) \exp(ij\underset{\sim}{k}\cdot\underset{\sim}{h})$$

$$\iint f^{*}(r'',z'',\underset{\sim}{K},\nu-m\Omega) \exp(-i\ell\underset{\sim}{K}\cdot\underset{\sim}{h}) \cdot$$

$$\langle \hat{\bar{w}}(r',\underset{\sim}{k},\omega-m\Omega)\ \hat{\bar{w}}^{*}(r'',\underset{\sim}{K},\nu-m\Omega)\rangle \frac{d^2k}{(2\pi)^2}\ \frac{d^2K}{(2\pi)^2} \quad . \tag{115}$$

The quantity in braces in Eq. (112) can be written out as follows:

$$\{\text{Eq. (112)}\} =$$

$$(\rho_0 U_r)^2 \iiiint f(r',z',\underset{\sim}{k},\omega-m\Omega) \cdot$$

$$f^*(r'',z'',\underset{\sim}{K},\nu-m\Omega) \cdot$$

$$\sum_{j=0}^{B-1} \exp[ij(2\pi m/B+\underset{\sim}{k}\cdot\underset{\sim}{h})]$$

$$\cdot \sum_{\ell=0}^{B-1} \exp[i\ell(2\pi m/B+\underset{\sim}{K}\cdot\underset{\sim}{h})] \cdot$$

$$< \hat{\hat{w}}(r',\underset{\sim}{k},\omega-m\Omega)\ \hat{\hat{w}}^*(r'',\underset{\sim}{K},\nu-m\Omega) > \frac{d^2k}{(2\pi)^2}\frac{d^2K}{(2\pi)^2} . \qquad (116)$$

The wavenumber-frequency spectrum [Eq. (106)] contains the factor $\delta(\underset{\sim}{K}-\underset{\sim}{k})\ \delta(k_2-s/r)$, so in the expression above, we can set $\underset{\sim}{K} = \underset{\sim}{k}$ and $k_2 = s/r$. By noting that $\underset{\sim}{h} = (2\pi r/B)\underset{\sim}{\epsilon}_2$, the summations over the indices j and ℓ can be carried out explicitly:

$$\sum_{j=0}^{B-1} \exp[i2\pi(m+s)j/B] = B \quad \text{if } m+s = pB;$$
$$= 0 \text{ otherwise}$$

where p is any integer. A similar result holds for the sum over ℓ. Thus, we can set $s = pB - m$ in Eq. (106) and change the sum over all integers s to a sum over all integers p. If we now integrate over $\underset{\sim}{k}$ and $\underset{\sim}{K}$, we obtain the following result:

$$\{\text{Eq. (115)}\} =$$

$$\frac{\epsilon_D^2 U(\rho_0 U_r)^2 B^2}{r}\ \delta(\nu-\omega)$$

$$\sum_p f(r',z',\underset{\sim}{k}_p,\omega-m\Omega)\ f^*(r'',z'',\underset{\sim}{k}_p,\nu-m\Omega)\ \hat{\hat{\phi}}(\underset{\sim}{k}_p) \qquad (117)$$

where k_p is defined as follows:

$$\underset{\sim}{k}_p = \left(\frac{\omega - pB\Omega}{U} \, , \, \frac{pB-m}{r} \right) \quad . \tag{118}$$

It would appear from Eq. (117) that the elemental loading functions $f(r,z,\cdots)$ and $f^*(r",z",\cdots)$ must be computed anew for each value of the integer p. But, if we assume that the rotor is lightly loaded, so that the flow relative to the rotor blades is roughly aligned with the blade chords, then this is not the case. In the integral equation from which the elemental loading function $f(r,z,\cdots)$ is computed [see Eq. (54)], the wavenumber appears in two roles. First, the chordwise component of $\underset{\sim}{k}_p$ appears in the expression for the chordwise distribution of the inflow velocity normal to the chord, which is the inhomogeneous or forcing term in the integral equation. The nominal inflow velocity relative to the blades is $\underset{\sim}{U}_r = \underset{\sim}{U} + \Omega r \underset{\sim}{e}_2$. If we assume that the blade is lightly loaded, then $\underset{\sim}{U}_r$ will be roughly parallel to the blade chord, so that the chordwise component of $\underset{\sim}{k}_p$ is

$$\underset{\sim}{U}_r \cdot \underset{\sim}{k}_p / U_r = (\omega - m\Omega)/U_r \quad ,$$

which is independent of p. The wavenumber $\underset{\sim}{k}_p$ also appears in the kernel function itself (see Appendix B) as the inter-blade phase angle σ, defined as follows:

$$\sigma \equiv \underset{\sim}{k}_p \cdot \underset{\sim}{h}$$

$$= 2\pi(p - m/B) \quad .$$

But the kernel function is a periodic function of the inter-blade phase angle, and the period is 2π. Thus, the term $2\pi p$ can be deleted from σ without affecting the kernel function. It is apparent, then, that the elemental loading function $f(r,z,...)$ does not depend on the integer p, so we can rewrite Eq. (117) as follows:

$$\{\text{Eq. (115)}\} = \frac{\epsilon_D^2 U (\rho_0 U_r)^2 B^2}{r} \, \delta(\nu - \omega) \cdot$$

$$\cdot \, f(r',z',\underset{\sim}{k}_0,\omega - m\Omega) \, f^*(r",z",\underset{\sim}{k}_0,\nu - m\Omega)$$

$$\cdot \sum \hat{\hat{\phi}} \, (\underset{\sim}{k}_p, r, \Delta r) \quad , \tag{119}$$

where $\underset{\sim}{k}_0$ is obtained by setting p = 0 in Eq. (118).

The expected value of the (m.n)th duct mode may now be written as

$$\langle \bar{p}_{mn}(\omega)\ \bar{p}^{*}_{mn}(\nu)\rangle = \frac{\varepsilon_D^2 U(\rho_0 U)^2 B^2\ \delta(\nu-\omega)}{4\Gamma^2 k^2_{n,m}(\omega)} \cdot$$

$$\int_{r_H}^{r_D} R(r',\omega) \int_{r_H}^{r_D} R(r'',\omega) \int_{-b'}^{+b'} \exp[i\mu(r',\omega)z']$$

$$\cdot \int_{-b''}^{+b''} \exp[-i\mu(r'',\omega)z''] \ f(r',z',\underset{\sim}{k}_0,\omega-m\Omega) \cdot$$

$$\cdot\ f(r'',z'',\underset{\sim}{k}_0,\nu-m\Omega)\ dz''\ dz' \cdot \left(\frac{U_r}{U}\right)^2 \cdot$$

$$\cdot \frac{1}{r} \sum_p \hat{\hat{\phi}}(\underset{\sim}{k}_p,r,\Delta r)\ dr''\ dr' \quad . \tag{120}$$

At this point, it is necessary to express the auto-correlation function $\phi(\underset{\sim}{x},r,\Delta r)$ as the product of three functions, each one of which depends only upon a single variable. That is,*

$$\phi(\underset{\sim}{x},r,\Delta r) = \phi_1\left(\frac{X_1}{L_1}\right)\ \phi_2\left(\frac{X_2}{L_2}\right)\ \phi_r\left(\frac{\Delta r}{L_r}\right) . \tag{121}$$

The three integral scales L_1, L_2, and L_r may be functions of the radius r. Procedures by which the functions ϕ_1, ϕ_2, ϕ_r and the length scales L_1, L_2, and L_r may be chosen to fit turbulence data collected from transducers placed in the inlet duct are described in Ref. (1). The Fourier transform of ϕ is then

$$\hat{\hat{\phi}}(\underset{\sim}{k},r,\Delta r) = L_1 L_2 \hat{\phi}_1(k_1 L_1)\ \hat{\phi}_2(k_2 L_2)\ \phi_r\left(\frac{\Delta r}{L_r}\right) , \tag{122}$$

*The representation given by Eq. (121) is physically meaningful only where $L_2 << 2\pi r$.

so

$$\hat{\phi}(\underset{\sim}{k}_p, r, \Delta r) = L_1 L_2 \hat{\phi}_1\left[\frac{(\omega - pB\Omega)L_1}{U}\right] \cdot$$

$$\hat{\phi}_2\left[\frac{(pB-m)L_2}{r}\right] \phi_r\left(\frac{\Delta r}{L_r}\right) \quad . \tag{123}$$

And the expected value of the (m,n)th mode is

$$\langle \bar{p}_{mn}(\omega)\ \bar{p}^*_{mn}(\nu)\rangle = \frac{\rho_0^2 U^3 B^2\ \delta(\nu-\omega)}{4r^2 k^2_{n,m}} \cdot$$

$$\int_{r_H}^{r_D} R(r',\omega) \int_{r_H}^{r_D} R^*(r'',\omega) \int_{-b'}^{+b'} f(r',z',\underset{\sim}{k}_0,\omega-m\Omega)$$

$$\exp[i\mu(r',\omega)z']\ dz' \int_{-b''}^{+b''} f(r'',z'',\underset{\sim}{k}_0,\nu-m\Omega)$$

$$\exp[-i\mu(r'',\omega)z'']\ dz'' \cdot \frac{\varepsilon_D^2}{r}\left(\frac{U_r}{U}\right)^2 L_1 L_2 \cdot$$

$$\cdot\ \phi_r\left(\frac{\Delta r}{L_r}\right) \sum_p \hat{\phi}_1\left[\frac{(\omega - pB\Omega)L_1}{U}\right] \hat{\phi}_2\left[\frac{(pB-m)L_2}{r}\right] dr''\ dr' \quad . \tag{124}$$

This rather cumbersome equation can be simplified if we assume that the radial integral scale, L_r, is very much shorter than the radius of the duct, r_D. If this is the case, both r' and r" may be replaced by $r = \frac{1}{2}(r'+r")$, everywhere but in the argument of ϕ_r. The integration variables can be changed from r' and r" to r and $\Delta r = y$, and the integration over y can be approximated as

$$\int_{-\infty}^{+\infty} \phi_r(y/L_r)dr = L_r \quad . \tag{125}$$

When this is done, we obtain the following result:

$$\langle \bar{p}_{mn}(\omega)\ \bar{p}^{*}_{mn}(\nu)\rangle = \frac{\rho_0 U^3 B^2 \delta(\nu-\omega)}{4\Gamma^2 k^2_{n,m}}$$

$$\int_{r_H}^{r_D} b^2 R^2(r,\omega)\ |C_{mn}(r,\omega)|^2 \cdot \frac{\epsilon_D^2}{r}\left(\frac{U_r}{U}\right)^2 L_1 L_2 L_r$$

$$\sum_p\ \hat{\phi}_1\left[\frac{(\omega-pB\Omega)L_1}{U}\right]\ \hat{\phi}_2\left[\frac{(pB-m)L_2}{r}\right]\ dr \quad , \tag{126}$$

where the chordwise integral $C_{mn}(r,\omega)$ is defined as

$$C_{mn}(r,\omega) \equiv \int_{-b}^{+b} f(r,z,\underset{\sim}{k}_0,\omega-m\Omega) \cdot$$

$$\exp[i\mu(r,\omega)z]\ \frac{dz}{b} \quad . \tag{127}$$

The mean-square value of the (m,n)th mode is given by

$$\langle p^2_{mn}\rangle = \iint \langle \bar{p}_{mn}(\omega)\ \bar{p}^{*}_{mn}(\nu)\rangle \cdot$$

$$\exp[i(\nu-\omega)t]\ \frac{d\nu}{2\pi}\ \frac{d\omega}{2\pi} \quad , \tag{128}$$

which is

$$\langle p^2_{mn}\rangle = \int \frac{\rho_0^2 U^3 B^2}{8\pi\Gamma k^2_{n,m}} \int_{r_H}^{r_D} b^2 R^2(r,\omega) \cdot$$

$$|C_{mn}(r,\omega)|^2\ \frac{\epsilon_D^2}{r}\ (U_r/U)^2\ L_1 L_2 L_r \cdot$$

$$\sum_p\ \hat{\phi}_1\left[\frac{(\omega-pB\Omega)L_1}{U}\right]\ \hat{\phi}_2\left[\frac{(pB-m)L_2}{r}\right]\ dr\ \frac{d\omega}{(2\pi)} \quad . \tag{129}$$

The spectral density of the (m,n)th mode is the integrand of the integration with respect to $\omega/2\pi$:

$$P_{mn}(\omega) = \frac{\rho_0^2 U^3 B^2}{8\pi\Gamma^2 k_{n,m}^2(\omega)} \int_{r_H}^{r_D} b^2 R^2(r,\omega) \cdot$$

$$|C_{mn}(r,\omega)|^2 \frac{\epsilon_D^2}{r} (U_r/U)^2 L_1 L_2 L_r \cdot$$

$$\sum_p \hat{\phi}_1\left[\frac{(\omega - pB\Omega)L_1}{U}\right] \hat{\phi}_2\left[\frac{(pB-m)L_2}{r}\right] dr \quad . \qquad (130)$$

Recalling the discussion of Sec. 6.3, $\hat{\phi}_1$ is small unless the following inequality is satisfied:

$$\left|\frac{\omega}{\Omega B} - p\right| < \frac{2\pi/\Omega B}{L_1/U} \quad .$$

Thus, if the axial integral scale L_1 is long enough so that the eddy passage time, L_1/U, is considerably longer than the blade passage interval, $2\pi/\Omega B$, the modal spectrum will contain distinct peaks at multiples of the blade passage rate. Now looking at the function $\hat{\phi}_2$, we see that the peaks exist only at those multiples of the blade passage rate which satisfy the following inequality:

$$|pB-m| < \frac{2\pi r}{L_2} \quad .$$

Thus, if the azimuthal integral scale is small compared to the mean circumference of the rotor, many peaks will appear in the spectrum. On the other hand, if L_2 is large, few peaks appear, and a mode selection process occurs by which modes with a number of azimuthal nodes equal to some multiple of the number of blades are most strongly excited. Finally, if L_1 is small, a broadband spectrum will result.

Recall that the spectral density of the inlet turbulence sensed by a blade-mounted transducer tends to peak

at multiples of the rotor rotation rate, whereas acoustic mode excitation peaks at multiples of the blade passage rate. On a multi-bladed rotor these peaks occur at much higher frequencies.

6.5 Sound Power Flux Generated by Inlet Turbulence/Rotor Interaction

The sound power flux within the duct is obtained from Eq. (34):

$$S(\omega) = \frac{\pi(r_D^2-r_H)^2}{\rho_0 U} \sum_m \sum_n G_{mn}(\omega)\, P_{mn}(\omega) \quad , \tag{131}$$

where $G_{mn}(\omega)$ is the quantity in braces given in Eq. (35). If we introduce $S_{mn}(\omega)$ as the sound power flux per mode, i.e.,

$$S_{mn}(\omega) \equiv \frac{\pi(r_D^2-r_H^2)}{\rho_0 U} G_{mn}(\omega)\, P_{mn}(\omega) \quad , \tag{132}$$

then the total sound power flux is obtained by summing over m and n:

$$S(\omega) = \sum_m \sum_n S_{mn}(\omega) \quad . \tag{133}$$

In the computer program, both $S(\omega)$ and $S_{mn}(\omega)$ have been divided by $\rho_0 c_0^2 r_D^3$ to make them dimensionless. Using the dimensionless variables defined in Appendix A, the following expressions are obtained:

$$\frac{S(\omega)}{\rho_0 c_0^2 r_D^3} = \sum_{m=-\infty}^{+\infty} \sum_{n=1}^{\infty} \frac{S_{mn}(\omega)}{\rho_0 c_0^2 r_D^3} \tag{134}$$

where

$$\frac{S_{mn}(\omega)}{\rho_0 c_0^2 r_D^3} = \frac{\beta^4 M\ M_T\ B^2(\omega/\Omega)}{\pi(1-\sigma_r^2)k_{n,m}\left(\frac{\omega M_T}{\Omega} \pm M\ \tilde{k}_{n,m}\right)^2} \cdot$$

$$\frac{\sigma_c^2}{2} \int_{\sigma_r}^{1} \psi_m^2(K_{m,n}x) \left(\frac{m}{x}\cos\chi - \tilde{\nu}_{n,m}\sin\chi\right)^2 \cdot$$

$$\cdot |C_{mn}(x,\omega/\Omega)|^2\ \varepsilon_D^2(x) \sqrt{1 + \left(\frac{M_T x}{M}\right)^2}\ \tilde{b}^2(x)$$

$$\tilde{L}_r(x)\ \tilde{L}_1(x)\ \tilde{L}_2(x) \cdot$$

$$\cdot \sum_p \hat{\phi}_1\left[\left(\frac{\omega}{\Omega} - pB\right)\frac{M_T \tilde{L}_1}{M_\theta}\right] \hat{\phi}_2\left[\frac{(pB-m)\tilde{L}_2}{x}\right] \frac{dx}{x} \quad . \qquad (135)$$

The chordwise integral $C_{mn}(x,\omega/\Omega)$ is defined as follows:

$$C(x,\omega/\Omega) = \int_{-1}^{+1} f(x,z/b,\underset{\sim}{k},\omega) \cdot$$

$$\exp[i\sigma_c \bar{b}(\bar{\gamma}_{n,m}\cos\chi + \frac{m}{x}\sin\chi)z/b]\ dz/b \quad . \qquad (136)$$

The elemental loading function f(...), the chordwise integral C_{mn}(...), and the modal power flux $S_{mn}/\rho_0 c_0^2 r_D^3$ are all computed numerically. The procedures used are described in Chapter 8.

CHAPTER 7

ROTOR WAKE TURBULENCE

7.1 Rotor Wake Turbulence Model

Figure 9 shows a cylindrical slice of the rotor and stator opened out to form two linear cascades. Axes (x_1,x_2) are fixed in the stator, while axes (X_1,X_2) move with the rotor blades. The equation relating the two sets of axes is

$$\underset{\sim}{X} = \underset{\sim}{x} + \underset{\sim}{D} + \Omega rt\underset{\sim}{e}_2 \quad , \tag{137}$$

where $\underset{\sim}{D}$ is a vector extending from the reference blade on the rotor to the reference vane on the stator. The reference blade and vane can be chosen arbitrarily, and $\underset{\sim}{D}$ is defined only to within an arbitrary additive constant vector parallel to the x_2 and X_2 axes. In Fig.9 the centerlines of the rotor blades wakes are shown as dashed lines. These strike an angle χ with the axis of rotation, as seen by an observer moving with the rotor blades. The unit vector $\underset{\sim}{n}$ is normal to the wake centerlines, so the components of $\underset{\sim}{n}$ along the X_1 and X_2 axes are $(-\sin\chi, \cos\chi)$. Note that χ and $\underset{\sim}{n}$ have here different definitions than they had in Chapter 4, where they were defined with regard to the rotor blades themselves rather than the rotor blade wakes. The two sets of definitions become identical only when the rotor is operating under no load, so that the wakes are lined up with the blade chords. Since the equations to be derived in this chapter are self-contained, no ambiguity should arise.

The wakes are supposed to be convected with the nominal flow downstream of the rotor. Reynolds, *et al.* have conducted surveys of the turbulence within the wakes, using transducers fixed with respect to the rotor (Refs.13,14). These measurements indicate that the turbulence intensity is maximum on the wake centerline, and diminishes monotonically with distance on either side of the wake centerline. The surveys were conducted relatively close to the blade trailing edges and show marked asymmetry of the wake widths on either side of the centerline. But at larger distances downstream, at distances comparable to the blade chord, the wakes become more symmetric.

Our mathematical model of rotor wake turbulence may be described as follows. Samples of the fluid velocity

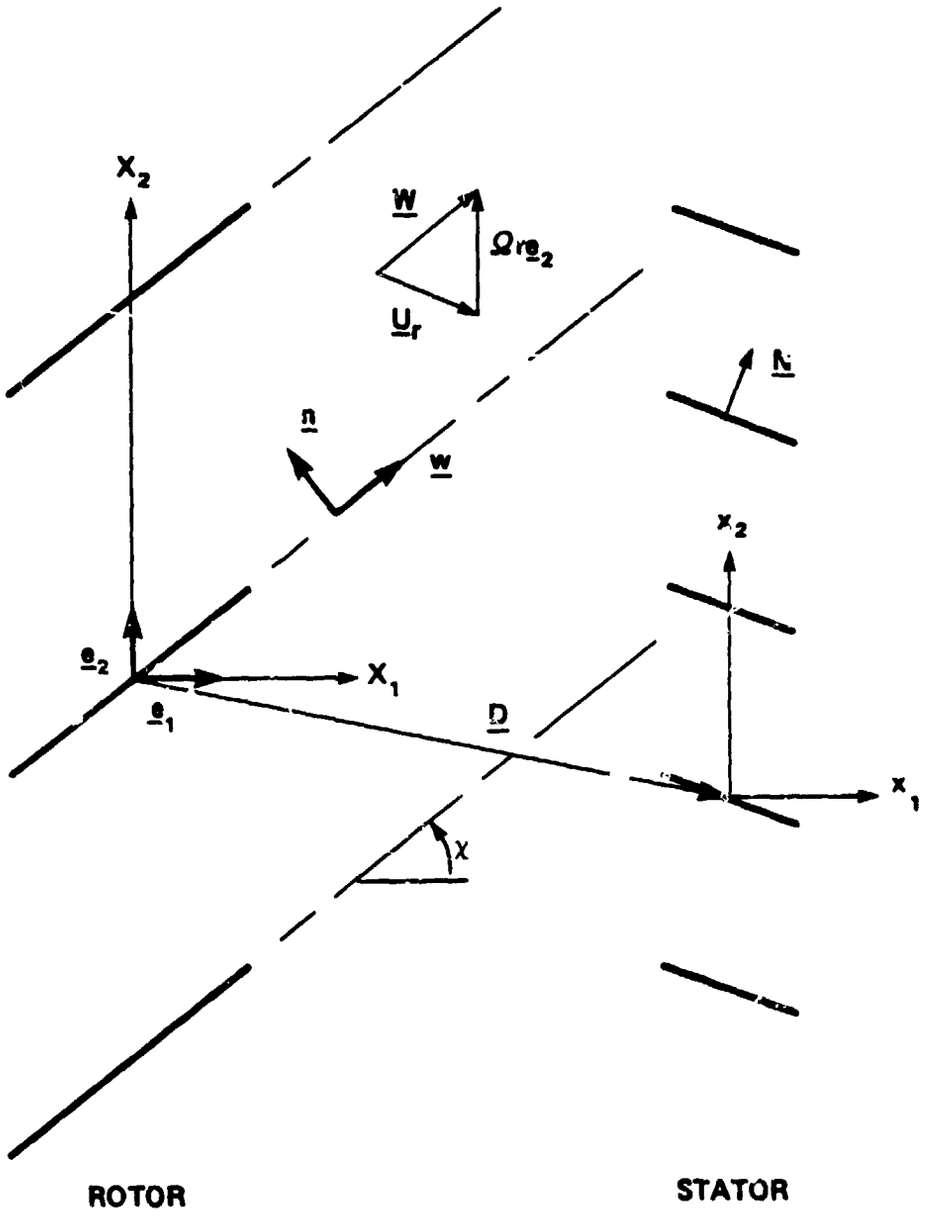

FIGURE 9. Rotor/Stator Geometry for Wake Turbulence Analysis

downstream of the rotor, as seen in a rotating frame of reference, are assumed to have the following form:

$$w(r,\underset{\sim}{X},t) = \varepsilon_w \, WF(\underset{\sim}{X}\cdot\underset{\sim}{n}) \, g(r,\underset{\sim}{X}-\underset{\sim}{W}t) \quad . \tag{138}$$

In this equation, $w(r,X,t)$ is the component of the fluctuating velocity downstream of the rotor which is normal to the stator vanes, while W is the magnitude of the mean flow velocity, and ε_w is the rms turbulence intensity on the wake centerline. The function $g(r,\underset{\sim}{X}-\underset{\sim}{W}t)$ is a random function of the variables indicated, and $F(\underset{\sim}{X}\cdot\underset{\sim}{n})$ is a deterministic function chosen so as to model the variation of the turbulence intensity with distance from the wake centerlines. Note that $\underset{\sim}{X}\cdot\underset{\sim}{n}$ is constant on planes parallel to the wake centerlines. To sustain the definition of ε_w as the rms turbulence intensity, $F(\underset{\sim}{X}\cdot\underset{\sim}{n})$ must be normalized so that $F(0) = 1$. Because all the wakes are assumed to be identical, $F(\underset{\sim}{X}\cdot\underset{\sim}{n})$ must be a periodic function, the period being the distance between wake centerlines, measured normal to the centerlines themselves.

It is convenient to express F as an infinite series of identical "haystack" functions, each representing the variation of the turbulence intensity across one of the wakes. The normal distance between wakes is $2\pi r \cos\chi/B$, so $F(\underset{\sim}{X}\cdot\underset{\sim}{n})$ can be written as follows:

$$F(\underset{\sim}{X}\cdot\underset{\sim}{n}) = \sum_m f\left(\frac{\underset{\sim}{X}\cdot\underset{\sim}{n}-mh\cos\chi}{\delta\cos\chi}\right) \tag{139}$$

where $h \equiv 2\pi r/B$. The denominator of the argument of $f(\ )$, $\delta\cos\chi$, is the width of the wake turbulence intensity, measured normal to the wake centerlines. Thus, δ itself is the corresponding width measured azimuthally. One example of a candidate "haystack" function, and in fact the one currently being used in the computer program, is the well-known Gaussian profile,

$$f(y/\delta) = \exp[-\pi(y/\delta)^2] \quad , \tag{140}$$

where $y = \underset{\sim}{X}\cdot\underset{\sim}{n}$. As defined here, δ is equivalent to an integral scale, in the sense that

$$\int f(y/\delta)\, dy = \delta \ . \tag{141}$$

Because $F(\underset{\sim}{X}\cdot\underset{\sim}{n})$ is a periodic function, it can be expressed as a Fourier series, which can be reduced to the form shown here:

$$F(\underset{\sim}{X}\cdot\underset{\sim}{n}) = \frac{B}{2\pi r} \sum_s \hat{f}\left(\frac{sB\delta}{r}\right) \exp\left(\frac{isB}{r\cos\chi}\ \underset{\sim}{X}\cdot\underset{\sim}{n}\right) \ , \tag{142}$$

where $\hat{f}(\alpha)$ is the Fourier transform of the "haystack" function $f(x)$:

$$\hat{f}(\alpha) \equiv \int f(x)\, \exp(-i\alpha x)\, dx \ . \tag{143}$$

For example, if $f(x) = \exp(-\pi x^2)$, then $\hat{f}(\alpha) = \exp(-\alpha^2/4\pi)$.

The random function $g(r,\underset{\sim}{X}-\underset{\sim}{W}t)$ is assumed to be a stationary random function, with respect to the spatial variable $\underset{\sim}{X}$. Therefore, the correlation function Φ_w is a function only of $\underset{\sim}{X}-\underset{\sim}{Y}$, and not of $\underset{\sim}{X}$ and $\underset{\sim}{Y}$ separately. Thus, Φ_w can be written as follows:

$$\langle w(r_1,\underset{\sim}{X}-\underset{\sim}{W}t)\ w(r_2,\underset{\sim}{Y}-\underset{\sim}{W}\tau)\rangle = \Phi_w[\underset{\sim}{X}-\underset{\sim}{Y}-\underset{\sim}{W}(t-\tau),\ \Delta r] \ , \tag{144}$$

where $r = \frac{1}{2}(r_1+r_2)$. Once again, the duct is annular, so Φ_w must be a periodic function, just as Φ_D was in Chapter 6. Φ_w also can be written as an Fourier series, just as Φ_D was. Thus, we have

$$\Phi_w(\underset{\sim}{X},\Delta r) = \sum_m \Phi_m \exp(imX_2/r) \tag{145}$$

The Fourier coefficients Φ_m are proportional to the Fourier transform of the nonperiodic function $\phi\ (\underset{\sim}{X},\Delta r)$, defined as follows,

$$\begin{aligned} \phi(\underset{\sim}{X},\Delta r) &= \Phi_w(\underset{\sim}{X},\Delta r) \qquad \text{if } |X_2|<\pi r \\ &= 0 \qquad\qquad\quad \text{if } |X_2|\geq r \end{aligned} \tag{146}$$

That is,

$$\Phi_m = \frac{1}{2\pi r}\Phi(X_1,m/r,\Delta r) \tag{147}$$

so

$$\Phi_w(\underset{\sim}{X},\Delta r) = \frac{1}{2\pi r}\sum_m \hat{\Phi}(X_1,m/r,\Delta r)\exp(imX_2/r) \qquad (148)$$

and the Fourier transform of Φ_ω is

$$\hat{\hat{\Phi}}_w(\underset{\sim}{\lambda},\Delta r) = \frac{1}{r}\sum_m \hat{\hat{\Phi}}(\underset{\sim}{\lambda},\Delta r)\ \delta(\lambda_2 - m/r). \qquad (149)$$

7.2 Wavenumber-Frequency Spectrum in Stator-Fixed Coordinates

In order to calculate the power spectral density of the sound generated by the interaction of rotor wake turbulence with the stator vanes, we must calculate the expected value of the wake wavenumber-frequency spectrum in a nonrotating reference frame:

$$\langle \hat{\hat{w}}(r_1,\underset{\sim}{k},\omega)\ \hat{\hat{w}}^*(r_2,\underset{\sim}{K},\nu)\rangle =$$

$$\int\int\int\int\int\int\int \langle w(r_1,\underset{\sim}{X}-\underset{\sim}{W}t)\ w(r_2,\underset{\sim}{Y}-\underset{\sim}{W}\tau)\cdot \qquad (150)$$

$$\exp(i\omega t - i\nu\tau - i\underset{\sim}{k}\cdot\underset{\sim}{X} + i\underset{\sim}{K}\cdot\underset{\sim}{Y})\ d^2x\ d^2y\ d\tau dt \quad .$$

The expected value of the wake turbulence, as discussed in the previous section, is

$$\langle w(r_1,\underset{\sim}{X}-\underset{\sim}{W}t)\ w^*(r_2,\underset{\sim}{Y}-\underset{\sim}{W}\tau)\rangle =$$

$$\varepsilon_w^2 W^2 F(\underset{\sim}{X}\cdot\underset{\sim}{\ })\ F^*(\underset{\sim}{Y}\cdot\underset{\sim}{n})\cdot$$

$$\cdot\ \Phi_w[\underset{\sim}{X}-\underset{\sim}{Y}-\underset{\sim}{W}(t-\tau),\ \Delta r] \quad . \qquad (151)$$

From here on, we will assume that the radial integral scale of the wake turbulence is small enough so that we can set $r_1 = r_2 = r$ *except* in the last argument of Φ_w, above. To reduce the integrals in Eq. (150), substitute Eq.(151) in for the integrand, and change the integration variables to $\underset{\sim}{X}$ and $\underset{\sim}{Y}$, where

$$\underset{\sim}{X} = \underset{\sim}{x} + \underset{\sim}{D} + \Omega r\tau\underset{\sim}{e}_2$$

$$\underset{\sim}{Y} = \underset{\sim}{y} + \underset{\sim}{D} + \Omega r\tau\underset{\sim}{e}_2 \quad . \qquad (152)$$

Having done this, introduce a second change of variables,

$$\underset{\sim}{\xi} = \underset{\sim}{X} - \underset{\sim}{Y} - \underset{\sim}{W}(t-\tau) \quad , \tag{153}$$

where ξ replaces X. The integration with respect to t and τ can now be carried out explicitly by recognizing the integral expression for the delta function [Eq. (98)]. The result at this point is

$$\langle \hat{\hat{w}}(r_1, \underset{\sim}{k}, \omega)\ \hat{\hat{w}}(r_2, \underset{\sim}{K}, \nu) \rangle =$$

$$(2\pi)^2\ \delta(\omega - \underset{\sim}{W}\cdot\underset{\sim}{k} + \Omega r k_2)\ \delta(\nu - \underset{\sim}{W}\cdot\underset{\sim}{k} + \Omega r K_2)\ \cdot$$

$$\cdot \iiiint F[(\underset{\sim}{\xi}+\underset{\sim}{Y})\cdot\underset{\sim}{n}]\ F^*(\underset{\sim}{Y}\cdot\underset{\sim}{n})\ \Phi(\underset{\sim}{\xi})\ \cdot$$

$$\exp[i(\underset{\sim}{K}-\underset{\sim}{k})\cdot\underset{\sim}{Y} - i\underset{\sim}{k}\cdot\underset{\sim}{\xi}]\ d^2\xi\ d^2Y\ \cdot$$

$$\cdot\ \exp[i(\underset{\sim}{K}-\underset{\sim}{k})\cdot\underset{\sim}{D}] \quad . \tag{154}$$

The remaining integrations can be completed by substituting for F and F* the Fourier series as given in Eq. (142). The result, using Eq. (149) for the Fourier transform of Φ_w, is shown below:

$$\langle \hat{\hat{w}}(r_1, \underset{\sim}{k}, \omega)\ \hat{\hat{w}}^*(r_2, \underset{\sim}{K}, \nu) \rangle \ =$$

$$\left(\frac{2\pi B\delta}{r}\right)^2 \frac{\exp[i(\underset{\sim}{K}-\underset{\sim}{k})\cdot\underset{\sim}{D}]}{r} \ \cdot$$

$$\delta(\omega - \underset{\sim}{W}\cdot\underset{\sim}{k} + \Omega r k_2)\ \delta(\nu - \underset{\sim}{W}\cdot\underset{\sim}{k} + \Omega r K_2)$$

$$\sum_m \sum_\ell \hat{f}\left(\frac{mB\delta}{r}\right)\hat{f}^*\left(\frac{\ell B\delta}{r}\right)\ \delta\left[\underset{\sim}{K}-\underset{\sim}{k} + \frac{(m-\ell)B}{r\cos\chi}\ \underset{\sim}{n}\right]$$

$$\hat{\hat{\phi}}\left(\underset{\sim}{k} - \frac{mB}{r\cos\chi}\underset{\sim}{n}, \Delta r\right) \cdot \sum_s \delta\left(k_2 - \frac{s+mB}{r}\right) \quad . \tag{155}$$

Finally, it is worthwhile to introduce $\underset{\sim}{U}_r$, the mean or nominal velocity relative to the stator,

$$\underset{\sim}{U}_r = \underset{\sim}{W} - \Omega r \underset{\sim}{e}_2 \tag{156}$$

and to re-arrange the arguments of the five delta functions into a form more convenient for subsequent calculations. The final result is shown below:

$$\begin{aligned}
&\langle \hat{\hat{w}}(r_1, \underset{\sim}{k}, \omega)\ \hat{\hat{w}}(r_2, \underset{\sim}{K}, \nu) \rangle = \\
&\frac{(2\pi\varepsilon_w WB\delta)^2}{r^3}\ \delta(\omega - \underset{\sim}{U}_r \cdot \underset{\sim}{k})\ \cdot \\
&\sum_m \sum_\ell \hat{f}\left(\frac{mB\delta}{r}\right)\ \hat{f}^*\left(\frac{\ell B\delta}{r}\right)\ \exp\left[\frac{i(m-\ell)}{r\cos\chi}\underset{\sim}{D}\cdot\underset{\sim}{n}\right]\ \cdot \\
&\cdot\ \hat{\hat{\phi}}\left(k - \frac{mB}{r\cos\chi}\ \underset{\sim}{n}, \Delta r\right)\ \delta[\nu - \omega - \Omega(\ell - m)B] \\
&\delta\left[\underset{\sim}{k} - \underset{\sim}{K} - \frac{(m-\ell)B}{r\cos\chi}\ \underset{\sim}{n}\right]\ \sum_s \delta\left(k - \frac{s+mB}{r}\right)\ .
\end{aligned} \tag{157}$$

7.3 Wake Turbulence Velocity Spectral Density in Rotating and Nonrotating Coordinates

In Sec. 6.3, the velocity spectral densities of inlet turbulence in fixed and rotating reference frames were derived from the inlet turbulence model adopted, in order to discuss the effects of rotation on the spectra. In this section, the velocity spectral densities of rotor wake turbulence also will be calculated in fixed and rotating coordinates, for purposes of comparison.

The mean-square velocity of the wake turbulence can be calculated by setting $r_1 = r_2 = r$ in Eq. (157), multiplying it by $(2\pi)^5 \exp[i(\nu-\omega)t + i(\underset{\sim}{k}-\underset{\sim}{K})\cdot\underset{\sim}{X}]$, and integrating over ν, $\underset{\sim}{K}$, and $\underset{\sim}{k}$:

$$\langle w^2(r,\underset{\sim}{x},t)\rangle =$$

$$\iiiint \langle \hat{\underset{\sim}{w}}(r,\underset{\sim}{k},\omega)\ \hat{\underset{\sim}{w}}^*(r,\underset{\sim}{K},\nu)\rangle \cdot$$

$$\exp[i(\nu-\omega)t+i(\underset{\sim}{k}-\underset{\sim}{K})\cdot\underset{\sim}{X}]\ \frac{d^2K\ d^2k\ d\nu}{(2\pi)^5} \quad . \tag{158}$$

The result is

$$\langle w^2(r,\underset{\sim}{x},t)\rangle =$$

$$\frac{(\varepsilon_w WB\delta)^2}{(2\pi r)^3 U_{r1}} \sum_m \sum_\ell \hat{f}\left(\frac{mB\delta}{r}\right)\ \hat{f}^*\left(\frac{\ell B\delta}{r}\right)$$

$$\exp\left\{\frac{i(m-\ell)B}{r\cos\chi}\ (\underset{\sim}{x}+\underset{\sim}{D})\cdot\underset{\sim}{n} + i\Omega(\ell-m)\ Bt\right\}$$

$$\sum_s \int \hat{\phi}\left(\underset{\sim}{k}_s - \frac{mB}{r\cos\chi}\ \underset{\sim}{n},0\right)\ \frac{d\omega}{2\pi} \quad , \tag{159}$$

where the wavenumber $\underset{\sim}{k}_s$ is defined by the following two equations:

$$\underset{\sim}{U}_r\cdot\underset{\sim}{k}_s = \omega$$

$$\underset{\sim}{e}_2\cdot\underset{\sim}{k}_s = \frac{s+mB}{r} \quad . \tag{160}$$

Behind the rotor, the mean-square velocity at a point fixed in the duct fluctuates at multiples of the blade passage rate, ΩB. The time-averaged mean-square velocity is obtained by setting $\ell = m$ and deleting the summation over ℓ. If we delete the integration with respect to ω, we

obtain the time-averaged rotor wake velocity spectral density. In the expression below, the components of $\underset{\sim}{k}_s$ have been written out explicitly,

$$S_w(\omega) = \frac{(\epsilon_w WB\delta)^2}{(2\pi r)^3 U_{1r}} \cdot$$

$$\sum_s \sum_m \left|\hat{f}\left(\frac{mB\delta}{r}\right)\right|^2 \hat{\hat{\phi}}_1\left(\frac{\omega+mB\Omega}{U_{1r}} - \frac{U_{r2}}{U_{r1}}\frac{s}{r}, \frac{s}{r}, r, 0\right) \qquad (161)$$

To simplify matters, assume that the rotor is operating at no load, so that the azimuthal velocity in the wake, as seen by an observer fixed in the duct, is zero. Then the first argument of $\hat{\phi}$ depends only on the index m:

$$S_w(\omega) = \frac{1}{U_{1r}}\left(\frac{\epsilon_w WB\delta}{2\pi r}\right)^2 \frac{1}{2\pi r} \cdot$$

$$\cdot \sum_s \sum_m \left|\hat{f}\left(\frac{mB\delta}{r}\right)\right|^2 \hat{\hat{\phi}}_1\left(\frac{\omega+mB\Omega}{U_{r1}}, \frac{s}{r}, r, 0\right) \qquad (162)$$

The spectrum consists of the sum of several "haystack" functions $\hat{\hat{\phi}}_1(\omega+mB\Omega/U_{r1}\ldots)$ centered at integer multiples of the blade passage rate. The width of these "haystacks" is roughly $4\pi\ U_{r1}/L_1$, where L_1 is the axial integral scale of the turbulence, and the frequency increment between them is ΩB, so the peaks are distinct only if

$$\frac{4\pi U_{r1}}{L_1} < \Omega B$$

or

$$L_1 > \left(\frac{2\pi r}{B}\right)\left(\frac{2U_{r1}}{\Omega r}\right) \cdot$$

The first factor on the right-hand side of this inequality is $2\pi r/B = h$, the gap between the rotor blades,

and the second is twice the ratio of the axial velocity behind the rotor to the rotational tip speed of the rotor. This latter ratio is roughly one half, so the peaks are distinct only if the integral scale of the wake turbulence is greater than the rotor blade gap. But the amplitude of the mth "haystack" is proportional to $|\hat{f}(mB\delta/r)|^2$, which is small unless $mB\delta/r < 2\pi$, or $m < 2\pi r/B\delta = h/\delta$, where $h = 2\pi r/B$ is the blade gap. This means that the high-order peaks are attenuated unless the width of the wakes, δ, is much smaller than the blade gap. Therefore, if we assume that the integral scales of the turbulence within the wakes are comparable to the wake width, then the velocity spectral density, in a nonrotating frame of reference, will not contain pronounced peaks at multiples of the blade passage rate. On the other hand, if the wake width is considerably smaller than the rotor blade gap, but the axial length scale is larger, then a "peaky" spectrum will result.

7.4 Spectral Density of Duct Modes Excited by Rotor Wake/Stator Interaction

In this section, we will derive an equation for the modal spectral density of the duct modes excited by the interaction of the rotor blade wakes and the stator vanes. The starting point is Eq. (50), which gives the Fourier transform of the complex amplitude of the (m,n)th duct mode generated by a given pressure distribution on the stator vanes. Using this equation, we can write out an equation for the expected value (or ensemble average) of the (m,n)th mode in the frequency domain:

$$\langle \bar{p}_{mn}(\omega)\, \bar{p}^*_{mn}(\nu) \rangle = \frac{1}{4\Gamma^2 k_{n,m}(\omega) k_{n,m}(\nu)} \cdot$$

$$\int_{r_H}^{r_D} R(r',\omega) \int_{r_H}^{r_D} R(r'',\nu) \int_{-b'}^{+b'} \exp[i\mu(r',\omega)z'] \cdot$$

$$\cdot \int_{-b''}^{+b''} \exp[-i\mu(r'',\omega)z''] \cdot \left\{ \sum_{j=0}^{V-1} \exp(i2\pi mj/V) \right.$$

(Cont.)

$$\cdot \sum_{\ell=0}^{V-1} \exp(i2\pi m\ell/V) < \bar{p}_j(r',z',\omega) \cdot$$

$$\cdot \bar{p}^*_\ell(r'',z'',\nu) > \Big\} \, dz'' \, dz' \, dr'' \, dr' \quad , \tag{163}$$

where $R(r,\omega)$ and $\mu(r,\omega)$ are defined in Eqs. (116,117).* The expected value of the stator vane loading can be obtained from Eq. (54),

$$<\Delta\bar{p}_j(r',z'\omega) \; \Delta\bar{p}^*_\ell(r'',z'',\nu)> =$$

$$(\rho_0 U_r)^2 \iint f(r',z',\underset{\sim}{k},\omega) \exp(ij\underset{\sim}{k}\cdot\underset{\sim}{H})$$

$$\cdot \iint f^*(r'',z'',\underset{\sim}{K},\nu) \exp(-i\ell\underset{\sim}{K}\cdot\underset{\sim}{H}) \cdot$$

$$\cdot <\hat{\bar{w}}(r',\underset{\sim}{k},\omega) \; \hat{\bar{w}}^*(r'',\underset{\sim}{K},\nu)> \; \frac{d^2k \; d^2K}{(2\pi)^4} \tag{164}$$

and the quantity in braces in Eq. (163) can be written out as follows:

$$\{\text{Eq. (163)}\} =$$

$$(\rho_0 U_r)^2 \iiiint f(r',z',k, \;) \; f^*(r'',z'',K, \;) \cdot$$

$$\sum_{j=0}^{V-1} \exp[ij(2\pi m/V+\underset{\sim}{k}\cdot\underset{\sim}{H})]$$

$$\sum_{\ell=0}^{V-1} \exp[i\ell(2\pi m/V+\underset{\sim}{K}\cdot\underset{\sim}{H})] \cdot$$

$$<\hat{\bar{w}}(r',\underset{\sim}{k},\omega) \; \hat{\bar{w}}^*(r'',\underset{\sim}{K},\nu) > \frac{d^2k \; d^2K}{(2\pi)^4} \quad . \tag{165}$$

*But substitute $-\theta$ for χ.

The complex wavenumber-frequency spectrum was derived in Sec. 5.2; it is rewritten below with different summation indices to avoid confusion later on.

$$\langle \hat{\hat{w}}(r',\underset{\sim}{k},\omega)\ \hat{\hat{w}}^*(r'',\underset{\sim}{K},\nu)\rangle =$$

$$\frac{(2\pi\epsilon_w WB\delta)^2}{r^3}\ \delta(\omega-\underset{\sim}{U}_r\cdot\underset{\sim}{k})\ \cdot$$

$$\sum_{m_1}\sum_{\ell_1}\ \hat{f}\left(\frac{m_1B\delta}{r}\right)\ \hat{f}\left(\frac{\ell_1B\delta}{r}\right)\ \exp\left[\frac{i(m_1-\ell_1)}{r\cos\chi}\ \underset{\sim}{D}\cdot\underset{\sim}{h}\right]$$

$$\hat{\hat{\phi}}\left(\underset{\sim}{k}-\frac{m_1B}{r\cos\chi}\ \underset{\sim}{h},\Delta r\right)\ \delta[\nu-\omega-\Omega(\ell_1-m_1)B]$$

$$\delta\left[\underset{\sim}{k}-\underset{\sim}{K}-\frac{(m_1-\ell_1)B}{r\cos\chi}\underset{\sim}{h}\right]\ \sum_s\ \delta\left(k_2-\frac{s+m_1B}{r}\right)\ . \qquad (166)$$

Equation (166) contains two summations over the number of stator vanes, V. These can be summed explicitly if we note that the wavenumber-frequency spectrum contains the factor

$$\delta[\underset{\sim}{k}-\underset{\sim}{K}-(m_1-\ell_1)\ B\underset{\sim}{n}/r\cos\chi]\ \delta\left(k_2-\frac{s+mB}{r}\right)\quad ,$$

which means that we can set $k_2 = (s+m_1B)/r$ and $K_2 = (s+\ell_1B)/r$ everywhere they appear. Also, the intervane gap on the stator is $\underset{\sim}{H} = (2\pi r\underset{\sim}{e}_2/V)$, so

$$\underset{\sim}{k}\cdot\underset{\sim}{H} = 2\pi(s+m_1B)/V$$

$$\underset{\sim}{K}\cdot\underset{\sim}{H} = 2\pi(s+\ell_1B)/V$$

and

$$\sum_{j=0}^{V-1} \exp[ij(2\pi m/V + \underset{\sim}{k}\cdot\underset{\sim}{H})]$$

$$= V \text{ if } m + s + m_1 B = p_1 V$$

$$= 0 \text{ otherwise; and}$$

$$\sum_{\ell=0}^{V-1} \exp[i\ell(2\pi m/V + \underset{\sim}{K}\cdot\underset{\sim}{H})]$$

$$= V \text{ if } m + s + \ell_1 B = q_1 V$$

$$= 0 \text{ otherwise,}$$

where p_1 and q_1 are arbitrary integers, positive, negative, or zero. If we eliminate m and s from the equations

$$m + s + m_1 B = p_1 V$$

$$m + s + \ell_1 B = q_1 V \quad ,$$

we obtain the following relationship between m_1, ℓ_1, and p_1, q_1:

$$(m_1 - \ell_1)B = (p_1 - q_1)V \quad .$$

This equation has integer solutions for arbitary integers m_1 and ℓ_1 only if $p_1 - q_1 = jB$ for some integer j. Then $m_1 - \ell_1 = jV$. If we set $\ell_1 = m_1 - jV$, then $s = q_1 V - m_1 B - jVB - m$. The summations over ℓ_1 and s_1 can thus be changed into summations over q_1 and j. When this is done, the quantity in braces in Eq.(163) becomes

$$\{\text{Eq. (163)}\} \frac{(\rho_0 U_r \epsilon_w WBV\delta)^2}{(2\pi r)^2 r} \quad .$$

$$\sum_{m_1} \sum_{q_1} \sum_{j} \hat{f}\left(\frac{m_1 B\delta}{r}\right) \hat{f}^*\left[\frac{(m_1 - jV)B\delta}{r}\right]$$

(Cont.)

$$\cdot \iint f(r',z',\underset{\sim}{k},\omega) \iint f^*(r'',z'',\underset{\sim}{K},\nu) \cdot$$

$$\hat{\hat{\phi}}\left(\underset{\sim}{k} - \frac{m_1 B}{r\cos\chi}\,\underset{\sim}{n},\Delta r\right)\ \delta\left[k_2 - \frac{(q_1 V - jBV - m)}{r}\right]$$

$$\cdot\ \delta\left(\underset{\sim}{K}-\underset{\sim}{k} + \frac{jBV}{r\cos\chi}\,\underset{\sim}{n}\right)\ \delta(\omega - JBV - \underset{\sim}{U}_r\cdot\underset{\sim}{k})\ d^2K\ d^2k$$

$$\cdot\ \delta(\nu-\omega-jBV)\ \cdot\ \exp\left(\frac{ijBV}{r\cos\chi}\,\underset{\sim}{n}\cdot\underset{\sim}{D}\right) \quad .$$

Those terms in this equation with j = 0 represent fluctuations at frequencies jBVΩ. The time-averaged modal spectral density is obtained by eliminating the summation on j and setting j = 0. Because of the factor $\delta(K-k)$ $\delta(\nu-\omega)$, we can set $\underset{\sim}{K} = \underset{\sim}{k}$ and $\nu = \omega$ wherever they appear. Integrating with respect to $\underset{\sim}{K}$ and $\underset{\sim}{k}$, we obtain

$$\{\text{Eq. (163)}\} = \frac{(\rho_0 U_r \varepsilon_w WBV\delta)^2}{(2\pi r)^2 r}\ \delta(\nu-\omega)\ \cdot$$

$$\sum_{m_1}\sum_{q_1}\left|\hat{f}\left(\frac{m_1 B\delta}{r}\right)\right|^2 \cdot f(r',z',\underset{\sim}{k},\omega)\ \cdot$$

$$f^*(r'',z'',\underset{\sim}{k},\omega)\ \hat{\hat{\phi}}\left(\underset{\sim}{k} - \frac{m_1 B}{r\cos\chi}\,\underset{\sim}{n},\Delta r\right) \quad , \qquad (167)$$

where now $\underset{\sim}{k}$ is a specific vector whose components in the axial and circumferential directions are

$$k_1 = \frac{\omega}{U_{r_1}} - \frac{U_{r1}}{U_{r_1}}\left(\frac{q_1 V - m}{r}\right)$$

$$k_2 = (q_1 V - m)/r \quad . \tag{168}$$

Equation (167) can be considerably simplified if we accept two approximations. The first is that the radial integral scale of the wake turbulence is much smaller than the stator vane chord. If this is so, we can replace r' and r" by their mean value $r = \frac{1}{2}(r'+r")$ everywhere but in the last argument of the correlation function ϕ. The second approximation is that the stator vanes are roughly aligned with the mean velocity in the wakes, so that the chordwise component of the wavenumber can be approximated as

$$k_c = (\underset{\sim}{U}_r \cdot \underset{\sim}{k})/U_r$$

$$= \omega/U_r \quad .$$

This expression contains neither of the summation indices m_1 or q_1. The inter-blade phase angle, which is the product of the circumferential component of the wavenumber and the inter-blade gap, does contain q_1, but only as an integral multiple of 2π. But the kernel function K_c is a periodic function of the inter-blade phase angle, and the period is 2π. The indicial chordwise loading function $f(r,z,k,\omega)$ is therefore independent of m_1 and q_1, and so can be removed from the summations in Eq. (167). We then have

$$\{\text{Eq. (163)}\} = \left(\frac{\rho_0 U_r \epsilon_w WBV\delta}{2\pi r}\right)^2 \frac{\delta(\nu-\omega)}{rU_{r_1}}$$

(Cont.)

$$\hat{f}(r,z',\underset{\sim}{k},\omega)\ \hat{f}^*(r,z'',\underset{\sim}{k},\omega)\ \cdot$$

$$\sum_{m_1}\sum_{q_1} \hat{\phi}(\underset{\sim}{k} - \frac{m_1 B}{r\cos\chi}\ \underset{\sim}{n},\Delta r) \quad . \tag{169}$$

The expected value of the (m,n)th duct mode may now be written as shown below, by substituting Eq. (169) into Eq. (163):

$$\langle \bar{p}_{mn}(\omega)\ \bar{p}^*_{m_1}(\nu)\rangle =$$

$$\left(\frac{\rho_0 \varepsilon_w B V \delta}{2\pi}\right)^2 \frac{\delta(\nu-\omega)}{4\Gamma^2 k^2_{n,m}(\omega)} \quad \cdot$$

$$\int_{r_H}^{r_D}\int_{r_H}^{r_D} \frac{U^2_r(r)W(r)}{U_{r_1}(r)r^3}\ \psi^2_m(\kappa_{m,n}r)\ \cdot$$

$$\left(\frac{m}{r}\cos\theta+\gamma_{n,m}\sin\theta\right)^2 \cdot b^2(r)|C_{mn}(r)|^2 \cdot$$

$$\sum_{m_1}\sum_{q_1} \left|\hat{f}\left(\frac{m_1 B\delta}{r}\right)\right|^2 \hat{\phi}(\underset{\sim}{k} - \frac{m_1 B}{r\cos\chi}\ \underset{\sim}{n})\ dr'\ dr'' \quad . \tag{170}$$

In this equation, $C_{mn}(r)$ is the chordwise integral of the elemental loading function,

$$C_{mn}(r) = \int_{-b}^{+b} f(r,z,\underset{\sim}{k},\omega)\ \exp(i\mu z)\ dz/b \tag{171}$$

and

$$\mu \equiv \gamma_{n,m}\cos\theta - \frac{m}{r}\sin\theta \quad . \tag{172}$$

In Chap. 6, the correlation function of the inlet turbulence was approximated as the product of three functions, each of which depended on only one variable. The object of this procedure is to facilitate the use of experimental data to select the appropriate correlation function. We will adopt the same tactic here:

$$\phi(\underset{\sim}{x},\Delta r) = \phi_1(x_1/L_1)\ \phi_2(x_2/L_2)\ \phi_r(\Delta r/L_r) \tag{173}$$

so that

$$\hat{\hat{\phi}}(\underset{\sim}{k},\Delta r) = L_1L_2\hat{\phi}_1(k_1L_1)\ \hat{\phi}_2(k_2L_2)\ \phi_r(\Delta r/L_r) \tag{174a}$$

and

$$\hat{\hat{\phi}}\ (\underset{\sim}{k} - \frac{m_1\underset{\sim}{Bn}}{r\cos\chi},\Delta r) = L_1L_2\ \hat{\phi}_1(\lambda_1L_1)\hat{\phi}_2(\lambda_2L_2)\phi_r(\Delta r/L_r)\ , \tag{174b}$$

where

$$\lambda_1 \equiv \frac{\omega+m_1B\Omega}{U_{r_1}} - \frac{U_{r_2}}{U_{r_1}}\left(\frac{q_1V-m_1B-m}{r}\right)$$

$$\lambda_2 \equiv \frac{q_1V-m_1B-m}{r}\ . \tag{175}$$

By changing the integration variables in Eq. (170) from r' and r" to $r = \frac{1}{2}(r'+r")$ and Δr, and by approximating the integral over Δr by the following infinite integral,

$$\int \phi(\Delta r/L_r)\ d(\Delta r) = L_r\ ,$$

the double integration over the radius in Eq. (170) can be reduced to a single integral:

$$\langle\bar{p}_{mn}(\omega)\ \bar{p}^*_{m\nu}(\nu)\rangle =$$

(Cont.)

$$\left(\frac{\rho_0 \varepsilon_w BV\delta}{2\pi}\right)^2 \frac{\delta(\nu-\omega)}{4\Gamma k^2_{n,m}(\omega)} L_1 L_2 L_r$$

$$\int_{r_H}^{r_D} \frac{U_r^2(r)W(r)}{U_{1r}(r)r^3} \psi_m^2(\kappa_{m,n}r) \cdot$$

$$\left(\frac{m}{r}\cos\theta+\gamma_{n,m}\sin\theta\right)^2 b^2(r) \left|C_{mn}(r)\right|^2$$

$$\sum_{m_1} \sum_{q_1} \left|\hat{f}\left(\frac{m_1 B\delta}{r}\right)\right|^2 \hat{\phi}_1(\lambda_1 L_1) \phi_2(\lambda_2 L_2)\, dr \quad . \qquad (176)$$

In this equation, the chordwise integral $C_{mn}(r,\omega)$ is defined just as it was in Chapter 6:

$$C_{mn}(r,\omega) = \int_{-b}^{+b} f(r,z,\underset{\sim}{k},\omega) \exp(i\mu z)\, dz/b \quad , \qquad (177)$$

where now

$$\mu = \gamma_{n,m}\cos\theta - \frac{m}{r}\sin\theta \quad . \qquad (178)$$

The mean-squared value of the (m,n)th mode can be calculated by integrating over ω and ν:

$$\langle p^2_{mn}\rangle = \int \langle \hat{p}_{mn}(\omega)\, \hat{p}^*_{mn}(\nu)\rangle \cdot$$

$$\exp[i(\nu-\omega)t] \frac{d\nu}{2\pi} \frac{d\omega}{2\pi} \quad . \qquad (179)$$

The result is

$$\langle p_{mn}^2 \rangle = \int \left(\frac{\rho_0 \varepsilon_w BV\delta}{2\pi}\right)^2 \frac{L_1 L_2 L_r}{4\Gamma k_{n,m}^2(\omega)}$$

$$\int_{r_H}^{r_D} \frac{U_r^2(r)W(r)}{U_{r_1}(r)r^3}\, \psi_m^2(\kappa_{m,n} r) \cdot$$

$$\left[\frac{m}{r}\cos\theta + \gamma_{n,m}(\omega)\sin\theta\right]^2 b^2(r)\left|C_{mn}(r,\omega)\right|^2$$

$$\sum_{m_1}\sum_{q_1}\left|\hat{f}\left(\frac{m_1 B\delta}{r}\right)\right|^2 \hat{\phi}_1(\lambda_1 L_1)\, \hat{\phi}_2(\lambda_2 L_2)\, dr \cdot \frac{d\omega}{2\pi} \quad , \qquad (180)$$

and the modal spectral density of the (m,n)th mode is the integrand of the integration with respect to $\omega/2\pi$:

$$P_{mn}(\omega) = \left(\frac{\rho_0 \varepsilon_w BV\delta}{2\pi}\right)^2 \frac{L_1 L_2 L_r}{4\Gamma^2 k_{n,m}^2(\omega)}$$

$$\int_{r_H}^{r_D} \frac{U_r^2(r)W(r)}{U_{r_1}(r)r^3}\, \psi_m^2(\kappa_{m,n} r) \cdot$$

$$\left[\frac{m}{r}\cos\theta + \gamma_{n,m}(\omega)\sin\theta\right]^2 b^2(r)\left|C_{mn}(r,\omega)\right|^2$$

$$\cdot \sum_{m_1}\sum_{q_1}\left|\hat{f}\left(\frac{m_1 B\delta}{r}\right)\right|^2 \hat{\phi}_1(\lambda_1 L_1)\, \hat{\phi}_2(\lambda_2 L_2)\, dr \, . \qquad (181)$$

As discussed in the previous section, the modal spectral density will be broadband in nature unless the rotor blade wake width is less than the rotor blade spacing, and the axial integral scale of the wake turbulence is considerably larger than the rotor blade gap.

7.5 Sound Power Flux Generated by the Interaction Between the Rotor Blade Wake Turbulence and the Stator Vanes

The sound power flux within the duct is obtained from Eq. (34):

$$S(\omega) = \frac{\pi(r_D^2-r_H)^2}{\rho_0 U} \sum_m \sum_n G_{mn}(\omega)\, P_{mn}(\omega) \quad , \tag{182}$$

where $G_{mn}(\omega)$ is the quantity in braces in Eq. (35). If we introduce $S_{mn}(\omega)$ as the sound power flux per mode, i.e.,

$$S_{mn}(\omega) \equiv \frac{\pi(r_D^2-r_H^2)}{\rho_0 U}\, G_{mn}(\omega)\, P_{mn}(\omega) \quad , \tag{183}$$

then the total sound power flux is obtained by summing over m and n:

$$S(\omega) = \sum_m \sum_n S_{mn}(\omega) \quad . \tag{184}$$

In the computer program, both $S(\omega)$ and $S_{mn}(\omega)$ have been divided by $\rho_0 c_0^2 r_D^3$ to make them dimensionless. Using the dimensionless variables defined in Appendix A , the following expressions are obtained:

$$\frac{S(\omega)}{\rho_0 c_0^2 r_D^3} = \sum_{m=-\infty}^{+\infty} \sum_{n=1}^{\infty} \frac{S_{mn}(\omega)}{\rho_0 c_0^2 r_D^3} \quad , \tag{185}$$

where

$$\frac{S_{mn}(\omega)}{\rho_0 c_0^2 r_D^3} = \frac{\beta^4 M_T (\omega/\Omega)(\varepsilon_w B V \delta)^2 \bar{L}_1 \bar{L}_2 \bar{L}_r M^3 \sigma_c^2}{64\pi^4 (1-\sigma_r)^2 \bar{k}_{n,m} \left(\frac{M_T \omega}{\Omega} \pm M\bar{k}_{n,m}\right)^2} \tag{186}$$

(Cont.)

$$\cdot \int_{\sigma_r}^{1} \frac{\bar{b}^2}{x^2 \cos\chi} \sqrt{1+\left(\frac{M_T x}{\bar{M}}\right)^2}\ \psi_m^2(X_{m,n}x)\ \left|C_{mn}(x,\frac{\omega}{\bar{\Omega}})\right|^2 \cdot$$

$$(\frac{m}{x}\cos\theta+\bar{\gamma}_{n,n}\sin\theta)^2 \sum_{m_1}\sum_{q_1}\left|\hat{f}\left(\frac{m_1 B\bar{\delta}}{x}\right)\right|^2 \cdot$$

$$\hat{\phi}_1(\lambda_1 L_1)\ \hat{\phi}_2(\lambda_2 L_2)\ \frac{dx}{x} \quad .$$

The numerical methods used in compute this integral are discussed in Chapter 8 .

CHAPTER 8

COMPUTER PROGRAMS

Computer programs have been written which compute the sound power per mode and the total sound power flux upstream and downstream of a turbofan for the three noise source mechanisms discussed in Chapters 5, 6, and 7. These computer programs are discussed in general terms in this Chapter; FORTRAN listings and sample displays of the input and output data are provided in Volume 2.

8.1 Rotor Mean Wake Velocity Deficit

The mean wake program computes the complex amplitude of each propagating mode excited by the interaction of the stator vanes with the mean velocity deficit wake of the rotor. The sound power flux per mode is also computed, and by summing over all propagating modes, the total sound power flux is obtained. Recall that a multivaned stator excites only a subset of the propagating modes at any given frequency; specifically, only modes whose number of diametral nodes m is related to the number of rotor blades and stator vanes by the equation $m = pV - qB$, where p and q are arbitrary integers. The program takes this selection mechanism into account in choosing which mode amplitudes to compute.

A dimensionless version of Eq. (87) is used to compute the complex amplitude of each of the modes at the first three harmonics of the blade passage rate. The dimensionless form of Eq. (87) is written out below:

$$\frac{P_{m,n,q}}{\rho_0 U^2} = \frac{(U_r/U)^2\, V}{2\pi(1-\sigma_r^2)\,\hat{k}_{n,m,q}} \cdot$$

$$\int_{\sigma_r}^{1} \frac{w_q}{U_r}\, \psi_m(X_{mn}x) \left(\frac{m}{x}\cos\theta + \bar{\gamma}_{n,m,q}\sin\theta\right) \cdot$$

$$\exp\left[i\,\bar{\gamma}_{n,m,q}\bar{\delta}_1 - \frac{m}{x}\bar{\delta}_2\right] \tilde{b}\, C_{mnq}(x)dx \quad . \qquad (187)$$

Given the modal amplitudes $p_{mnq}/\rho U^2$, the total sound power is obtained from Eq. (28). In dimensionless form, this is

$$\frac{\overline{\text{Power}}}{\rho_0 U^3 \Gamma} = \sum_m \sum_n G_{mn}(sB\Omega) \left| \frac{P_{m,n,q}}{\rho_0 U^2} \right|^2 , \qquad (188)$$

where $G_{mn}(qB\Omega)$ is the quantity in braces in Eq. (28) or (29).

In Eq. (187), $C_{mnq}(x)$ is the chordwise integral of the elemental blade loading function $f_q(r,z)$ multiplied by an exponential function:

$$C_{mnq}(x) \equiv \int_{-b}^{+b} f_q(r,z) \exp\left[i \frac{\sigma_c \tilde{b}}{2} \cdot \left(\bar{\gamma}_{n,m,q} \cos\theta - \frac{m}{x} \sin\theta \right) \frac{z}{b} \right] \frac{dz}{b} .$$

Because $f_q(r,z)$ has a square root singularity at the leading edge ($z=-b$), it is necessary to change the integration variable from z to ψ, where $z = b\cos\psi$. We then have

$$C_{mnq}(x) = \int_0^{\pi} f_z(r,z) \sin\psi \cdot \exp\left[i \frac{\sigma_c \tilde{b}}{2} \left(\bar{\gamma}_{n,m,q} \cos\theta - \frac{m}{x} \sin\theta \right) \cos\psi \right] d\psi \qquad (189)$$

This integral is easy to compute numerically using Simpson's rule, because the product $f_q(r,z)\sin\psi$ is finite at the leading edge ($\psi=0$). The spanwise integration requires special treatment, however, because w_q is the qth Fourier coefficient of the component of the rotor mean wake normal to the stator chord,

$$w_q = W_q \sin(\theta+\chi) \exp - \frac{iqB}{r} (D_2 - D_1 \tan\chi)$$

contains a phase angle which varies rapidly over the span when the separation between rotor and stator is large or when the rotor wake angle χ is a strong function of the radius r. To handle this rapidly varying phase, an

adaptation of Filon's rule of integration has been used in place of Simpson's rule for the spanwise integration (see Appendix G).

8.2 Inlet Turbulence and Rotor Wake Turbulence

Random loads on the rotor or stator blades caused by convected turbulence generate continuous noise spectra, as opposed to the purely tonal noise generated by the rotor mean velocity deficit wakes. To plot these continuous spectra accurately, it is necessary to compute the modal power flux in the turbofan duct at many more frequencies than are required for the mean wake tone noise. To save computer time, therefore, it was decided first to compute and store the elemental blade loading functions $f(r,z,\tilde{k},\omega)$ over a predetermined range of frequency and wavenumber, and then to interpolate between these values to compute the power spectral density at intermediate values of the frequency. The advantage gained by doing this arises from the fact that the elemental loading functions can be computed and stored once and for all for a given rotor/stator geometry. Once this has been accomplished, parameter variations (frequency, turbulence length scales, etc.) for the chosen rotor/stator geometry can be conducted conveniently and economically. The elemental loading functions have been found to be reasonably smoothly varying functions of the frequency (and for convected turbulence frequency and wavenumber are related), so acceptable accuracy (within 5%) can be obtained by computing and storing the loading functions at integer multiples of the rotor rotation rate Ω. Care must be taken, however, to assure that the array of stored loading functions encompasses the required range of frequency, especially for the inlet turbulence case, because in that situation the frequency appears in the combination $\omega - m\Omega$, where m, the number of diametral nodes, can take on large positive and negative values.

The inlet turbulence and rotor wake turbulence programs print out the spectral density of the power flux per mode for each propagating mode, and by summation, the spectral density of the total sound power flux. Dimensionless expressions for the spectral density of the power flux per mode are given in Eq. (135) (inlet turbulence) and Eq. (186) (rotor wake turbulence). Both equations require numerical integration over the chord and span of the blade (or vane). The integral over the chord is basically the same as the integral required in the mean wake program; the same change of integral variable is used

to eliminate the singularity at the leading edge. Once this change of variable has been effected, a straightforward application of Simpson's rule is sufficient for both the chordwise and spanwise integrations.

8.3 Integral Equation for the Blade Loading

As discussed in Chapter 3, the elemental blade loading function $f(\cdot,y/b,\ldots)$* is the solution of an integral equation,

$$\exp(ik_c z) = \int_{-b}^{+b} K_c(\cdot, \frac{z-y}{b}, \cdots)\, f(\cdot,y/b,\cdots)\, dy/b \ ,$$

whose kernel function $K_c(\cdot,(z-y)(b,\cdots)$ is derived in Appendix B. Given the elemental blade loading function, the pressure on the blades is obtained by multiplying $f(\cdot,y/b,\cdots)$ by $\rho_0 U_r \hat{w}(r,\underset{\sim}{k},\omega)$ and inverting the Fourier transforms with respect to time and/or space as appropriate.

The integral equation contains two basic difficulties. They are

a. the solution $f(\cdot,z/b,\cdots)$ is singular as $(z+b)^{-\frac{1}{2}}$ at the leading edge ($z=-b$), and

b. the kernel function $K_c(\cdot,y/b,\cdots)$ contains both a Cauchy singularity $(1/y)$ and a logarithmic singularity at $y = 0$.

Difficulty (a) is circumvented by introducing the independent variable transformations

$$z/b = \cos\theta$$

$$y/b = \cos\psi$$

Equation (B.1) then becomes

*In previous chapters, the elemental loading function $f(\ )$ has been written as having dimensional arguments. Use of dimensionless arguments in Chapter 8 is convenient and should cause no confusion.

$$\exp(ik_c b \cos\theta) = \int_0^{\pi} K_c(\cdot,\cos\theta-\cos\psi,\cdots)\, F(\psi)\, d\psi \quad , \tag{190}$$

where $F(\psi) = f(\cdot,\cos\psi,\cdots)\sin\psi$. Whereas $f(\cdot,\cos\psi,\cdots)$ is singular at $\psi = \pi$, $F(\psi)$ is not. Thus the integral equation is solved for $F(\psi)$ rather than for $f(\cdots)$ itself.

To solve Eq. (190), the method of collocation is used. (Refs. 18, 19). That is, the integral on the right-hand side of Eq. (190) is required to equal the forcing function on the left-hand side at the N points.

$$\theta_m = (m-1/2)\pi \; ; \quad m = 1,\cdots N \quad , \tag{191}$$

The equations to be solved are then

$$\exp(ik_c b \cos\theta_m) = I(\theta_m) \; ; \quad m = 1,2,\cdots N \tag{192}$$

where

$$I(\theta) \equiv \int_0^{\pi} K_c(\cdot,\cos\theta-\cos\psi,\cdots)F(\psi)\, d\psi \quad . \tag{193}$$

In computing $I(\theta)$, the left-hand side of Eq. (193), the points

$$\psi_n = n\pi/N \; , \quad n = 0,1,2,\cdots N$$

are used.* Having the collocation and integration points evenly interlaced has the dual effects of avoiding the point $\psi = \theta$, where K_c is singular, and of insuring that the solution obtained satisfies the Kutta condition, which requires that $f(\cdots) = 0$ at the trailing edge.

---

*Because $F(0) = -$, use of $N + 1$ integration points as called for in Eq. (193) introduces only N unknowns $f(f\pi/n)$, $n=1,\ldots N$.

The logarithmic portion of the kernel function must be singled out for special treatment. Thus,

$$K_c(\cdot,y/b,\cdots) = K_1(\cdot,y/b,\cdots) + G(\cdot,y/b,\cdots) \log |y/b|$$

and $I(\theta) = I_1(\theta) + I_L(\theta)$,

where

$$I_1(\theta) = \int_0^\pi K_1(\cdot,\cos\theta-\cos\psi,\cdots)F(\psi)\, d\psi$$

$$I_L(\theta) = \int_0^\pi G(\cdot,\cos\theta-\cos\psi,\cdots) \cdot \log |\cos\theta-\cos\psi| F(\psi)\, d\psi \quad .$$

The trapezoidal rule suffices to compute $I_1(\theta)$,

$$I_1(\theta) = \sum_{n=0}^{N} B_n K_1(\cdot,\cos\theta-\cos\psi_n,\cdots)F(\psi_n)\ \pi/N$$

where $B_0 = B_N = 1/2$, while $B_n = 1$ otherwise; but a special integration rule, devised by Whitehead (Refs. 18, 19) is required for the logarithmic portion of the kernel. Whitehead's integration rule is given below,

$$I_L(\theta) = \sum_{\ell=0}^{N} B_\ell G(\cdot,\cos\theta-\cos\psi_\ell,\cdots) \cdot \log |\cos\theta-\cos\psi_\ell|\ S_\ell(\theta)\ \pi/N \ ,$$

where the B_ℓ's are the same weighting functions as defined above, and

$$S_\ell(\theta) = - \{\log(2) + 2 \sum_{s=1}^{N} (B_s/s) \cos(s\theta) \cos(s\ell\pi/N)\} \quad .$$

By combining $I_1(\theta)$ and $I_L(\theta)$, the integral equation is reduced to the following set of algebraic equations for the unknowns $F(n\pi/N)$:

$$\exp[i(k_c b) \cos(m-1/2)\pi/N] = \sum_{n=0}^{N} A_{mn} F(n\pi/N) \quad ,$$

where

$$A_{mn} = B_n\{K_c(x)+G(x)[S_n(\theta_m)-\log|x|]\ \pi/N$$

and

$$x \equiv \cos(\theta_m) - \cos(\psi_n) \quad .$$

Any standard matrix package that handles equations with complex coefficients can be used to solve these equations.

FORTRAN listings for computer subprograms which compute the elemental loading function f( ), based upon the equations set forth in this section are provided in Volume 2. These subroutines have been used to compute the blade lift and pitching moment coefficients for a cascade of oscillating blades in uniform flow, and for a rigid cascade of blades in a sinusoidal gust, for comparison with results of similar calculations published in the literature (Refs. 18, 19). Agreement was obtained to four significant figures in every case tried. Comparisons have also been made with the loading function itself, published in graphical form by Kaji (Ref. 5). Again agreement was excellent, within the limitations imposed by the small scale in the figures provided in Kaji's paper.

CHAPTER 9

SAMPLE COMPUTATIONS

No computations have been made with the Inlet Turbulence/Rotor Interaction program, and only a few have been made with the Mean Wake/Stator Interaction and Wake Turbulence/Stator Interaction Programs. Typical results from these latter computations are presented in this chapter only as examples of output data generated by the programs; a systematic set of parameter variation studies has not been performed.

The Mean Wake/Stator Interaction Program computes the sound power per mode and the total sound power radiating upstream and downstream of a turbofan at the blade passage frequency and its first two harmonics. The sound radiating upstream from a 15 blade fan and 11 blade stator is displayed in Fig. 10*. As indicated in the Figure, whereas at the blade passage frequency only one propagating mode is excited, many are excited at higher frequencies.

Typical results obtained with the Wake Turbulence/Stator Interaction program are shown in Fig. 11. In this figure, the upstream sound power spectral density for various values of the turbulence length scales is plotted as a function of the frequency. The axial, radial and azimuthal length scales were assumed to be equal. The width of the turbulent wake is $0.072r_D$ and the rms turbulence intensity is assumed to be 1% of the nominal flow velocity. (The sound power is directly proportional to the rms turbulence intensity, so the sound power at any other intensity may be found by shifting the vertical scale in the figure.) It may be seen that increasing the turbulence length scales caused bands of noise to coalesce around harmonics of the blade passage frequncy. However, the length scales required to produce this effect are probably unrealistically long. Individual modal amplitudes are not plotted because of the large number of propagating modes (about 130 modes at three times blade passage frequency).

*The fan/stator geometry is that of NASA Fan Stage 55 (Ref. 20). The input variables used for the computation may be found in Volume 2 (Mean Wake Program).

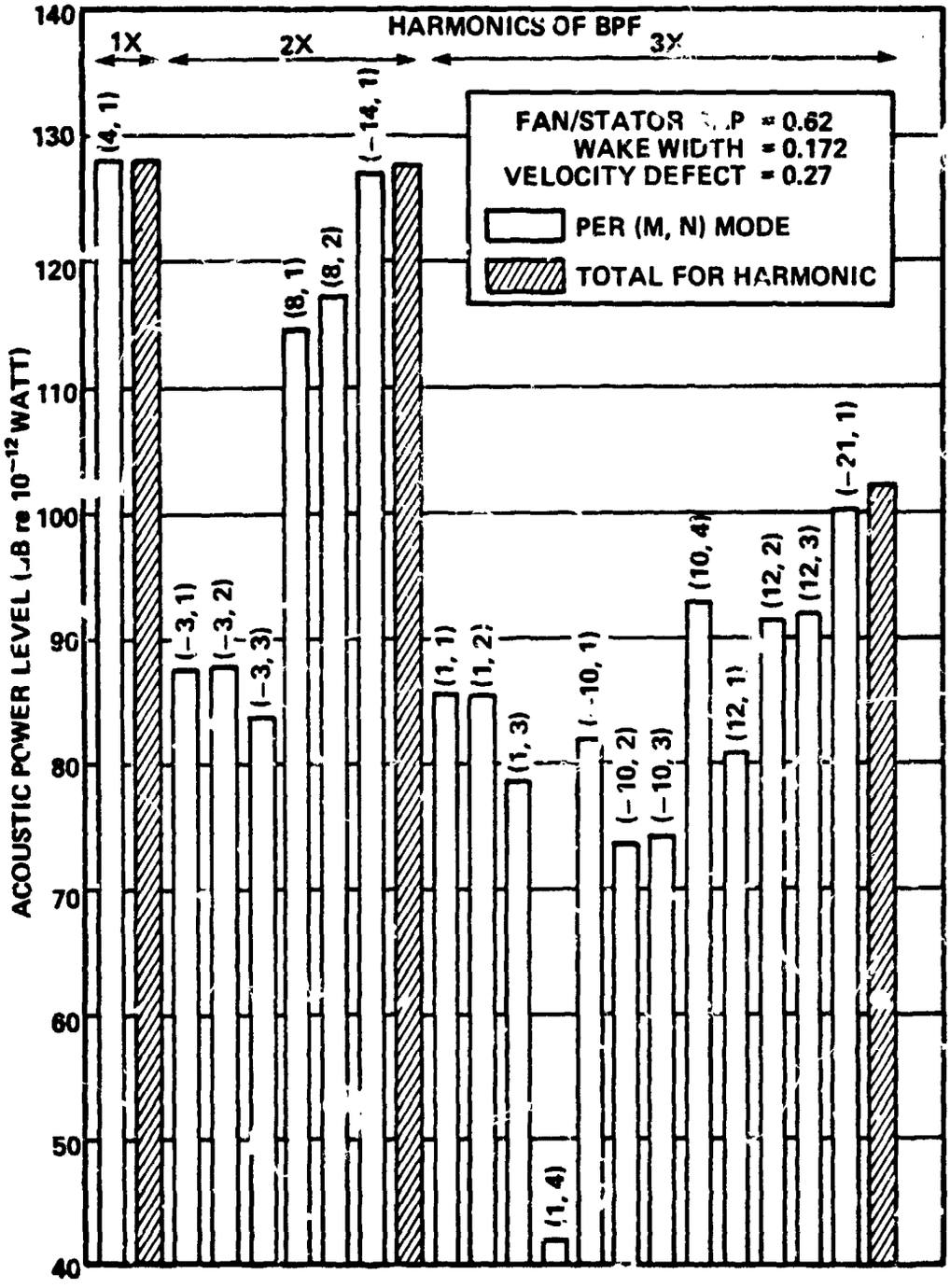

FIG. 10. SOUND POWER/MODE AND TOTAL SOUND POWER: MEAN WAKE/ STATOR INTERACTION.

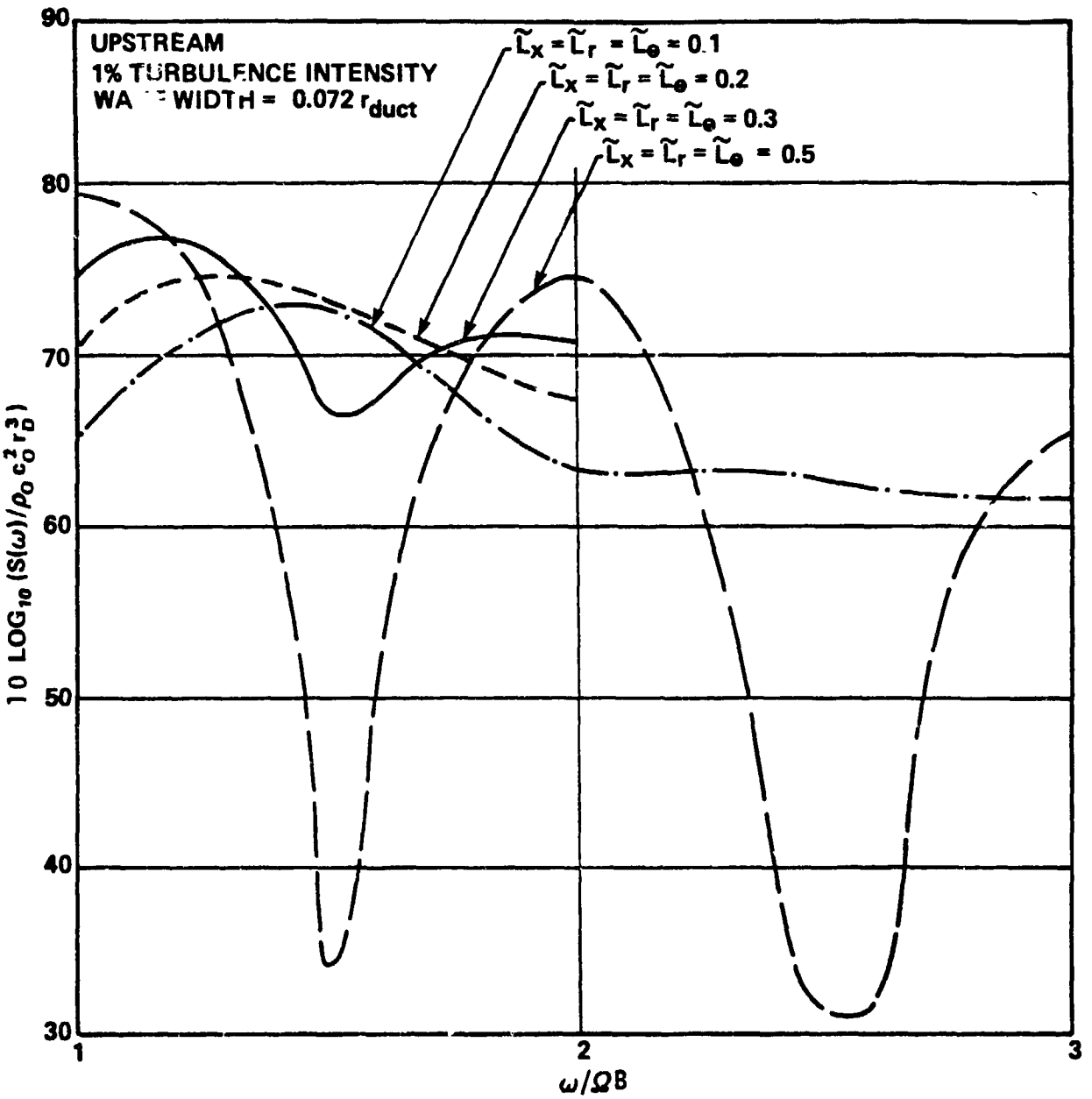

FIG. 11. SOUND POWER: WAKE TURBULENCE/STATOR INTERACTION.

C.2

CHAPTER 10

CONCLUDING REMARKS

Equations have been derived for the amplitudes (or amplitude spectral densities) of the propagating duct modes excited by a turbofan (fan/stator stage) operating at subsonic tip speed within an infinite hard-walled annular duct. Three noise source mechanisms were considered:

a) random noise generated by inlet turbulence impinging on the rotor blades;

b) random noise generated by rotor blade wake turbulence impinging on the stator vanes; and

c) tone noise generated by the mean velocity defect wakes of the rotor blades impinging on the stator vanes.

Equations have also been derived for the acoustic pressure at an arbitrary point within the duct, and for the sound power flux (or sound power spectral density) in the duct either upstream of the fan or downstream of the stator. These latter equations require a summation over all those duct modes that are excited by the particular noise source mechanism of interest and which propagate at the selected frequency.

A package of FORTRAN computer programs has been developed which computes the duct mode amplitudes (or spectral densities of the mode amplitudes) for each of the three noise source mechanisms, and sums these mode amplitudes to compute the sound power flux (or sound power spectral density) within the duct. The inlet turbulence and rotor wake turbulence programs print out, at any desired frequency, the sound power spectral density per mode for all propagating modes and the total sound power spectral density. The mean wake program prints out, at the blade passage frequency and its first two harmonics, the mode amplitude and sound power per mode for each mode excited. The total sound power flux is also printed out at each frequency.

A very limited set of preliminary computations has been carried out using the mean wake and wake turbulence programs. The output data display the expected qualitative behavior, but no attempt has yet been made to make any systematic comparisons with experimental data. No computations have been made with the inlet turbulence program other than those required to verify that the program runs.

REFERENCES

1. Mark, W.D., "Characterization of Rotor Inlet Turbulence for Rotor Noise Predictions." Bolt Beranek & Newman Inc. Technical Memorandum No. 486, December 1978.

2. Kemp, N.H. and W.R. Sears, "Aerodynamic Interference Between Moving Blade Rows," J. Aeron. Sci., 20, 9, 585-597, 1953.

3. Kemp, Nelson H. and W.R. Sears, "The Unsteady Forces Due to Viscous Wakes in Turbomachines," J. Aeron. Sci., 22, 7, 478-483, 1955.

4. Fleeter, Sanford, "Fluctuating Lift and Moment Coefficients for Cascaded Airfoils in a Nonuniform Compressible Flow," J. Aircraft, 10, 2, 93-98, 1973.

5. Kaji, S., "Noncompact Source Effect on the Prediction of Tone Noise from a Fan Rotor," AIAA Paper 75-446, Hampton, VA, March 1975.

6. Kobayashi, H., "Three Dimensional Effects on Pure Tone Fan Noise Due to Inflow Distortion," AIAA Paper 78-1120, July 1978.

7. Kobayashi, H., and Groeneweg, J.F., "Effects of Inflow Distortion Profiles on Fan Tone Noise," AIAA Journal, Vol. 18, No. 8, pp. 899-906, August 1980.

8. Namba, M., "Three-Dimensional Analysis of Blade Force and Sound Generation for an Annular Cascade in Distorted Flows," Journal of Sound and Vibration, Vol. 50, Feb. 1977, pp. 479-508.

9. Namba, M., "Lifting Surface Theory for a Rotating Subsonic or Transonic Blade Row," Aeronautical Research Council, R&M No. 3740, 1974.

10. Hanson, D.B., "Spectrum of Rotor Noise Caused by Atmospheric Turbulence," Journal of the Acoustic Society of America, Vol. 56, July 1974, pp. 110-126.

11. Kerschen, E.J., "Noise Caused by the Interaction of a Rotor with Anisotropic Turbulence," AIAA Journal, Vol. 19, No. 6, pp. 717-723, June 1981.

12. Reynolds, B., Laksminarayana, B., and Ravindranath, A., "Characteristics of the Near Wake of a Compressor or Fan Rotor Blade," AIAA Journal, Vol. 17, No. 9, pp. 959-967, Sept., 1979.

13. Reynolds, B., and Laksminarayana, B., "Characteristics of Lightly Loaded Fan Rotor Blade Wakes," NASA Constructor Report 3188, October 1979.

14. Ravindranath, A., and Laksminarayana, B., "Three Dimensional Mean Flow and Turbulence Characteristics of the Near Wake of a Compressor Rotor Blade," NASA Contractor Report 159518, June 1980.

15. Bliss, D.B., Chandiramani, K.L., and Piersol, A.G., "Data Analysis and Noise Prediction for the QF-1B Experimental Fan Stage," NASA Contractor Report 135066, August 1976.

16. Hanson, D.B., "Unified Analysis of Fan Stator Noise," The Journal of the Acoustical Society of America, Vol. 54, December 1973, pp. 1571-1591.

17. Goldstein, M.E., Aeroacoustics, McGraw-Hill International Book Co., New York, 1976, p. 193.

18. Whitehead, D.S., "Force and Moment Coefficients for Vibrating Aerofoils in Cascade," ARC Reports and Memoranda No. 3254, February 1960.

19. Smith, S.N., "Discrete Frequency Sound Generation in Axial Flow Turbomachines," ARC Reports and Memoranda No. 3709, March 1972.

20. Lewis, G.W., Jr., and Tysl, E.R., "Overall and Blade-Element Performance of a 1.20 Pressure-Ratio Fan Stage at Design Blade Setting Angle," NASA TM X-3101, September 1974.

APPENDIX A

LIST OF SYMBOLS

A_{mn}	mode amplitude (Eq. 23)
B	# or rotor blades
b	blade/vane semi-chord
b_r	blade/vane semi-chord at radius r
b_t	blade/vane semi-chord at tip
C_{mn}	chordwise integral (Eq. 130)
C_c	speed of sound
$\underset{\sim}{D}$	displacement vector extending from rotor blade to stator vane (Eq. 62)
d	axial distance from rotor to stator
exp ( )	exponential function
$\underline{e}_1$, $\underline{e}_2$	unit vectors (Fig. 4)
$F(\underset{\sim}{X} \cdot \underset{\sim}{u})$	amplitude of turbulence intensity in rotor blade wake
f (r, z, $\underline{k}$, ω)	elemental blade/vane chordwise pressure distribution (Eq. 55)
$f_q(r,z)$	elemental vane chordwise pressure distribution at qth harmonic of the blade passage frequency (Eq. 85)
f(y)	mean rotor wake velocity deficit profile (Chapter 3): or rotor wake rms turbulence intensity profile (Chapter 5)

$G_{mn}(\omega)$	See Eqs. (134) and (35)
$g\ (r,\ \underset{\sim}{x}-\underset{\sim}{w}t)$	See Eq. (141)
H	inter-vane gap (stator)
h	inter-blade gap (rotor)
I	axial intensity
i	$\sqrt{-1}$
$J_m(\ )$	mth order Bessel function of 1st kind
$\underset{\sim}{K} = (K_1, K_2)$	wavenumber vector
$k_{n,m}(\omega)$	See Eq. (39)
$\underset{\sim}{k} = (k_1, k_2)$	wavenumber vector
$\underset{\sim}{k}_p$	particular value of wavenumber vector as defined in Eq. (118)
L_i	Turbulence length scale in the ith direction.
M	axial flow Mach No.
M_r	Mach number of flow relative to blades/vanes
M_T	relative Mach number at the rotor blade tip.
$\underline{N}$	unit vector normal to stator vanes
$\underline{n}$	unit vector normal to rotor blades (Chapter 4); or normal to rotor wake centerlines (Chapter 3 and 5)
p	acoustic pressure
$p_{mn}(\omega)$	duct mode amplitude
$P_{mn}(\omega)$	amplitude spectral density of (m,n)th mode
$R\ (r,\omega)$	See Eq. (116)

r	radial coordinate
r_H	hub radius
r_D	duct radius
$S(\omega)$	total intensity spectral density
$S_{mn}(\omega)$	intensity spectral density of (m,n)th mode
t	time
U	axial fluid velocity
U_r	fluid velocity relative to rotor or stator vanes
V	number of stator vanes
$\underset{\sim}{W}$	velocity downstream of the rotor (defined in rotor-fixed coordinates)
w	component of fluctuating velocity normal to rotor/stator blades
$\underset{\sim}{X} = (X_1, X_2)$	rotor-fixed coordinates
x	axial coordinate
$\underset{\sim}{x} = (x_1, x_2)$	stator-fixed coordinates
$\underset{\sim}{Y}$	integration point (r, y_1, ϕ)
$Y_m(\ )$	mth order Bessel function of 2nd kind
z	chordwise variable

GREEK LETTERS

α	Fourier transform variable
β	$\sqrt{1-M^2}$
β_r	$\sqrt{1-M_r^2}$
$\gamma_{m,n}(\omega)$	See Eq. 11
$\Delta p_s(r,y,\ldots)$	pressure loading on blades (Eq. 53)
Γ	$\pi\ (r_D^2 - r_H^2)$
δ	half-velocity width of rotor mean wake (Chapter 5), or width of turbulent rotor wake (Chapter 7)
$\underline{\delta} = (\delta_1, \delta_2)$	blade/vane sweep
ε_D	rms intensity of the component of the inlet turbulence normal to the blade surface.
ε_W	rms intensity of turbulence on centerlines of rotor wakes (component normal to stator vanes)
θ	stagger angle of stator vanes
$\kappa_{m,n}$	eigenvalues of annular duct modes
$\underline{\lambda} = (\lambda_1, \lambda_2)$	Fourier transform variable
$\mu(r,\omega)$	See Eq. (117)
ν	radian frequency
$\underline{\xi}$	integration variable (Eq. 153)
π	3.14159...

ρ_o	nominal fluid density
σ	interblade phase angle
σ_r	r_H/r_D
σ_c	$2b_T/r_D$
τ	time
ϕ	polar angle
χ	rotor blade stagger angle
$X_{m,n}$	$\kappa_{m,n}r_D$
$\psi_m(\kappa_{m,n}r)$	normal mode
ω	radian frequency
Ω	rotor rotation rate (radians/sec.)
Φ	
Φ_0	

APPENDIX B

KERNEL FUNCTION FOR A LINEAR CASCADE IN SUBSONIC FLOW

The kernel function for a cascade of thin airfoils in oscillating subsonic flow has been dervied by several investigators, using a variety of methods (Refs. 1–6). Of the various approaches employed to date, the method of Fourier transforms is perhaps the most straightforward. This procedure was used in Ref. 3, for example, but the inversion of the Fourier transform was accomplished numerically. More recently, Goldstein (Ref. 7) pointed out that the Fourier transform of the kernel function contains no branch points, so the inversion can be accomplished quite easily by using the Cauchy residue theorem. Goldstein outlined the procedure to be followed, but did not actually carry out the calculation of the kernel function. The purpose of this Appendix is to set forth the details of the inversion, and to record the end result. For the convenience of the reader, as well as to document the notation used, a brief derivation of the transform of the kernel function is also presented.

The cascade geometry is shown in Fig. B.1. The airfoil semichord is b, and the gap between neighboring airfoils is bh, with components bh_1 projected along the chord, and bh_2 normal to the chord. The airfoils are shown as having no camber, because the ultimate objective is to calculate the pressure field scattered by the cascade when it is subjected to vorticity convected with the mean flow. However, other situations, such as a cascade of oscillating airfoils, can be handled as well. For the purpose of calculating the kernel function, we need only suppose that a known chordwise pressure distribution exists on each airfoil, and calculate the resulting velocity field.

The first step is to calculate the upwash generated by a single airfoil. Let the pressure be given by the real part of $p \exp(i\omega t)$, and the corresponding velocity field be the real part of $(w_1, w_2) \exp(i\omega t)$. Then p satisfies the convected wave equation, and the velocity field is related to the gradient of p through the momentum equations. These equations are*

*A list of symbols for Appendix B is provided on page B12.

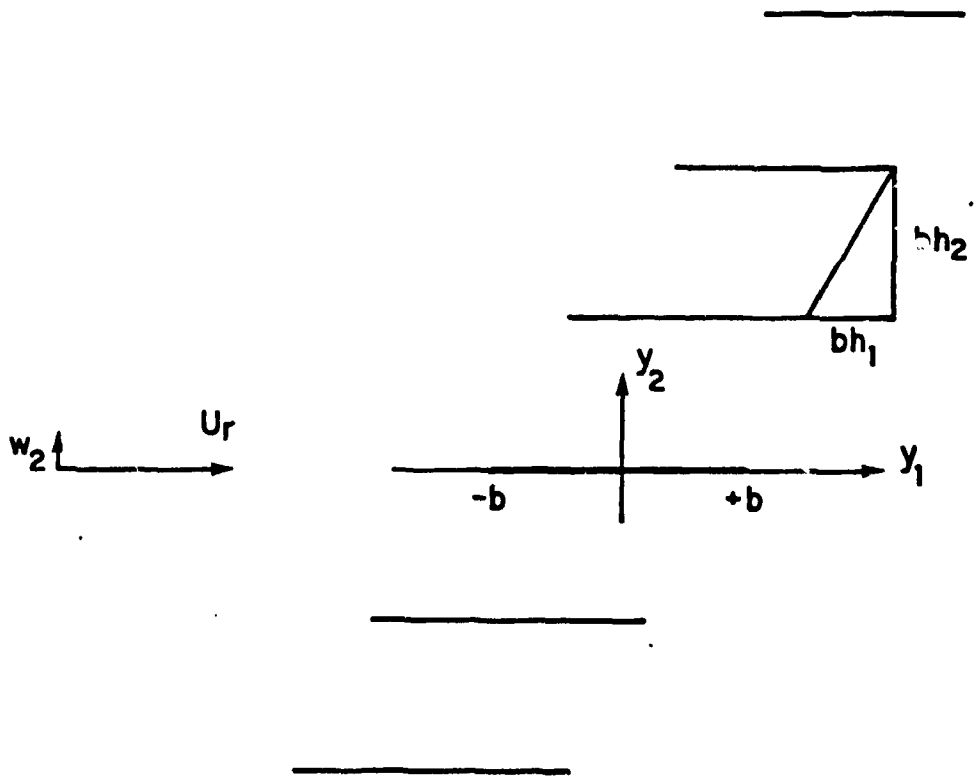

FIG. B.1. CASCADE GEOMETRY.

$$\frac{\partial^2 p}{\partial y_1^2} + \frac{\partial^2 p}{\partial y_2^2} - \frac{1}{c_0^2}\left(i\omega + U_r \frac{\partial}{\partial y_1}\right)^2 p = 0 \quad , \tag{B.1}$$

$$(i\omega + U_r \frac{\partial}{\partial y_1})\, w_j + \frac{1}{\rho_0}\frac{\partial p}{\partial y_j} = 0 \; ; \quad j=1,2 \quad . \tag{B.2}$$

The following definition of the Fourier transform pair is chosen:

$$\bar{p} = \int_{-\infty}^{+\infty} p \exp(-i\alpha y_1)\, dy_1$$

$$p = \frac{1}{2\pi}\int_{-\infty}^{+\infty} \bar{p} \exp(+i\alpha y_1)\, d\alpha \quad . \tag{B.3}$$

The Fourier transforms of Eq. (B.1)* and the second of Eqs. (B.2) are

$$\frac{d^2\bar{p}}{dy_2^2} - \lambda^2 \bar{p} = 0 \quad , \tag{B.4}$$

$$(i\omega + i\alpha U_r)\, \bar{w}_2 + \frac{1}{\rho_0}\frac{\partial \bar{p}}{\partial y_2} = 0 \quad , \tag{B.5}$$

where

$$\lambda \equiv \{\alpha^2 - M_r^2\,(\alpha+\omega/U_r)^2\}^{\frac{1}{2}} \quad . \tag{B.6}$$

The pressure p generated by an isolated airfoil is bounded at infinity, and, because the airfoils are assumed to have zero thickness, is antisymmetric in y_2. A solution of Eq. (B.4) satisfying these conditions is

*All equation references are to equations in this Appendix.

$$\bar{p} = -\frac{\Delta\bar{p}(\alpha)}{2} \exp(-\lambda|y_2|) \cdot \mathrm{sgn}(y_2) \ , \qquad (B.7)$$

provided that λ is defined so that its real part is non-negative on the path of integration used to invert the Fourier transform. In Eq. (B.7), $\Delta\bar{p}(\alpha)$ is the Fourier transform of the chordwise pressure distribution on the airfoil. (Δp is positive if the pressure is greatest on the lower face of the airfoil.) By eliminating $\bar{p}$ between Eqs. (B.5) and (B.7), we obtain the Fourier transform of the upwash generated by a single airfoil. The upwash itself is

$$\frac{\bar{w}_2(y_1,y_2)}{U_r} = -\frac{1}{2\pi} \int_{-\infty}^{+\infty} \frac{\lambda}{2i(\alpha+\omega/U_r)} \frac{\Delta\bar{p}(\alpha)}{\rho_0 U_r^2}$$

$$\cdot \exp(i\alpha y_1 - \lambda|y_2|) \, d\alpha \ .$$

The upwash generated by a cascade of airfoils, located at the points $(y_1,y_2) = m(bh_1,bh_2)$, $m = 0, \pm1, \pm2, \ldots$, is obtained by summing the contributions of the individual airfoils:

$$\frac{w_2(y_1,y_2)}{U_r} = -\frac{1}{2\pi} \sum_{m=-\infty}^{+\infty} \int_{-\infty}^{+\infty} \frac{\lambda}{2i(\alpha+\omega/U_r)} \frac{\Delta\bar{p}_m(\alpha)}{\rho_0 U_r^2}$$

$$\cdot \exp\{i\alpha(y_1 - mbh_1) - \lambda|y_2 - mbh_2|\} \, d\alpha$$

This infinite series can be summed analytically if the transformed pressure distributions on successive airfoils in the cascade $[\Delta\bar{p}_m(\nabla)]$ are related by a constant increment in phase angle. That is, for any integer m,

$$\Delta\bar{p}_m(\alpha) = \Delta\bar{p}_0(\alpha) \exp(im\sigma) \ ,$$

where $\Delta\bar{p}_0(\alpha)$ is the transform of the pressure on the "zeroth" or reference airfoil, and σ (called the interblade phase angle) is a constant, $0 \le \sigma < 2\pi$. To calculate the upwash near any selected blade, say blade s, introduce

$$x_1 \equiv y_1 - sbh_1$$

$$x_2 \equiv y_2 - sbh_2$$

and

$$n \equiv m - s \quad .$$

Then

$$\frac{w_2}{U_r}(x_1+sbh_1, x_2+sbh_2) =$$

$$-\frac{\exp(is\sigma)}{2\pi}\int_{-\infty}^{+\infty}\frac{\Delta\bar{p}_0(\alpha)}{\rho_0 U_r^2}\,\frac{\lambda\, S(\alpha)\,\exp(i\alpha x_1)}{2i(\alpha+\omega/U_r)}\,d\alpha \quad , \qquad (B.8)$$

where the infinite series

$$S(\alpha) \equiv \sum_{n=-\infty}^{+\infty} \exp\{in\sigma - \lambda|x_2 - nbh_2| - i\alpha nbh_1\}$$

can be summed:

$$S(\alpha) = \frac{1}{2}\left\{\frac{\exp(\frac{1}{2}\Delta_+ - \lambda x_2)}{\sinh(\frac{1}{2}\Delta_+)} - \frac{\exp(\frac{1}{2}\Delta_- + \lambda x_2)}{\sinh(\frac{1}{2}\Delta_-)}\right\} \quad , \qquad (B.9)$$

where

$$\Delta_\pm \equiv \pm\lambda h_2 + i(\sigma - \alpha bh_1) \quad . \qquad (B.10)$$

Now, use the convolution theorem to calculate the inverse of Eq. (B.8):

$$\frac{w_2}{U_r}(x_1+sbh_1, x_2+sbh_2) =$$

$$\exp(is\sigma) \int_{-b}^{+b} K_c(x_1-\zeta, x_2) \frac{\Delta p_0(\zeta)}{\rho_0 U_r^2} \frac{d\zeta}{b} \quad . \tag{B.11}$$

K_c is the desired cascade kernel function:

$$K_c(x_1, x_2) = -\frac{b}{2\pi} \int_{-\infty}^{+\infty} \frac{\lambda S \exp(i\alpha x_1)}{2i(\alpha+\omega/U_r)} d\alpha \quad . \tag{B.12}$$

The factor b is included to make K_c dimensionless.

It is convenient to introduce dimensionless variables, as follows:

$$K \equiv \omega b/\beta_r^2 c_0 \qquad \hat{x}_1 \equiv x_1/b$$

$$\hat{\alpha} \equiv \alpha b - M_r K \qquad \hat{x}_2 \equiv x_2/b \quad . \tag{B.13}$$

The shifted transform variable $\hat{\alpha}$ completes the square in λ:

$$\lambda = \frac{\beta_r}{b}\sqrt{\hat{\alpha}^2-K^2} \quad .$$

Then

$$K_c = -\frac{\beta_r \exp(iKM_r\hat{x}_1)}{2\pi i} \int_{-\infty}^{+\infty} \frac{\gamma S \exp(i\hat{\alpha}\hat{x}_1)}{2(\hat{\alpha}+K/M_r)} d\hat{\alpha} \quad , \tag{B.14}$$

where now

$$\gamma \equiv (\hat{\alpha}^2-K^2)^{\frac{1}{2}} \tag{B.15}$$

$$S \equiv \frac{1}{2}\left\{\frac{\exp(\frac{1}{2}\Delta_+ - \beta_r\gamma\hat{x}_2)}{\sinh(\frac{1}{2}\Delta_+)} - \frac{\exp(\frac{1}{2}\Delta_- + \beta_r\gamma\hat{x}_2)}{\sinh(\frac{1}{2}\Delta_-)}\right\} \tag{B.16}$$

Notice that γS is an even function of γ, so that even though the integrand contains the variable

$$\gamma = \sqrt{\hat{\alpha}^2 - K^2} \quad ,$$

there can be no branch points at $\hat{\alpha} = \pm K$. Thus, if we apply the residue theorem to evaluate the kernel function by closing the path of integration on a large arc in the upper or lower $\hat{\alpha}$ plane, no residual integrals around branch cuts appear; the kernel function is simply the sum of the residues in the upper or lower half plane. To insure that the integrals on the arcs vanish as their radii are allowed to become infinitely large, the integrand in Eq. (B.14) must be modified. First, note that

$$S = \frac{1}{(\beta_r\gamma)^2}\frac{\partial^2 S}{\partial \hat{x}_2^2}$$

so K_c can be written as follows

$$K_c = -\frac{\exp(iKM_r\hat{x}_1)}{2\pi i\beta_r} \cdot \frac{\partial^2}{\partial \hat{x}_2^2}\int_{-\infty}^{+\infty}\frac{S\,\exp(i\hat{\alpha}\hat{x}_1)}{2\gamma(\hat{\alpha}+K/M_r)}\,d\hat{\alpha} \quad . \tag{B.17}$$

The integral above can be evaluated via the residue theorem by using the contours shown in Fig. B.2, and the differentiation with respect to $\hat{x}_2$ carried out afterwards.

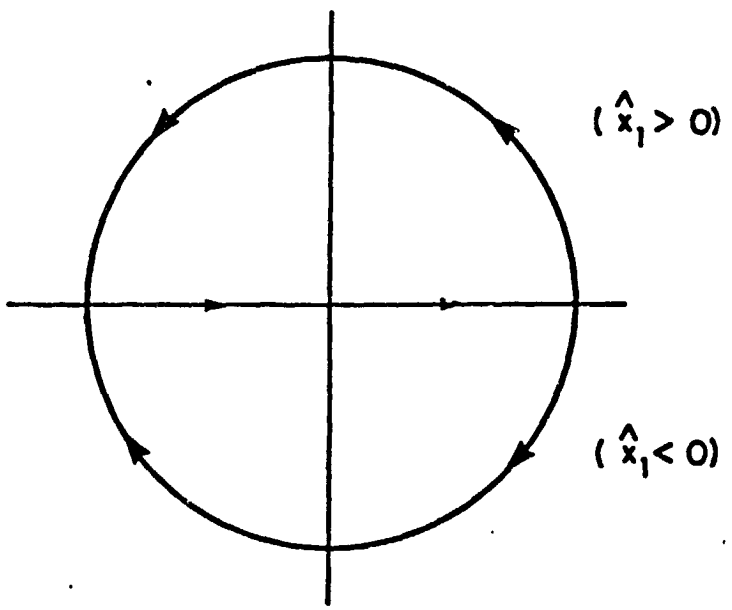

FIG. B.2. INTEGRATION CONTOUR.

If $\hat{x}_1>0$, the integral around the semicircle in the upper half plane vanishes when the radius of the contour goes to infinity. Thus,

$$K_c = -\frac{1}{\beta_r}\exp(iKM_r\hat{x}_1) \cdot \frac{\partial^2}{\partial\hat{x}_2^2}\left\{\begin{matrix}\text{sum of residues in}\\ \text{upper half plane}\end{matrix}\right\} . \qquad (B.18)$$

On the other hand, when $\hat{x}_1<0$ the integral around the contour in the lower half plane vanishes, so

$$K_c = +\frac{1}{\beta_r}\exp(iKM_r\hat{x}_1) \cdot \frac{\partial^2}{\partial\hat{x}_2^2}\left\{\begin{matrix}\text{sum of residues}\\ \text{in lower half plane}\end{matrix}\right\} \qquad (B.19)$$

The integrand in Eq. (B.17) has poles at $\alpha = -K/M_r$, and at points $\alpha_n^{\pm}$, where $\sinh(1/2\Delta_{\pm}) = 0$:

$$\Delta_{\pm} = 2n\pi i \quad (n = \text{any integer}).$$

[c.f. Eq. (B.16)]. When $\Delta_{\pm}$ is real, some of these poles lie directly on the real axis. To arrive at the correct expression of K_c, it is necessary to invoke the casuality condition by stipulating that ω has a small negative imaginary part. Once the kernel function has been evaluated, we can let $\mathrm{Im}(\omega)\to 0$. The effect of this procedure is to eliminate the possibility that acoustic waves not generated by the cascade itself are inadvertantly included in the solution.

If $\mathrm{Im}(\omega)<0$, the pole at $\alpha = -K/M_r$ is clearly in the upper half plane. The residue is

$$R_K = \frac{M_r}{2\beta_r K}\,\frac{\sinh(\beta_r^2 Kh_2/M_r)\exp(-iK\hat{x}_1/M_r)}{\cosh(\beta_r^2 Kh_2/M_r)-\cos(\Gamma+Kh_1/M_r)} . \qquad (B.20)$$

The roots α_n of the equation $\sinh(1/2\Delta_\pm) = 0$ are given by

$$\alpha_n^\pm = \frac{\Gamma_n h_1}{d^2} \pm \frac{\beta_r h_2}{d}\left[K^2 - \left(\frac{\Gamma_n}{d}\right)^2\right]^{\frac{1}{2}} \tag{B.21}$$

where

$$\Gamma_n \equiv \Gamma - 2n\pi$$

$$d = \sqrt{h_1^2+\beta_r^2 h_2^2} \quad . \tag{B.22}$$

If the square root in Eq. (B.21) is defined as follows,

$$[Re^{i\theta}]^{\frac{1}{2}} \equiv \sqrt{R}\, e^{i\theta/2} \quad , \quad 0 \leq \theta < 2\pi \tag{B.23}$$

where $\sqrt{R}$ is the positive square root of R, then solutions $\alpha_n^\pm$ having the plus (minus) sign in Eq. (B.21) are located in the upper (lower) half plane. In either case, the residue is

$$R_n(\alpha_n^\pm) = \frac{\beta_r h_2}{2d^2} \frac{\exp(i\alpha_n^\pm \hat{x}_1)}{\left(\alpha_n^\pm - \frac{\Gamma_n h_1}{d^2}\right)\left(\alpha_n^\pm + \frac{K}{M_r}\right)} \quad . \tag{B.24}$$

Using Eqs. (B.18) and (B.19), and carrying out the indicated differentiations, we obtain the final result:

$$K_c = -\frac{\beta_r^2 K}{2M_r}\frac{\sinh\left(\frac{\beta_r^2 K h_2}{M_r}\right)\exp\left(-\frac{i\beta_r^2 K\hat{x}_1}{M_r}\right)}{\cosh\left(\frac{\beta_r^2 K h_2}{M_r}\right)-\cos\left(\Gamma+\frac{Kh_1}{M_r}\right)}$$

$$-\frac{\beta_r^2 h_2}{2d^2}\sum_{n=-\infty}^{+\infty}\frac{(\alpha_n^{+2}-K^2)\exp[i(\alpha_n^{+}+KM_r)\hat{x}_1]}{\left(\alpha_n^{+}-\frac{\Gamma_n h_1}{d^2}\right)\left(\alpha_n^{+}+\frac{K}{M_r}\right)} \qquad (B.25)$$

if $\hat{x}_1 > 0$, and

$$K_c = \frac{\beta_r^2 h_2}{2d^2}\sum_{n=-\infty}^{+\infty}\frac{(\alpha_n^{-2}-K^2)\exp[i(\alpha_n^{-}+KM_r)\hat{x}_1]}{\left(\alpha_n^{-}-\frac{\Gamma_n h}{d^2}\right)\left(\alpha_n^{-}+\frac{K}{M_r}\right)} \qquad (B.26)$$

if $\hat{x}_1 < 0$. Having calculated the kernal function for $IM(K) < 0$, we can now let $IM(K) \to 0$. Then the roots become, using the branch of the square root given in α_n Eq. (B.22),

$$\alpha_n^{\pm} = \frac{\Gamma_n h_1}{d^2} \pm i\frac{\beta_r h_2}{d}\sqrt{\left(\frac{\Gamma_n}{d}\right)^2 - K^2} \qquad (B.27)$$

if $|\Gamma_n/d| > K$, and

$$\alpha_n^{\pm} = \frac{\Gamma_n h}{d^2} \mp \frac{\beta_r h_2}{d}\sqrt{K^2 - \left(\frac{\Gamma_n}{d}\right)^2} \qquad (B.28)$$

if $|\Gamma n/d| < K$. In Eqs. (B.27) and (B.28), α_n^{+} is to be calculated using the upper set of signs, and a_n using the lower set of signs. The $\sqrt{\ }$ sign means the positive square root.

LIST OF SYMBOLS FOR
APPENDIX B

b	airfoil semi-chord
c_0	speed of sound
d	$\sqrt{h_1^2+\beta_r^2 h_2^2}$
h_1	(inter-blade stagger gap)/b
h_2	(inter-blade normal gap)/b
i	$\sqrt{-1}$
K	reduced frequency [Eq. (13)]
M_r	Mach number
p	pressure
S	Eqs. (9, 16)
t	time
U_r	nominal fluid velocity
(w_1,w_2)	perturbation fluid velocity
(x_1,x_2)	coordinates [Eq. (13)]
(y_1,y_2)	coordinates (Fig. 1)
α	Fourier transform variable
$\hat{\alpha}$	$\alpha b-M_r K$
β_r	$\sqrt{1-M_r^2}$
γ	$\sqrt{\hat{\alpha}^2-K^2}$
Δ_t	Eq. (10)

λ	Eq. (6)
π	3.14159 ...
ρ_0	nominal flow density
σ	interblade phase angle
ω	frequency

APPENDIX C

NUMERICAL COMPUTATION OF THE NORMAL MODES IN AN ANNULAR DUCT

As discussed in Chapter 2, the normal modes in an annular duct are functions of the form

$$\psi_m(\kappa_{mn}r) = A\, J_m(\kappa_{mn}r) + B\, Y_n(\kappa_{mn}r) \quad , \tag{C.1}$$

where $J_m(\ )$ and $Y_m(\ )$ are Bessel functions of the first and second kinds, and κ_{mn} are the roots of the following transcendental equation:

$$\begin{vmatrix} J'_m(\kappa_{mn}r_H) & Y'_m(\kappa_{mn}r_H) \\ J'_m(\kappa_{mn}r_D) & Y'_m(\kappa_{mn}r_D) \end{vmatrix} = 0 \tag{C.2}$$

The roots $\kappa_{mn}r_D$ of Eq. (C.1) are found by first estimating the root as follows:

$$\kappa_{mn}r_D \doteq \begin{cases} m & \text{if } n = 1 \\ \kappa_{m,n-1}r_D + \pi & \text{if } n > 1 \end{cases} \quad . \tag{C.3}$$

This estimate is refined by incrementing the estimated value of $\kappa_{mn}r_D$ by $\pi/10$ until the determinent in Eq. (C.2) changes sign. The step size is then halved and changed in sign. This process continues until the absolute value of the determinent is reduced to a preassigned value.

Once the eigenvalue κ_{mn} has been computed, the constants A and B are assigned one of the following two sets of values:

$$\left.\begin{aligned} A &= 1 \\ B &= -\frac{A\, J'(\kappa_{mn}r_D)}{Y'_m(\kappa_{mn}r_D)} \end{aligned}\right\} \text{or} \left\{\begin{aligned} A &= -\frac{B\, Y'_m(\kappa_{mn}r_D)}{J'_m(\kappa_{mn}r_D)} \\ B &= 1 \end{aligned}\right. \quad .$$

Of these two sets of values, the one for which (A^2+B^2) is the smaller value is chosen. The desired normalization, namely,

$$\int_{r_D}^{r_H} \psi_m^2(\kappa_{mn}r)\, r dr = \frac{1}{2}\,(r_D^2 - r_H^2)$$

is obtained by computing the value of the integral on the left-hand side of the equation above, using the formula

$$\int_{r_H}^{r_D} \psi_m^2(\kappa_{m,n}r)\, r dr = \frac{1}{2}\left(r^2 - \frac{m^2}{\kappa_{mn}^2}\right) \psi_m^2(\kappa_{mn}r)\Bigg|_{r=r_H}^{r_D} .$$

The constants A and B are then divided by whatever common factor is required to produce the correct normalization.

APPENDIX D

FILON'S INTEGRATION RULE

Filon's integration rule applies to integrals of the form

$$\int_a^b f(x) \exp(igx)\, dx \qquad (D.1)$$

wherein the phase angle gx is large, so that use of the trapezoidal rule or Simpson's rule would require that the interval of integration be divided into many subintervals to obtain an accurate answer. Filon's rule is obtained by assuming that the function f(x) can be approximated by a quadratic function, but the exponential function exp(igx) is integrated exactly, without approximation. To extend this procedure to integrals wherein the phase angle is not a linear function of x, we need only approximate the phase angle as a linear function of x within each subinterval. The most straightforward procedure is to approximate both f(x) and g(x) as linear functions of x. For example, to compute the following integral

$$I \equiv \int_a^b f(x) \exp[ig(x)]\, dx \quad ,$$

divide the interval (a,b) into N equal subintervals of length h = (b-a)/N. The integral over the nth subinterval is then

$$I_n = \int_{x_n}^{x_n\text{th}} f(x) \exp[ig(x)]\, dx \quad .$$

To compute this integral, approximate both f(x) and g(x) as linear functions:

$$f(x) = f_n + (f_{n+1}-f_n)\left(\frac{x-x_n}{h}\right)$$

$$g(x) = g_n + (g_{n+1}-g_n)\left(\frac{x-x_n}{h}\right) \quad ,$$

where $f_n = f(x_n)$, and so on. Carrying out the integrations, we obtain

$$I_n = h(a^* f_n + a f_{n+1}) \exp(ig_0) \quad ,$$

where

$$g_0 \equiv \frac{1}{2} (g_n + g_{n+1})$$

$$\lambda \equiv \frac{1}{2} (g_{n+1} - g_n)$$

$$a \equiv \frac{\sin\lambda}{2\lambda} + i\left(\frac{\sin\lambda}{2\lambda^2} - \frac{\cos\lambda}{2\lambda}\right)$$

and a^* is the complex conjugate of a. When $\lambda \to 0$, the integral over the nth subinterval becomes

$$I_n = \frac{h}{2} (f_n + f_{n+1}) \quad ,$$

which is the trapezoidal rule.

If an even number of subintervals are used, it is also possible to approximate f(x) as a quadratic function (over any two neighboring subintervals) while leaving the phase angle g(x) as a linear function of x. This integration scheme reduces to Simpson's rule when g(x) is constant. Both the trapezoidal and the quadratic versions of Filon's rule have been tried; the quadratic version did not seem to improve the convergence significantly over the simpler trapezoidal rule, so the latter is used in the rotor mean wake program.